INTERACTION BETWEEN TRICEPS SURAE MUSCLES AND THE ACHILLES TENDON IN YOUNG AND OLDER ADULTS: MECHANISMS AND FUNCTIONAL CONSEQUENCES

William H. Clark

A dissertation submitted to the faculty at the University of North Carolina at Chapel Hill in partial fulfillment of the requirements for the degree of Doctor of Philosophy in the Joint Department of Biomedical Engineering at the University of North Carolina at Chapel Hill and North Carolina State University.

Chapel Hill
2020

Approved by:

Jason R. Franz

Xiaogang Hu

Katherine R. Saul

Eric D. Ryan

Michael D. Lewek

ABSTRACT

William H. Clark: Interaction Between Triceps Surae Muscles and the Achilles Tendon in Young and Older Adults: Mechanisms and Functional Consequences
(Under the direction of Jason R. Franz)

Push-off intensity is largely governed by the interaction between the triceps surae muscles (i.e., gastrocnemius and soleus) and the architecturally complex Achilles tendon (AT). Recent evidence suggests that the gastrocnemius and soleus muscles transmit their forces through bundles of tendon fascicles (i.e., "subtendons") that form the AT. Using ultrasound imaging, we and others have revealed non-uniform displacement patterns within the AT – evidence for sliding between adjacent subtendons that may facilitate independent muscle actuation. This dissertation contends that independent muscle actuation is biomechanically important; despite sharing a common tendon, the triceps surae muscles undergo different fascicle kinematics during walking and contribute differently to powering walking. However, in older adults, we have observed more uniform AT tissue displacement with the potential to disrupt independent muscle actuation. This dissertation aims to fill two major gaps. First, to our knowledge, no empirical studies have characterized the origins of sliding between human Achilles subtendons. Second, more uniform AT tissue displacements correlates with reduced push-off intensity, alluding to unfavorable shifts in muscle fascicle behavior during walking – a finding that is unsubstantiated but has wide-reaching translational implications.

In study 1, we introduced a dual-probe imaging approach and presented evidence that triceps surae muscle dynamics precipitate non-uniform AT displacement patterns. In study 2, we

revealed that older adults have more uniform AT tissue displacements that are accompanied by potentially unfavorable changes in muscle contractile behavior during isolated contractions. In study 3, we combined electromyography, ultrasound imaging, and musculoskeletal modeling and revealed the gastrocnemius muscles play a more significant role than the soleus in governing changes in forward propulsion during walking. In study 4, again during walking, we suggest that the capacity for sliding between subtendons facilitates independent muscle actuation in young adults but restricts actuation in older adults, likely contributing to reduced push-off intensity. In study 5, using electrical stimulation, we reveal evidence that localized AT displacements respond in anatomically consistent ways to different patterns of muscle activation. Together, these studies accelerate our understanding of musculoskeletal mechanisms underlying age-related mobility impairment and could accelerate the development of engineered tissues and orthopaedic surgical intervention.

Dedicated to my life partner, Sam. Forever and Always.

ACKNOWLEDGEMENTS

So many people have played an integral role in helping me with this accomplishment. First, I would like to thank my advisor, Dr. Jason Franz. Thank you for helping me grow as a researcher and as a person. You have showed me what it means to be an effective and caring advisor who wants nothing but the best for their trainees. I will always be grateful for your continued support and guidance. Second, thank you to my committee members, Drs. Xiaogang Hu, Kate Saul, Eric Ryan, and Mike Lewek. Thank you for challenging me to think critically about the science, showing me continued respect, and helping me build my confidence as a researcher. Third, to the past and present members of the Applied Biomechanics Lab, thank you for you continued support in research, but more importantly, thank you for your continued support outside of research. You all provided a fantastic lab environment and I really enjoyed all the fun conversations we had. I cannot overstate how important you were in this accomplishment. Finally, I want to thank my friends and family. Thank you to my parents and sister who have always supported me and have been the role models I look up to. To my partner, Sam, your unwavering support and unfailing encouragement has been most essential. I appreciate you every day. Shout out to my dog, Keto, and cat, Linguine.

TABLE OF CONTENTS

LIST OF TABLES

LIST OF FIGURES

CHAPTER 1: INTRODUCTION

Older adults experience reductions in walking speed and push-off intensity, thereby negatively influencing mobility and quality of life (Hardy, Perera, Roumani, Chandler, & Studenski, 2007; Purser et al., 2005; Studenski et al., 2011). Push-off intensity (i.e., net ankle joint moment and mechanical power), as detailed in the following sections, is primarily influenced by the Achilles tendon, a critical passive elastic structure that transmits substantial contractile forces from the gastrocnemius and soleus muscles that make up the triceps surae (Fukashiro, Hay, & Nagano, 2006; Oda et al., 2007; Orselli, Franz, & Thelen, 2017; Zajac, 1989). There is strong evidence that a precipitous decline in mechanical output from the triceps surae plays a vital role in age-related decreases in walking speed (Barrett & Lichtwark, 2008; Beijersbergen, Granacher, Vandervoort, DeVita, & Hortobagyi, 2013; DeVita & Hortobagyi, 2000). However, declines in muscles strength and power capacity do not fully explain reductions in moment or power generation during walking, nor do targeted resistance training programs that increase these parameters translate to improvements in push-off intensity or walking speed (Beijersbergen et al., 2013; DeVita & Hortobagyi, 2000; Foure, Nordez, McNair, & Cornu, 2011). This dissertation is motivated by the overarching working hypothesis that the interaction between tissue behavior within the architecturally complex Achilles tendon and the contractile behavior of individual triceps surae muscles is a poorly understood, yet vastly important, biomechanical phenomena that influences walking mobility and is uniquely compromised by aging. To fully assess this hypothesis, there is a critical need for innovation in our measurement techniques towards

characterizing the underlying tissue behavior affecting age-related mobility loss – with far reaching implications for the design and control of wearable assistive devices and for targeted therapeutics.

Ultrasound Imaging in Biomechanics Research

Conventional analyses of age-related changes in walking biomechanics typically involve comparing young and older adult cohorts via joint-level kinematics (e.g., joint angles) and kinetics (e.g., joint moments/powers) in response to altered task demand (Sikdar, Wei, & Cortes, 2014). Although important, these analyses do not provide direct assessment of underlying tissue behavior and often rest upon inferences about the pathophysiological mechanisms undergirding age-related reductions in ankle moment and power generation. Unlike conventional biomechanical analyses, advances in ultrasound imaging have enabled the direct assessment of *in vivo* muscle contractile behavior and tendon tissue behavior (Cronin, af Klint, Grey, & Sinkjaer, 2011; Sikdar et al., 2014). At the muscle-level, cine B-mode ultrasound imaging, together with automated tracking techniques (e.g., UltraTrack), provides dynamic measurements of triceps surae kinematics (e.g., fascicle length and pennation angle) with high validity and reliability (Farris & Lichtwark, 2016). At the tendon-level, tissue displacements are largely perpendicular to the ultrasound beam direction, thereby reducing the accuracy of motion tracking due to low lateral resolution (Chernak & Thelen, 2012). Fortunately, advances in two-dimensional ultrasound elastography enable sub-pixel motion estimates that exploit the phase information present in ultrasound radiofrequency data and thus provide reliable estimates of Achilles tendon tissue displacements (Chernak & Thelen, 2012; Chernak Slane & Thelen, 2014). However, tracking muscle- or tendon-level behavior separately fails to fully capture the complex interactions between triceps surae muscles and their series elastic subtendons (Zelik & Franz, 2017). If we plan to apply new imaging techniques and

take the next step in moving science forward, we must have a fundamental appreciation for the architecture and function of the Triceps Surae Muscle-Tendon Unit.

Triceps Surae Muscle-Tendon Architecture and Function

The timing and magnitude of peak ankle moment and peak ankle power is largely governed by the forces generated and work performed by the biarticular gastrocnemius and uniarticular soleus muscles of the triceps surae (Whittington, Silder, Heiderscheit, & Thelen, 2008; Zelik, Huang, Adamczyk, & Kuo, 2014). Despite collectively transferring their force through a common distal tendon, the triceps surae muscles undergo different shortening behaviors during walking (Barber et al., 2017; Cronin, Avela, Finni, & Peltonen, 2013; Cronin & Finni, 2013) and, biomechanically, contribute differently to walking subtasks. However, the relative contribution of these individual muscles to forward propulsion versus vertical support is equivocal. Gastrocnemius activation exhibits larger changes than the soleus in response to conditions that alter the demand for forward propulsion (Gottschall & Kram, 2003; Miyoshi, Nakazawa, Tanizaki, Sato, & Akai, 2006). Similarly, gastrocnemius muscle stimulation elicits larger anterior shifts in the stance phase center of pressure than soleus muscle stimulation (Francis, Lenz, Lenhart, & Thelen, 2013). Conversely, soleus muscle work derived from computational simulations changes more than that for the gastrocnemius in response to altered propulsive demands (Lenhart, Francis, Lenz, & Thelen, 2014; Neptune, Sasaki, & Kautz, 2008). Despite the relatively disparate literature on this topic to date, likely due to a wide range of measurement techniques and research questions, these cumulative findings highlight the importance of gastrocnemius versus soleus muscle actuation during walking.

Achilles Tendon Architecture and Function

This dissertation contends that these muscle-level differences (i.e., gastrocnemius versus soleus muscle contractile behavior) are facilitated by the architecturally complex Achilles tendon, which itself consists of three distinct bundles of tendon fascicles, known as "subtendons", that twist as they descend to the calcaneus (Del Buono, Chan, & Maffulli, 2013; Doral et al., 2010; Edama et al., 2015; Edama et al., 2016; Handsfield et al., 2017; Pekala et al., 2017; Szaro, Witkowski, Smigielski, Krajewski, & Ciszek, 2009). Using ultrashort echo time magnetic resonance imaging, combined with literature reports of cadaveric studies (Bojsen-Moller & Magnusson, 2015; Edama et al., 2015; Sarrafian, 1993; Szaro et al., 2009), Handsfield et al. (2017) developed a 3D computational model of generalized Achilles tendon anatomy that included subtendon morphology (Handsfield et al., 2017). Based on these cumulative reports, the Achilles tendon is comprised of a posterior (superficial) section with tendon fascicles arising from the medial and lateral gastrocnemius and a more anterior (deep) section with tendon fascicles arising from the soleus. In comparative literature, sliding between adjacent subtendons has been commonly observed in rat and equine tendons and has the potential to allow independent actuation of triceps surae muscles (Finni et al., 2018; Gains et al., 2020; Maas, Noort, Baan, & Finni, 2020; Thorpe, Udeze, Birch, Clegg, & Screen, 2013). In humans, evidence for sliding is generally attributed to observations of non-uniform Achilles tendon tissue displacement patterns (i.e., significant differences in tissue displacements attributed to the gastrocnemius versus soleus subtendon). Non-uniform Achilles tendon tissue displacement patterns have been shown during passive ankle rotation (Arndt, Bengtsson, Peolsson, Thorstensson, & Movin, 2012), eccentric loading (Slane & Thelen, 2014, 2015), and walking (Franz, Slane, Rasske, & Thelen, 2015). However, despite the evidence of different shortening behaviors between triceps surae muscles, to

our knowledge, no empirical studies have characterized the origins of sliding between adjacent subtendons within the human Achilles tendon.

Origins of Achilles Tendon Non-Uniformity

Recent model predictions implicate differences in gastrocnemius versus soleus muscle forces as a plausible candidate for non-uniform Achilles tendon tissue displacement patterns (Handsfield et al., 2017). In the aforementioned modeling study, Handsfield et al. (2017) tuned a finite-element model of the Achilles tendon to replicate published estimates of *in vivo* Achilles tendon tissue displacements (Slane & Thelen, 2014). The authors interrogated their model to reveal that without differential muscle forces, Achilles tendon tissue non-uniformity decreased by 85% (Handsfield et al., 2017). This prediction has support in comparative literature of the rat Achilles tendon. Using electrical stimulation in combination with tracking the movement of sutured subtendons, Finni et al. (2018) found that the soleus subtendon undergoes substantially greater strain during soleus muscle stimulation, thus increasing the magnitude of non-uniform Achilles tendon tissue displacements (Finni et al., 2018). One implication of these findings is that triceps surae muscle dynamics themselves may precipitate non-uniform displacement patterns in the human Achilles tendon – a finding for which experimental evidence has not yet been presented.

Age-Related Changes to Muscle-Tendon Interaction

With advancing age, reduced mechanical output from the interaction between triceps surae muscles and the Achilles tendon is likely multifactorial. At the muscle-level, in older adults, gastrocnemius and soleus contractile behavior is deleteriously affected by changes in myofilament protein biology, muscle coordination, and loss of viable motor units (Miller, Callahan, & Toth, 2014). The resultant effects on triceps surae muscle force generation contributes to age-related reductions in plantarflexor mechanical output and are exacerbated by changes in tendon

morphology. At the tendon-level, older adults experience changes in viscoelastic and quasi-static properties of tendon fascicles that affect the ability of the tendon to store and return elastic energy (i.e., stress relaxation, stiffness, structural alignment) (Thorpe et al., 2013). To fully capture these age-related changes in muscle- and tendon-level behavior and their relevance to plantarflexor mechanical output, a detailed assessment of muscle- and tendon-level length-tension during walking is warranted. In previous studies, compared to those in young adults, our research group has observed more uniform Achilles tendon tissue displacements in older adults during walking (Franz & Thelen, 2015). These findings agree well with animal models of the aging tendon that present with a proliferation of collagen cross-linking and prominent reductions in sliding between subtendons (Thorpe, Udeze, Birch, Clegg, & Screen, 2012; Thorpe et al., 2013). Thus, an important inspiration for this dissertation arises; if triceps surae muscle dynamics can precipitate anatomically consistent patterns of localized tissue displacements within the architecturally complex Achilles tendon, would an age-related reduction in the capacity for sliding between adjacent subtendons negatively influence muscle contractile behavior during walking? Understanding the functional consequences of age-associated reductions in the capacity for sliding between adjacent subtendons within the human Achilles tendon may provide important insight into functionally limiting impairments in elderly gait. Indeed, simulating a reduced capacity for inter-fascicle sliding in the Achilles tendon, and thus a loss of mechanical independence between the gastrocnemius and soleus muscles, predicts unfavorable shifts in muscle fascicle behavior during walking (Franz & Thelen, 2016).

Dissertation Objectives

The purpose of this dissertation was first to investigate individual triceps surae (i.e., medial gastrocnemius and soleus) muscle dynamics as a determinant of non-uniform Achilles tendon

tissue displacement patterns during isolate contractions. In the first study (Chapter Two), published in *PeerJ*, we introduced a novel dual-probe imaging technique that quantified *in vivo* gastrocnemius and soleus muscle dynamics in synchrony with localized tendon tissue displacements within their associated Achilles subtendons. After establishing mechanistic causal links in young adults, we investigated aging effects on triceps surae muscle-Achilles subtendon interaction (Chapter Three), a study that was invited and later published in a special issue on aging in the *Journal of Connective Tissue Research*. In Chapter Four, published in the *Annals of Biomedical Engineering*, we combined electromyography, ultrasound imaging, and musculoskeletal modeling to establish the differential role of triceps surae muscles in young adults and thus the need for relative independence in force transmission through the Achilles tendon. In Chapter Five, we investigated changes in gastrocnemius versus soleus muscle shortening as a determinant for previously observed correlations between more uniform Achilles tendon tissue displacements and reduced plantarflexor mechanical output in older adults. Finally, in Chapter Six, using surface muscle electrical stimulation, we made an early effort to establish mechanistic cause and effect relations between activation of triceps surae muscles and resultant localized Achilles subtendon tissue displacement patterns. Together, these studies accelerate our understanding of musculoskeletal mechanisms underlying age-related mobility impairment toward improving the health and welfare of our rapidly aging population. Moreover, characterizing the underlying tissue behavior affecting age-related mobility loss could accelerate the development of engineered tissues, regenerative medicine therapies, and orthopaedic surgical intervention.

CHAPTER 2: DO TRICEPS SURAE MUSCLE DYNAMICS GOVERN NON-UNIFORM ACHILLES TENDON DEFORMATIONS?[1]

INTRODUCTION

The Achilles tendon (AT) is a critical passive elastic structure that transmits contractile forces from the gastrocnemius and soleus muscles (i.e., triceps surae) to generate a moment about the ankle, thereby powering activities such as walking (Fukashiro et al., 2006). In young adults, the power generated via triceps surae muscle-tendon interaction during walking is responsible for 70%-80% of the mechanical power needed for forward propulsion and swing initiation (Neptune, Zajac, & Kautz, 2009; Whittington et al., 2008; Zelik et al., 2014). The architecturally complex AT consists of three distinct bundles of tendon fascicles, known as "sub-tendons" (Handsfield et al., 2017), arising from the medial and lateral gastrocnemius and soleus muscles (Bojsen-Moller & Magnusson, 2015; Edama et al., 2015; Szaro et al., 2009). Recent advances in the use of dynamic, *in vivo* ultrasound imaging have revealed non-uniform displacement patterns within the AT. Those non-uniform patterns are commonly interpreted as evidence for sliding between adjacent sub-tendons, which has the potential to facilitate independence between the individual triceps surae muscles (Arndt et al., 2012; Chernak Slane & Thelen, 2014; Franz & Thelen, 2015). However, the mechanisms governing these non-uniform displacement patterns, and their relevance to triceps surae muscle contractile dynamics, remain elusive.

[1] This chapter previously appeared as an article in *PeerJ*. The original citation is as follows: Clark, W. H., & Franz, J. R. (2018). Do triceps surae muscle dynamics govern non-uniform Achilles tendon deformations? *PeerJ* 6:e5182. doi:10.7717/peerj.5182

To our knowledge, no empirical studies have characterized the origins of sliding between adjacent sub-tendons within the human AT. However, recent model predictions implicate differential gastrocnemius versus soleus muscle dynamics as a plausible candidate (Handsfield et al., 2017). Using anatomy derived from MRI, Handsfield et al. (2017) tuned a finite-element model of the AT to replicate published estimates of *in vivo* AT tissue displacements during isolated contractions (Chernak Slane & Thelen, 2014). The authors interrogated their model to reveal that without differential muscle forces, AT tissue non-uniformity decreased by 85% (Handsfield et al., 2017). One implication of this prediction is that triceps surae muscle dynamics may precipitate non-uniform displacement patterns in the human AT – a finding for which experimental evidence has not yet been presented. Indeed, other factors, including differences in sub-tendon material or architectural properties or in calcaneal insertion have also been implicated (Franz & Thelen, 2015; Thorpe et al., 2012, 2013).

Cine B-mode imaging has revealed important disparities between the individual triceps surae muscles. For example, Ishikawa et al. (2005) found that gastrocnemius muscle fascicles remain isometric or shorten during the late stance phase of walking while soleus muscle fascicles lengthen (Ishikawa, Niemela, & Komi, 2005). Cronin et al. (2013) added that the contractile behavior of the gastrocnemius, but not the soleus, changed with walking speed (Cronin et al., 2013). These data allude to the potential for functional benefits at the muscle level conferred by independent actuation – actuation that may be facilitated by the AT itself (Huijing, Yaman, Ozturk, & Yucesoy, 2011; Kawakami, Ichinose, & Fukunaga, 1998; Tian, Herbert, Hoang, Gandevia, & Bilston, 2012). However, we recently observed cine B-mode imaging of gastrocnemius and soleus muscle dynamics alone are unable to reliably estimate interactions between these muscles and their series elastic sub-tendons (Zelik & Franz, 2017). Thus, to gain mechanistic insight into the role of

triceps surae muscle dynamics in precipitating non-uniform displacement patterns within the AT, there is a critical need for innovation in our measurement techniques; to understand the complexities of muscle and tendon behavior, you must measure muscle and tendon behavior.

Our goal was to investigate individual triceps surae (i.e., medial gastrocnemius and soleus) muscle dynamics as a determinant of non-uniform AT tissue displacement patterns during isolated contractions. We used a dual-probe ultrasound imaging technique to quantify *in vivo* gastrocnemius and soleus muscle dynamics in synchrony with localized tendon tissue displacements within their associated sub-tendons. We hypothesized that superficial versus deep differences in AT tissue displacements would be accompanied by and correlate with anatomically consistent differences in medial gastrocnemius (GAS) versus soleus (SOL) muscle shortening. We also tested the secondary hypothesis that the relationship between AT tissue displacements and GAS versus SOL muscle shortening would vary with ankle angle, which we would interpret in the context of altered triceps surae force generating capacity (Huijing et al., 2011; Kawakami et al., 1998; Tian et al., 2012) and tendon slack (Herbert et al., 2011; Hug, Lacourpaille, Maisetti, & Nordez, 2013).

METHODS

Subjects and Protocol

We estimated that n=8 subjects would have 80% power to detect ($p<0.05$) previously reported differences between peak GAS and SOL sub-tendon displacements (i.e., 5.95 mm versus 8.49 mm) in young subjects during an isolated ankle task (Slane & Thelen, 2015). We recruited 12 subjects to participate and excluded 3 subjects during our quality control process. Specifically, we excluded subjects for whom the average frame-to-frame correlation in our speckle tracking

algorithm, later described, for any one condition fell below 80%. Thus, we report data for 9 subjects (age: 25.1 ± 5.6 years, mass: 69.8 ± 6.9 kg, height: 1.7 ± 0.1 m, 4 females and 5 males). Subjects provided written informed consent as per the UNC Chapel Hill IRB and walked without an assistive aid, had no orthopedic disorders within the last six months nor any neurological disorder or disease, and did not have a leg prosthesis. Subjects first walked on a treadmill (Bertec Corp., Columbus, OH) for 6 min at 1.25 m/s to pre-condition their triceps surae muscle-tendon units and reach steady-state behavior (Hawkins, Lum, Gaydos, & Dunning, 2009). Subjects then performed three ramped maximum isometric voluntary contractions at each of five ankle angles (10º dorsiflexion to 30º plantarflexion in 10º increments) in a dynamometer (Biodex, Shirly, NY), with the knee flexed to replicate that near the push-off phase of walking (~20 degrees). To elicit a symmetric loading-unloading profile, subjects started from rest and increased their plantarflexor moment until reaching their voluntary maximum at 2 seconds, before steadily returning to rest at 4 seconds. Prior to data collection, subjects briefly practiced this 4 second ramped contraction using a real-time display of their net ankle moment for positive reinforcement. We fully-randomized the ankle angles, and subjects rested at least one minute between each contraction. Subjects were barefoot throughout the experiment to allow proper placement of the ultrasound transducers.

Measurements

We synchronized two 10 MHz linear array ultrasound transducers to simultaneously record GAS and SOL fascicle kinematics with tissue displacements in their associated tendinous structures (Figure 1). A 60 mm Telemed Echo Blaster 128 ultrasound transducer (LV7.5/60/128Z-2, UAB Telemed, Vilnius, Lithuania) placed over the mid-belly of the GAS of subjects' right leg recorded cine B-mode images at 61 frames/s through a longitudinal cross section using an image

depth of 65 mm. This Telemed transducer placement and depth also enabled imaging of the SOL in the same image plane (Cronin et al., 2013; Tian et al., 2012). Simultaneously, a 38-mm transducer (L14-5W/38, Ultrasonix Corporation, Richmond, BC) operating at 70 frames/s recorded 128 lines of ultrasound radiofrequency (RF) data from subjects' right free AT, distal to the SOL muscle-tendon junction, using an image depth of 20 mm and secured using a custom orthotic. Placement of this probe was prescribed by the fit of our custom orthotic, secured with straps just proximal to the malleoli and thus selected to replicate the placement used in prior studies (i.e., ~6 cm proximal to the calcaneal insertion) (Franz et al., 2015).

Eight cameras from a 14-camera motion capture system (Motion Analysis, Corp., Santa Rosa, CA) operating at 100 Hz recorded the 3D positions of 14 retroreflective markers placed on the subjects' right lower leg and ultrasound transducers. An inverse kinematics routine (Silder et al., 2008) estimated ankle and knee joint angles and we recorded the plantarflexor moment from the dynamometer at 1000 Hz.

We collected binary synchronization signals from the Telemed and Ultrasonix machines at 1000 Hz. These signals co-registered the onset of ultrasound data collected from the GAS, SOL, and free AT with the plantarflexor moment and marker trajectories. We analyzed all data between key-frames at the beginning and end of each ramped contraction, defined using a threshold of 5% peak moment. From the ultrasound data, we quantified time series of (*i*) GAS and SOL fascicle kinematics and (*ii*) tendon tissue kinematics, each interpolated to 1000 data points per trial, as described below.

Muscle Kinematics

Following best practices outlined by Farris and Lichtwark (2016), the same investigator performed all muscle tracking. First, we defined a static polygon region of interest (ROI)

surrounding each muscle and their aponeuroses (Figure 1). We then defined one GAS and one SOL muscle fascicle in the mid-region of the imaged plane, considered representative of the muscle belly, from their superficial to deep aponeurosis in the first "key-frame" of every trial. Open source MATLAB routines based on an affine extension to an optic flow algorithm quantified time series of GAS and SOL fascicle lengths ($L_{fascicle}$) and pennation angles (α) (Farris & Lichtwark, 2016). Pennation angles corresponded to the oblique angle between the image horizontal axis and the defined fascicle of the respective muscle. Finally, to more directly place these muscle dynamics in the context of tendon tissue displacement, we combined muscle fascicle lengths and pennation angles to compute muscle length longitudinal to its line of action (L_{muscle}):

$$L_{muscle} = L_{fascicle} \cos \alpha$$

Tendon Kinematics

A 2D speckle tracking algorithm estimated localized displacements of AT tissue using previously published techniques (Chernak & Thelen, 2012; Chernak Slane & Thelen, 2014). In brief, we defined a rectangular ROI, measuring ~15 x 3 mm on a B-mode image of the free AT created from the raw RF data at the first "key-frame" of each trial. The ROI contained a grid of nodes with 0.83 x 0.42 mm spacing defined to encompass only tendinous tissue. A 2 mm x 1 mm kernel containing up-sampled (4x) RF data, centered at each nodal position, provided a search window over which we defined two-dimensional (2D) normalized cross-correlation functions between successive frames. We defined localized frame-to-frame nodal displacements that maximized these 2D cross-correlations, with the cumulative displacement representing the average of forward and backward tracking results. Nodal displacements were regularized using second order polynomials (Pan et al., 2009). From these cumulative displacements, we quantified the

average longitudinal nodal displacements originating from two equally sized tendon depths (Szaro et al., 2009) - superficial and deep - corresponding to tendon tissue thought to arise from GAS and SOL, respectively. This orientation represents the anatomical arrangement most prevalent in cadaveric studies (Anson & McVay, 1971; Edama et al., 2015; Gils, Steed, & Page, 1996; Szaro et al., 2009). Although previous authors have acknowledged that in some anatomical observations the individual sub-tendons varied in their thickness, in the majority of the anatomical observations, the gastrocnemius sub-tendon was the same size as the soleus sub-tendon (Anson & McVay, 1971; Del Buono et al., 2013; Doral et al., 2010; Gils et al., 1996). Here, we report these average longitudinal displacements as representing that of tissue within the corresponding GAS and SOL sub-tendons (Figure 1). Finally, we quantified tendon non-uniformity by reporting the difference between peak tendon tissue displacements of the superficial and deep regions of the tendon.

Statistical Analysis

For each outcome measure, we took the average of the three conditions for each ankle angle. A two-way repeated measures ANOVA tested for main effects of and interactions between ankle angle and muscle-tendon unit (i.e., GAS and SOL) on peak muscle shortening and peak tendon tissue displacement using an alpha level of 0.05. When a significant main effect was found, post-hoc pairwise comparison identified the ankle angles at which GAS versus SOL differences were significant. For peak plantarflexor moment, a one-way repeated measures ANOVA tested for significant main effects of ankle angle and Pearson's correlation coefficients assessed the relation to muscle and sub-tendon tissue kinematics. We then calculated Pearson's correlation coefficients between: (*i*) GAS and SOL muscle shortening and displacement in their associated regions of the AT (i.e., superficial and deep, respectively) and (*ii*) muscle shortening differences (i.e., GAS versus SOL) and tendon non-uniformity (i.e., superficial versus deep). As a secondary analysis,

we calculated Pearson's correlation coefficients between GAS and SOL muscle shortening and displacement in their unassociated region of the AT (i.e., GAS versus deep, SOL versus superficial). Finally, we qualitatively assessed the independent contributions of fascicle length versus pennation angle on GAS and SOL muscle length changes. We plotted percent change in fascicle length versus percent change in the cosine of pennation angle (i.e., contributors to muscle length change) and noted apparent trends against the line of unity with a ratio of 1:1.

RESULTS

Peak plantarflexor moment decreased progressively from dorsiflexion to plantarflexion across the range of angles tested ($p<0.01$). Muscle and sub-tendon tissue kinematics were relatively independent of ankle angle; only SOL fascicle and longitudinal muscle shortening exhibited significant main effects ($p's=0.03$), with pairwise comparisons revealing smaller changes at 30º plantarflexion compared to the other conditions. However, consistent with this observation, SOL tendon displacements also tended to be smaller at 30º plantarflexion ($p=0.064$). Across all ankle angles, the SOL shortened by an average of 78% more than the GAS during moment generation ($p<0.01$) (Figure 2A), due both to greater fascicle shortening and a larger increase in pennation (p's<0.01) (Figure 3). However, change in fascicle length had a greater influence than change in the cosine of pennation on longitudinal GAS and SOL muscle shortening (Figure 3).

SOL versus GAS differences at the muscle level were accompanied by, on average, 51% more displacement in the deep versus superficial region of the AT ($p<0.01$) (Figure 2B). Moreover, the magnitude of peak GAS and SOL muscle shortening positively correlated with peak displacements in their associated regions of the AT (GAS: $R^2=0.48$; SOL: $R^2=0.63$; $p's<0.01$) (Figure 4A). Superficial versus deep differences in AT displacement positively correlated with

anatomically consistent differences in GAS versus SOL muscle shortening (R^2=0.37, p<0.01) (Figure 4B). The strength of these latter correlations varied systematically with ankle angle, becoming stronger with increased ankle dorsiflexion (Table 1). Conversely, those correlations became non-significant at 20º (p=0.10) and 30º (p=0.99) plantarflexion. We also found moderate to strong correlations between GAS and SOL muscle shortening and displacement in their unassociated region of the AT (R^2=0.38 and R^2=0.65, respectively; p's<0.05). Finally, across all conditions, peak muscle shortening (GAS: R^2=0.37; SOL: R^2=0.47) and sub-tendon tissue displacements (GAS: R^2=0.51; SOL: R^2=0.49) significantly and positively correlated with peak plantarflexor moment.

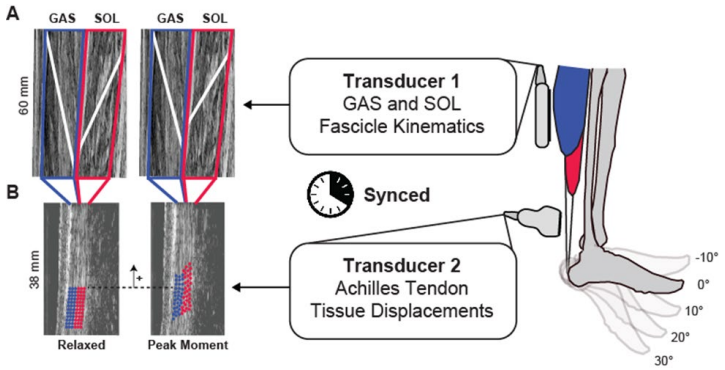

Figure 1: We used a dual-probe ultrasound imaging approach that enables the simultaneous assessment of the medial gastrocnemius (GAS) and soleus (SOL) muscle fascicle kinematics with tissue displacements in their associated sub-tendons of the free Achilles tendon (AT). (A) Time series of fascicle lengths and pennation angles were derived from cine B-mode images. (B) A custom 2D speckle tracking algorithm estimated localized displacements of two equally sized tendon depths - superficial and deep - corresponding to tendon tissue thought to arise from GAS and SOL, respectively.

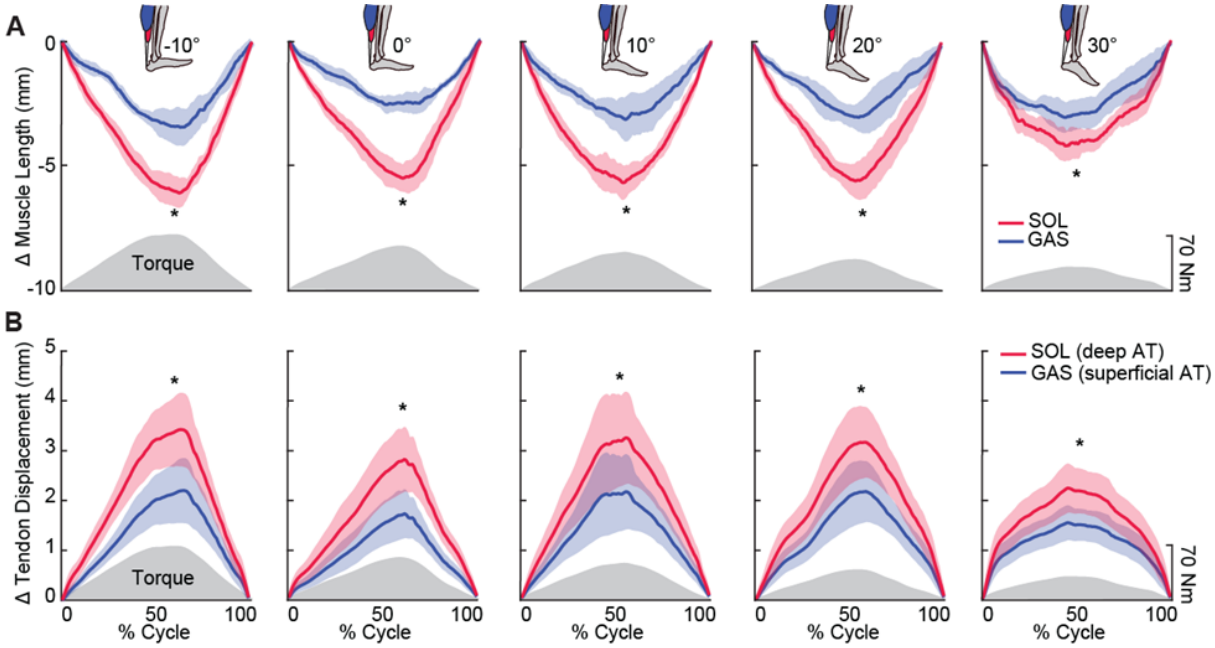

Figure 2: Group mean (standard error) (A) muscle shortening and (B) sub-tendon displacements (nodal displacement relative to initial position; proximal positive) across the range of ankle angles tested. Gray shaded regions show the group mean net profile during each loading-unloading cycle. Across all conditions, SOL shortened by an average of 78% more than GAS during force generation. This was accompanied by, on average, 51% more lengthening in the deep versus superficial region of the free AT. Asterisks (*) indicate statistically significant (p<0.05) differences between GAS and SOL.

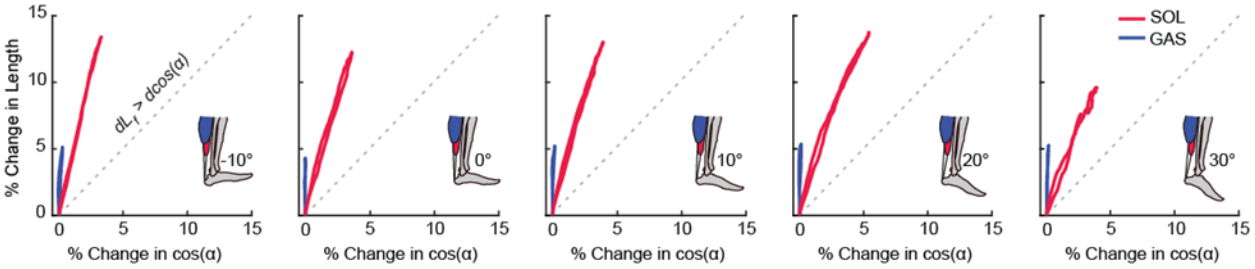

Figure 3: Group mean percent change in fascicle length versus percent change in the cosine of pennation angle for the gastrocnemius (GAS) and soleus (SOL) across the range of ankle angles tested. The dashed line represents a line of unity (i.e., equal contributions from fascicle shortening and fascicle rotation). SOL consistently exhibited more fascicle shortening and fascicle rotation than GAS. For all conditions, fascicle shortening had a greater influence on longitudinal muscle shortening than fascicle rotation.

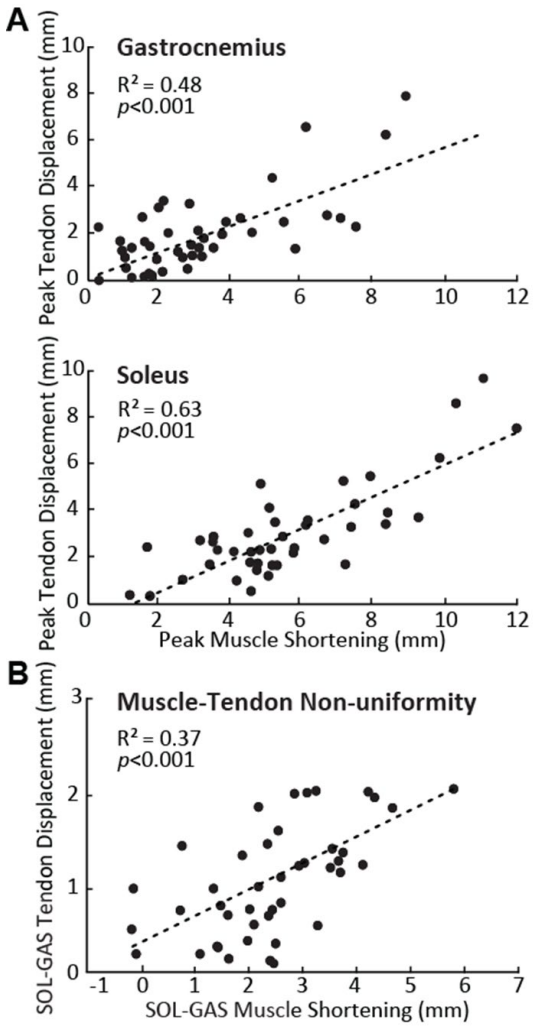

Figure 4: (A) Correlations between peak GAS or SOL muscle shortening and displacement in their associated regions of the AT. (B) Correlation between superficial versus deep differences in AT displacement and GAS versus SOL differences in muscle. All correlations are pooled across all conditions.

Table 1.
Correlations (R^2) and *p*- values between peak muscle shortening and peak sub-tendon tissue displacements at each ankle angle.

		-10°	0°	10°	20°	30°
GAS	R^2	**0.52**	0.20	**0.67**	**0.50**	0.32
	p- value	**0.044**	0.073	**0.007**	**0.031**	0.114
SOL	R^2	**0.77**	0.38	**0.75**	**0.76**	0.36
	p- value	**0.004**	0.075	**0.003**	**0.002**	0.088
SOL-GAS	R^2	**0.78**	**0.60**	**0.45**	0.33	0.04
	p- value	**0.004**	**0.015**	**0.049**	0.104	0.991

Bold numbers represent significant correlations ($p < 0.05$).
GAS: Gastrocnemius, SOL: Soleus

DISCUSSION

We investigated the role of triceps surae muscle dynamics in precipitating non-uniform tissue displacements in the architecturally complex Achilles tendon (AT). We also used a dual-probe ultrasound imaging technique empowering the simultaneous measurement of GAS and SOL muscle fascicle dynamics together with tissue displacements within their associated sub-tendons of the AT. Our results build on dual-probe approaches applied previously to GAS quantifying muscle fascicle and muscle-tendon junction kinematics (Ishikawa & Komi, 2008; Matijevich, Branscombe, & Zelik, 2018). Our findings largely supported our first hypothesis; independent of ankle angle, SOL shortened more than GAS during moment generation – muscle-level differences were accompanied by and correlated with anatomically consistent differences in sub-tendon tissue displacements. As we elaborate, these findings provide empirical evidence for a mechanistic link between non-uniform displacement patterns within the human AT and the operating behavior of the triceps surae muscles.

Previous anatomical work has shown that the human free AT near our imaging location consists predominantly of superficial tendon fascicles arising from GAS and deep tendon fascicles arising from SOL (Szaro et al., 2009). Consistent with this architecture, the SOL muscle and its associated deep region of the AT in all cases both underwent larger kinematic changes during moment generation compared to those structures associated with GAS. Although not previously quantified simultaneously, these triceps surae muscle (Fukashiro et al., 2006; Hoang, Herbert, Todd, Gorman, & Gandevia, 2007; Lauber, Lichtwark, & Cresswell, 2014; Maganaris, Baltzopoulos, & Sargeant, 1998) and AT tissue (Franz et al., 2015) kinematics are generally consistent with those reported for a variety of activities spanning isolated contractions to functional activities. For example, we reported larger tissue displacements in the deep AT (i.e., SOL sub-

tendon) than in the superficial AT (i.e., GAS sub-tendon) during the stance phase of walking, a phase in which GAS and SOL muscle fascicles exhibit different operating behavior (Ishikawa, Komi, Grey, Lepola, & Bruggemann, 2005). In their review, Bojsen-Møller and Magnusson (2015) summarize evidence for heterogeneous loading within the AT and at least conceptualize the potential for differential GAS and SOL activations, and thus muscle contractile dynamics, to precipitate non-uniform patterns of AT tissue displacements (Bojsen-Moller & Magnusson, 2015).

Despite conceptual descriptions (Bojsen-Moller & Magnusson, 2015) and recent model predictions (Handsfield et al., 2017), we lacked evidence for the role of muscle dynamics in governing non-uniform mechanical behavior within the AT. Consistent with our first hypothesis, here we found that differences between peak SOL and GAS muscle shortening positively correlated with those between peak SOL and GAS sub-tendon tissue displacement during fixed-end contractions. Coupled with anatomically consistent differences in muscle shortening and tendon tissue displacements described above, these correlations suggest that triceps surae muscle dynamics can give rise to sliding between adjacent sub-tendons within the human AT.

We qualitatively assessed the contributions of fascicle length versus pennation angle to differences between GAS and SOL muscle contractile behavior. Fascicle length and pennation angles of the GAS and SOL, including their changes during isometric contractions, agree well with published values (Maganaris, 2003; Maganaris et al., 1998; Tilp, Steib, Schappacher-Tilp, & Herzog, 2011). In all cases, fascicle shortening contributed more than fascicle rotation to the longitudinal GAS and SOL muscle length changes. Moreover, the SOL exhibited both larger fascicle shortening and fascicle rotation than GAS. In fact, we noted very little pennation angle change in the GAS during moment generation. Thus, differences in triceps surae contractile

behavior arise from a combination of larger fascicle shortening and rotation in SOL versus GAS, contributing to the non-uniform length change dynamics ultimately borne by the AT.

The strength of the correlation between tendon displacement non-uniformity and GAS versus SOL muscle differences in shortening increased with ankle dorsiflexion, which we interpret as support for our secondary hypothesis. Correlations were strongest at the most dorsiflexed ankle angle (i.e., 10º), decreasing progressively with increasing plantarflexion. This observation may reflect the effects of decreased tendon slack, decreased muscle passive tension, and/or larger peak moments conveyed by increasing ankle dorsiflexion. Indeed, muscle and tendon mechanical behavior may exhibit complex changes in response to ankle rotation (Hug et al., 2013). More tendon slack would imply greater tendon length change, and thus tendon tissue displacements, prior to the onset of force transmission (Zajac, 1989). We suspect that differences in tendon slack explain the relatively invariant tendon kinematics across the range of ankle angles tested, despite systematic changes in peak moment. Similarly, more tendon slack and/or differences between GAS and SOL tendon slack lengths may explain why these correlations became insignificant with increasing ankle plantarflexion. We also found that ankle dorsiflexion maximized peak moment, and presumably AT force transmission, consistent with prior studies (Ackland, Lin, & Pandy, 2012; Scovil & Ronsky, 2006; Zajac, 1989). Thus, larger forces may themselves convey stronger correlations between muscle and tendon tissue dynamics. Simultaneously, or perhaps alternatively, ankle angle effects on the mechanical properties of the individual triceps surae muscles and sub-tendons themselves could influence the relation between muscle and tendon behavior. Additional study here is certainly warranted.

Although sliding between adjacent sub-tendons in the AT may convey some independence between GAS and SOL muscle-tendon actuators, myofascial force transmission through

connective tissues between these muscles is also prevalent. Oda et al. (2007) found that an isolated stimulus to GAS elicited a similar time course and magnitude of length change in both GAS and SOL (Oda et al., 2007). Kinugasa et al. (2013) also suggested that interaponeurosis shear, elicited by adjacent muscle dynamics, influences displacements of the distal muscle-tendon junctions (Kinugasa, Oda, Komatsu, Edgerton, & Sinha, 2013). More recently, Finni et al. (2017) added that the strength of this lateral connectivity increases with muscle activation (Finni, Cronin, Mayfield, Lichtwark, & Cresswell, 2017). However, non-uniform AT displacement patterns are also present during passive ankle rotation in the absence of triceps surae muscle loading (Arndt et al., 2012; Chernak Slane & Thelen, 2014). For this study, we interpret our findings in the context of their relevance to independent actuation; follow-up studies are necessary to better understand the relative role of lateral force transmission. Indeed, we found that SOL muscle shortening exhibited strong positive correlations with GAS sub-tendon displacement, and vice versa. One interpretation of this finding is that SOL, having by far the largest force-generating capacity of the triceps surae muscles (Albracht, Arampatzis, & Baltzopoulos, 2008; Ogihara et al., 2017) coupled with having greater fascicle shortening and rotation than GAS, has a preferential influence on tendon tissue displacements in the free AT. Taking together, our results reflect independent and inter-dependent mechanical behavior between individual triceps surae muscle-tendon units. Indeed, intermuscular force transmission is documented within the triceps surae (Huijing et al., 2011; Tian et al., 2012).

There are other possible factors contributing to AT tissue non-uniformity that may act in concert with triceps surae muscle dynamics. Material property differences between adjacent sub-tendons may elicit non-uniform displacement patterns. Indeed, Matson et al. (2012) reported up to two-fold variations in elastic modulus between different leg tendons (Matson, Konow, Miller, Konow, & Roberts, 2012). In addition, architectural differences between sub-tendons (e.g., lengths

and cross-sectional areas) may influence their mechanical properties (e.g., stiffness) and thus displacement patterns (Szaro et al., 2009). As another example, differences between sub-tendon slack lengths could also contribute. We consider the present study a first step toward an improved understanding of the relative contributions of these factors in governing triceps surae muscle-tendon behavior.

If triceps surae muscle dynamics can precipitate non-uniform Achilles tendon tissue displacements, can tendon-level changes influence muscle contractile behavior? For example, our findings may be important for understanding the functional consequences of age-associated reductions in inter-fascicle sliding within the human AT. Compared to those in young adults, we have observed more uniform AT tissue displacements in older adults during walking (Franz & Thelen, 2015), which may reflect collagen cross-linking and interfascicle adhesions (Thorpe et al., 2013). These tendon-level changes correlate with a reduced plantarflexor moment during walking in older adults, alluding to unfavorable functional consequences. Moreover, simulating a reduced capacity for inter-fascicle sliding in the AT, and thus a loss of mechanical independence between the GAS and SOL, predicts unfavorable shifts in muscle fascicle behavior during walking (Franz & Thelen, 2016). Our present work provides a foundation for using dual-probe imaging to gain mechanistic insight into these earlier observations.

There are several limitations of this study. First, we only report data for the medial gastrocnemius and SOL, including a generalized anatomical approximation of their associated sub-tendons (Edama et al., 2015; Gils et al., 1996; Szaro et al., 2009). Second, two-dimensional imaging may not fully capture the three-dimensional behavior of the triceps surae muscles and AT. For example, the SOL muscle is comprised of anterior, posterior, medial, and lateral components that differ in architecture (Chow et al., 2000). We only imaged the posteromedial SOL, which may

not represent other regions. Third, muscle tracking reliability depends on meticulous fascicle determination and incumbent semi-automated tracking limitations (Farris & Lichtwark, 2016). To minimize these effects, one investigator performed all analyses. Fourth, the pennation angle defined by UltraTrack is not representative of a true pennation angle due to the software identifying the line of action as the horizontal axis of the image. We have also previously described the limitations of our 2D speckle tracking estimates of AT tissue displacements (Franz et al., 2015). We add here that cross-correlation estimates of tissue motion can be subject to spatial averaging. However, based on a previously published validation (Chernak & Thelen, 2012; Chernak Slane & Thelen, 2014), we do not suspect this significantly influenced our findings nor interpretation. We also opted to report sub-tendon tissue displacements, an outcome we can measure with a higher level of confidence than sub-tendon elongation. Specifically, estimating sub-tendon tissue elongation relative to a motion capture estimate of calcaneal insertion can be prone to errors associated with coronal plane ankle rotation, tendon slack, and the complexities of AT curvature - errors that require further study (Csapo, Hodgson, Kinugasa, Edgerton, & Sinha, 2013; Matijevich et al., 2018). Fifth, we made no attempt to estimate forces transmitted through the AT, which are heterogeneous and highly complex (Bojsen-Moller & Magnusson, 2015). We also note that ankle and knee angles became slightly (<5º) more extended from rest to peak moment generation. The sub-tendon tissue displacements reported here likely reflect some combination of that due to muscle shortening at the proximal attachment and that due to calcaneus displacement (via ankle rotation) at the distal attachment. However, Handsfield et al. (2017) found a very negligible effect of retrocalcaneal tendon insertion on GAS-SOL differences in sub-tendon tissue displacement, even for 25º of ankle rotation (Handsfield et al., 2017). Finally, although we report anatomically

consistent behavior between muscle and sub-tendons, our conclusions are based in part on correlations that cannot definitively convey causal links.

CONCLUSION

We present evidence that triceps surae muscle dynamics may precipitate non-uniform displacement patterns in the architecturally complex Achilles tendon. Moreover, we used a dual-probe imaging approach to empower simultaneous assessment of muscle and tendon toward an improved mechanistic understanding of triceps surae behavior. Our findings may be important for understanding age-associated changes in AT displacement patterns, which we suspect alter muscle contractile behavior in older adults.

CHAPTER 3: TRICEPS SURAE MUSCLE-SUBTENDON INTERACTION DYNAMICS DIFFERS BETWEEN YOUNG AND OLDER ADULTS[2]

INTRODUCTION

The timing and magnitude of peak ankle moment, governed by the mechanical output of the lateral and medial gastrocnemius (GAS) and soleus (SOL) muscles (i.e., triceps surae) and their common series elastic structures, is an important determinant of walking performance (Sawicki, Lewis, & Ferris, 2009). However, despite sharing a common tendon, muscles comprising the triceps surae undergo different fascicle kinematics during walking and, biomechanically, contribute differently to forward propulsion and vertical support (McGowan, Neptune, & Kram, 2008). This differential behavior at the muscle level alludes to the possibility that these muscles act, at least in part, as functionally independent actuators. Building on this premise, more recent evidence shows that the architecturally complex Achilles tendon consists of distinct subtendons arising from each of the individual triceps surae muscles (Edama et al., 2015; Handsfield et al., 2017). Comparative data and our own *in vivo* evidence allude to the prevalence of sliding between these adjacent subtendons that has the potential to facilitate independence between the GAS and SOL (Arndt et al., 2012; Clark & Franz, 2018b; Slane & Thelen, 2014). Unfortunately, animal models of the aging tendon present with a proliferation of collagen cross-

[2] This chapter previously appeared as an article in *Connective Tissue Research*. The original citation is as follows: Clark, W. H., & Franz, J. R. (2020). Triceps Surae Muscle-Subtendon Interaction Differs Between Young and Older Adults. *Connect Tissue Res*, 61:1, 104-113. doi:10.1080/03008207.2019.1612384

linking and prominent reductions in interfascicle sliding (Thorpe et al., 2012, 2013). Those observations also appear to be clinically meaningful; during walking, age-associated reductions in measures of subtendon sliding within the human Achilles tendon correlate with smaller peak ankle moments during push-off in older adults (Franz & Thelen, 2015). Although this alludes to a mechanistic link between Achilles subtendon tissue displacements and altered muscle contractile behavior due to aging, we are not aware of direct empirical data that would support such a conclusion.

There is strong evidence that a precipitous decline in peak ankle moment plays a vital role in age-related mobility deficits (Beijersbergen et al., 2013; DeVita & Hortobagyi, 2000). Reduced mechanical output from the triceps surae is likely multifactorial, and the functional consequences of, for example, sarcopenia and distal leg muscle weakness are well-documented. However, declines in muscle strength alone cannot fully explain age-related reductions in push-off intensity during walking, nor do simple strengthening exercises directly translate to improvements in ankle moment or walking speed (Beijersbergen et al., 2013; Foure et al., 2011). The current study is motivated by the overarching working hypothesis that changes in the interaction between triceps surae muscle behavior and Achilles subtendon tissue displacements contributes to a reduced capacity for ankle moment generation during walking in older versus young adults (Browne & Franz, 2017). Finni et al. (2018) revealed that independent GAS versus SOL muscle stimulation elicits large differences in the Achilles subtendon strain patterns and mechanical output in rats (Finni et al., 2018). Thus, as a logical and needed extension, we aim to determine the mechanistic link between these structures in humans.

Indirect evidence from young adults is consistent with the notion that subtendon-level changes can alter the contractile behavior of individual triceps surae muscles. For example, we recently investigated the relation between Achilles subtendon tissue displacement patterns and individual triceps surae muscle fascicle shortening using synchronized, dual-probe ultrasound imaging (Clark & Franz, 2018b). There, consistent with our conceptual premise, we revealed that differences between GAS and SOL subtendon displacements were accompanied by and correlated with anatomically consistent differences between GAS and SOL muscle shortening. In young adults, this implicates triceps surae muscle contractile behavior in precipitating sliding between adjacent subtendons comprising the Achilles tendon. By logical extension, this outcome also suggests that reduced interfascicle sliding at the tendon-level due to aging could unfavorably couple GAS and SOL behavior at the muscle-level. Length changes of GAS (Mian, Thom, Ardigo, Minetti, & Narici, 2007) and SOL (Rubenson, Pires, Loi, Pinniger, & Shannon, 2012) muscle fascicles have been measured separately during activities spanning isolated contractions to walking in young and older subjects. As one example, older adults walk with shorter GAS (Mian et al., 2007) and SOL (Panizzolo, Green, Lloyd, Maiorana, & Rubenson, 2013) muscle fascicle lengths, most likely due to an age-related increase in Achilles tendon compliance (Onambele, Narici, & Maganaris, 2006). However, only young adult studies have simultaneously measured fascicle behavior in both GAS and SOL (McGowan et al., 2008; Neptune et al., 2009). Moreover, no study to date has compared simultaneous muscle- and tendon-level measurements between cohorts of young and older adults. Thus, we have an incomplete understanding of how age-related tendon-level changes influence muscle-level behavior.

As an important step toward establishing mechanistic causal links, the purpose of this study was to investigate aging effects on the relation between non-uniform Achilles subtendon

displacement patterns and triceps surae muscle contractile behavior using dual-probe ultrasound imaging during a series of ramped maximum isometric voluntary contractions. We hypothesized that, compared to young adults, older adults would have (*i*) more uniform Achilles subtendon tissue displacements that (*ii*) would be accompanied by anatomically consistent (i.e., smaller differences, same sign) GAS versus SOL muscle length change behavior. Finally, based on evidence that the human AT becomes more compliant in old age, we tested the secondary hypothesis that older adult subtendons would be more sensitive than younger adult subtendons to changes in force transmission that follow from changes in ankle joint position (i.e., more displacement per unit force).

METHODS

Subjects and Protocol

We report data for nine younger subjects (age: 25.1 ± 5.6 years, mass: 69.8 ± 6.9 kg, height: 1.7 ± 0.1 m, four females) and ten older adult subjects (age: 74.3 ± 3.4 years, mass: 67.2 ± 9.0 kg, height: 1.7 ± 0.1 m, four females). Each subject provided written informed consent as per the University of North Carolina at Chapel Hill Internal Review Board (16-0379). All subjects did not require an assistive aid to walk, were free from any neurological disorder or disease, did not have a leg prosthesis, and have not had an orthopedic disorder within the last six months. To precondition their Achilles tendon and triceps surae, subjects first walked on a treadmill (Bertec Corporation, Columbus, OH) for six min at a self-selected walking speed (above 1.0 m/s) (Hawkins et al., 2009). Thereafter, while sitting in a Biodex System 4-Pro (Biodex, Shirly, NY), subjects completed a series of three ramped maximum isometric voluntary contractions at four separate ankle angles (from a 0º neutral ankle angle to a 30º plantarflexion in 10º increments) with

the knee flexed to replicate the push-off phase of walking (~20-30º). We instructed subjects to "push like a gas pedal" (i.e., attempt to isolate their triceps surae), and perform a four second, symmetric loading-unloading profile. To comply, subjects started at rest and increased ankle moment until they reached a voluntary maximum at two seconds, before steadily returning to rest at four seconds. Before the first recorded trial, subjects practiced the ramped contractions using a real-time display of their ankle moment. During data collection, we fully-randomized ankle angle and provided one minute of rest between contractions. Subjects were barefoot throughout the data collection to facilitate proper placement of the ultrasound transducers.

Measurements

We utilized the same methodological approach as previously reported in our younger adult data collection (Clark & Franz, 2018b). Two linear array 10 MHz ultrasound transducers simultaneously recorded GAS and SOL fascicle kinematics and tissue displacements in their associated tendinous structures (Supplementary Figure 1). The first transducer (LV7.5/60/128Z-2, UAB Telemed, Vilnius, Lithuania), placed over the GAS mid-belly of the subject's right leg, recorded cine B-mode images at 61 frames/s through a longitudinal cross section using an image depth of 65 mm. The transducer placement and depth enabled synchronized assessment of GAS and SOL in the same image plane (Tian et al., 2012). Simultaneously, a second ultrasound transducer (L14-5W/38, Ultrasonix Corporation, Richmond, BC) placed over the subjects' right free AT, distal to the SOL muscle-tendon junction, recorded 128 lines of ultrasound radiofrequency data at 70 frames/s using an image depth of 20 mm. We secured the second ultrasound probe with a custom orthotic, secured just proximal to the malleoli to replicate the placement used in prior studies (i.e., ~ six cm proximal to the calcaneal insertion point) (Franz et al., 2015).

Operating at 100 Hz, eight cameras (Motion Analysis Corporation, Santa Rosa, CA) recorded the three-dimensional positions of 14 retroreflective markers placed on the subjects' lower right leg and each ultrasound transducer. We synchronized binary ultrasound signals (i.e., signals indicating the start and stop of collection) from each transducer at 1000 Hz using a wave form generator (SDG1025, SIGLENT, Shenzhen). The Biodex dynamometer (Biodex, Shirly, NY) recorded ankle moment at 1000 Hz. Post collection, we estimated ankle and knee joint angles using a custom inverse kinematics routine (Silder, Heiderscheit, & Thelen, 2008). We co-registered ultrasound signals, ankle moment, and marker trajectories with GAS, SOL, and free Achilles tendon ultrasound data. Using a key-frame threshold of 5% peak ankle moment, we analyzed all co-registered data between key-frames at the beginning and end of each ramped contraction. Finally, we quantified time series of (*i*) triceps surae muscle kinematics (i.e., GAS and SOL muscle length change) and (*ii*) Achilles subtendon tissue kinematics (i.e., GAS and SOL subtendon displacements), each interpolated to 1000 data points per trial, described in detail below.

Muscle Kinematics

We controlled for tracking limitations and inter-investigator variability by following the best practices outlined by Farris and Lichtwark (2016), with the same investigator interrogating and performing all triceps surae tracking (Farris & Lichtwark, 2016). First, we defined a static region of interest surrounding each muscle and their aponeuroses (Supplementary Figure 1). In the first key-frame of each trial, we defined one GAS and one SOL muscle fascicle, drawn from their superficial to deep aponeurosis. We selected a fascicle that was in the mid-region of the imaged plane and most represented the muscle belly. An open source MATLAB routine, UltraTrack (Farris & Lichtwark, 2016), based on an affine extension to an optic flow algorithm quantified time series of GAS and SOL fascicle length and pennation angle. For direct comparison of

longitudinal tissue displacements, we multiplied muscle fascicle length by the cosine of pennation angle to compute longitudinal muscle length along the Achilles tendon line of action.

Tendon Kinematics

Using previously published techniques (Chernak Slane & Thelen, 2014), we quantified localized displacements of Achilles subtendon tissue using a custom two-dimensional speckle tracking algorithm. Briefly, we created a rectangular region of interest (~15 x 3 mm grid of nodes with 0.83 x 0.42 mm spacing, encompassing only tendinous tissue) on a B-mode image of the free Achilles tendon reconstructed from the raw radiofrequency data at the first key-frame of each trial. Centered at each nodal position, a 2 mm x 1 mm kernel containing up-sampled (4x) radiofrequency data acted as a search window for successive two-dimensional normalized cross-correlation functions. Frame-to-frame nodal displacements that maximized the two-dimensional cross-correlations were regularized using second order polynomials. These cumulative displacements represented the average of forward and backward tracking results and quantified the longitudinal displacement originating from two equally sized tendon depths - superficial and deep - corresponding to tendon tissue thought to arise from GAS and SOL, respectively. This orientation (i.e., free Achilles tendon ~ six cm proximal to the calcaneal insertion point) exemplifies the most prevalent anatomical arrangement in cadaveric studies (Anson & McVay, 1971; Gils et al., 1996; Szaro et al., 2009), with the GAS subtendon and SOL subtendon each representing 50% of the longitudinal cross section of the Achilles tendon (Doral et al., 2010). We report these average displacements as GAS and SOL subtendon tissue displacements. We report Achilles subtendon non-uniformity as the difference between peak GAS and peak SOL subtendon tissue displacements.

Statistics

For each outcome measure, we took the average of the three conditions for each ankle angle for statistical analysis in SPSS. First, a Shapiro-Wilks test assessed normal distributions for each outcome measure. Subsequently, a three-way mixed factorial analysis of variance (ANOVA) tested for main effects of and interactions between age, ankle angle, and muscle-tendon unit (i.e., MTU, GAS vs. SOL) on peak muscle shortening and peak subtendon tissue displacements using an alpha level of 0.05. Post-hoc comparisons identified the ankle angles at which the muscle-tendon units were significantly different. Specifically, we used independent samples and Mann-Whitney tests for outcome measures found normally and not normally distributed, respectively. A two-way repeated measures ANOVA tested for significant main effects of and interactions between age and ankle angle on peak ankle moment. Pearson's correlation coefficients assessed the relation between muscle and subtendon kinematics (i.e., GAS muscle and GAS subtendon, SOL muscle and SOL subtendon) in young and in older adults. We then calculated Pearson's correlation coefficients between tendon non-uniformity (i.e., difference between GAS subtendon displacement and SOL subtendon displacement) and muscle level differences (i.e., difference between GAS muscle shortening and SOL muscle shortening). Finally, we calculated Pearson's correlation coefficients between GAS and SOL peak subtendon displacement and mass normalized peak ankle moment.

RESULTS

Across conditions, subjects' knee flexion angle averaged 24.4 ± 5.1º. In young and older adults, peak ankle moment decreased progressively with increasing plantarflexion (p<0.001, Supplementary Figure 2). Compared to young adults, older adults' peak ankle moment was

significantly lower at each ankle angle (p-values≤0.024) and averaged 34% lower across all angles (Age, p<0.001). Average GAS and SOL muscle and subtendon profiles for each ankle angle are shown in Figure 5. We found significant age×MTU interactions for peak subtendon displacement and peak muscle shortening (p-values≤0.002). In young adults, peak SOL subtendon tissue displacements averaged 51% more than GAS subtendon tissue displacements (MTU, p<0.001), and peak SOL muscle shortening averaged 76% more than peak GAS muscle shortening (MTU, p=0.025, Figure 6). In older adults, peak SOL subtendon tissue displacements averaged 31% more than GAS subtendon tissue displacements (MTU, p=0.006, Figure 6). However, compared to young adults, those differences, indicative of tendon non-uniformity, averaged 63% smaller in older adults (Age, p<0.001, Figure 7). Also in older adults, peak SOL muscle shortening was indistinguishable from peak GAS muscle shortening (Age, p=0.502, Figure 6). Moreover, differences between GAS and SOL peak muscle shortening were 61% smaller in older adults (Age, p=0.002, Figure 7).

For young adults, the magnitude of peak GAS and peak SOL muscle shortening pooled across ankle angles positively correlated with peak displacements in their associated regions of the Achilles tendon (GAS: R^2=0.486; SOL: R^2=0.618; p-values<0.001, Figure 8A). In older adults, those correlations remained relatively strong and significant only for SOL (GAS: R^2=0.089, p=0.061; SOL: R^2=0.382, p<0.001). Only in young adults did tendon non-uniformity (i.e., differences between peak SOL subtendon displacement and peak GAS subtendon displacement) positively correlate with anatomically consistent differences between GAS and SOL muscle shortening (R^2=0.310, p<0.001; Figure 8B). Indeed, we found no such relation in older adults (R^2=0.008, p=0.579). Peak GAS subtendon displacement and peak SOL subtendon displacement positively correlated with peak ankle moment in young (GAS: R^2=0.357; SOL: R^2=0.364; p-

values<0.001) and in older adults (GAS: R^2=0.506; SOL: R^2=0.561; *p*-values<0.001) (Figure 9). However, older adult GAS and SOL subtendons were significantly more sensitive to changes in ankle moment (Angle×Age interactions, *p*-values<0.001). Finally, peak ankle moment positively correlated with tendon non-uniformity (Young: R^2=0.186; Older: R^2=0.341; *p*-values≤0.009) but not with differences between GAS and SOL peak muscle shortening (Young: R^2=0.036; Old: R^2=0.077; *p*-values≥0.084).

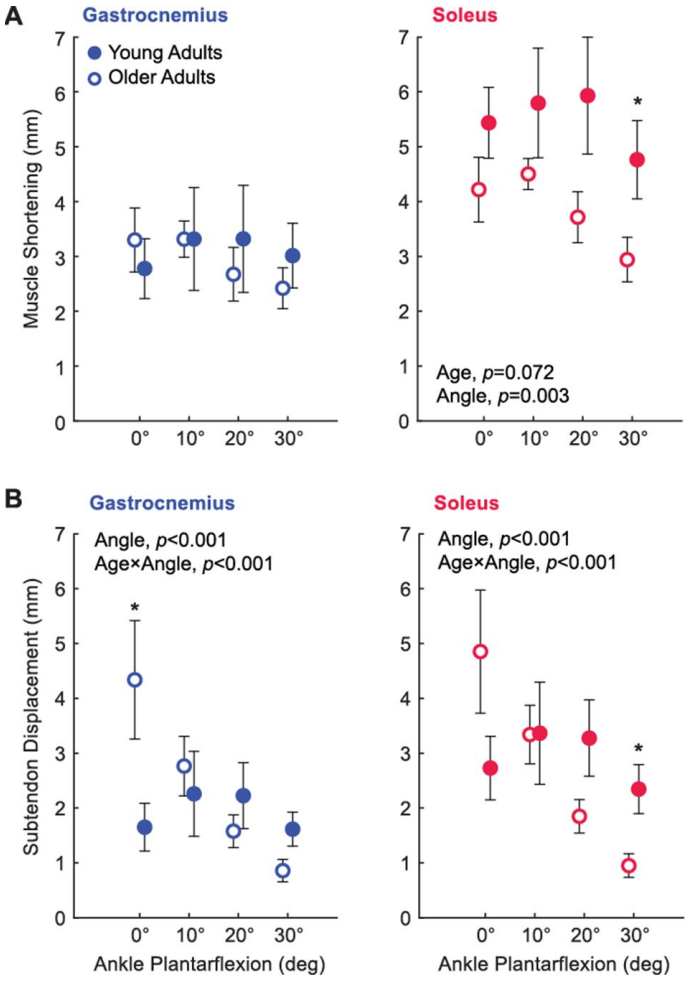

Figure 5: (A) Group mean medial gastrocnemius (GAS) and soleus (SOL) peak muscle shortening for young and older adults. (B) Group mean GAS and SOL peak subtendon displacement. Asterisks (*) represent significant differences between young and older adults (p<0.05). Bars represent standard error.

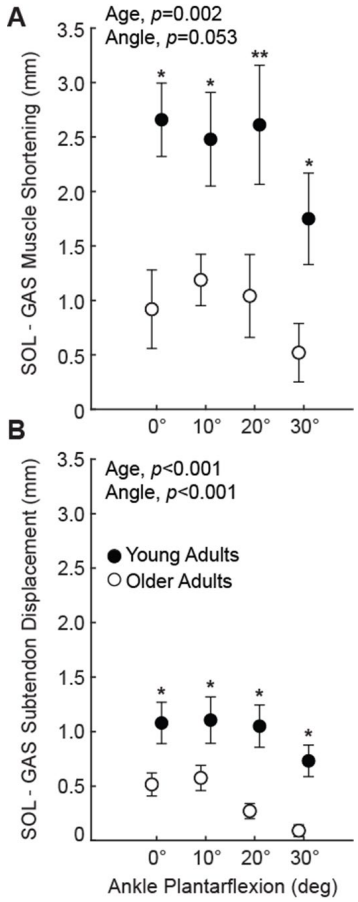

Figure 6: (A) Compared to young, differences between soleus (SOL) muscle shortening and medial gastrocnemius (GAS) muscle shortening decreased by 61% in older adults. (B) Achilles tendon non-uniformity (differences between peak SOL subtendon displacement and peak GAS subtendon displacement) decreased by 63%. Asterisks (*) represent significant differences between young and older adults (p<0.05). Double asterisk (**) indicates a Mann-Whitney comparison with p-value equal to 0.05. Bars represent standard error.

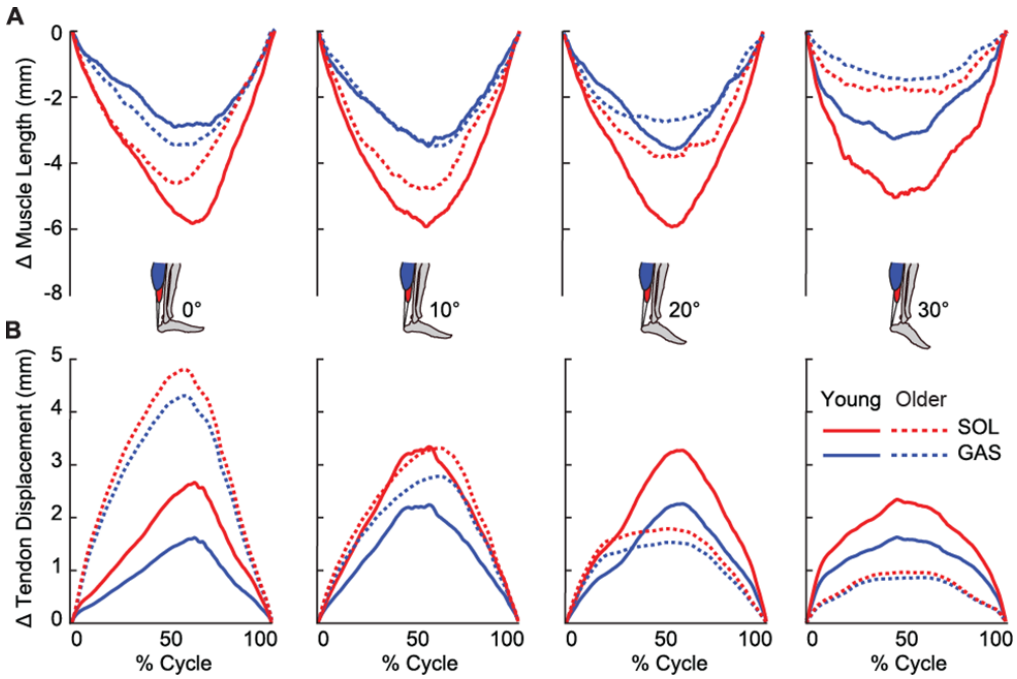

Figure 7: Group mean (A) muscle shortening and (B) subtendon displacements across the range of ankle angles tested (plantarflexion, positive). Young adult (solid line) and older adult (dashed line) medial gastrocnemius (GAS) muscle and subtendon shown in blue and soleus (SOL) muscle and subtendon shown in red.

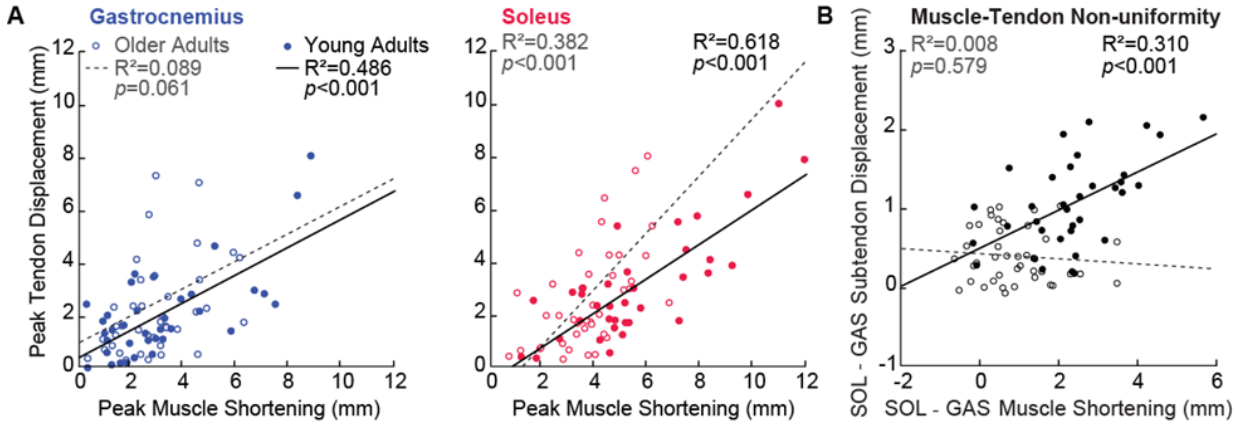

Figure 8: (A) Correlations between peak GAS or peak SOL muscle shortening and displacement in their associated Achilles subtendons. (B) Correlation between Achilles tendon non-uniformity and GAS versus SOL differences in muscle. All correlations are pooled across all conditions.

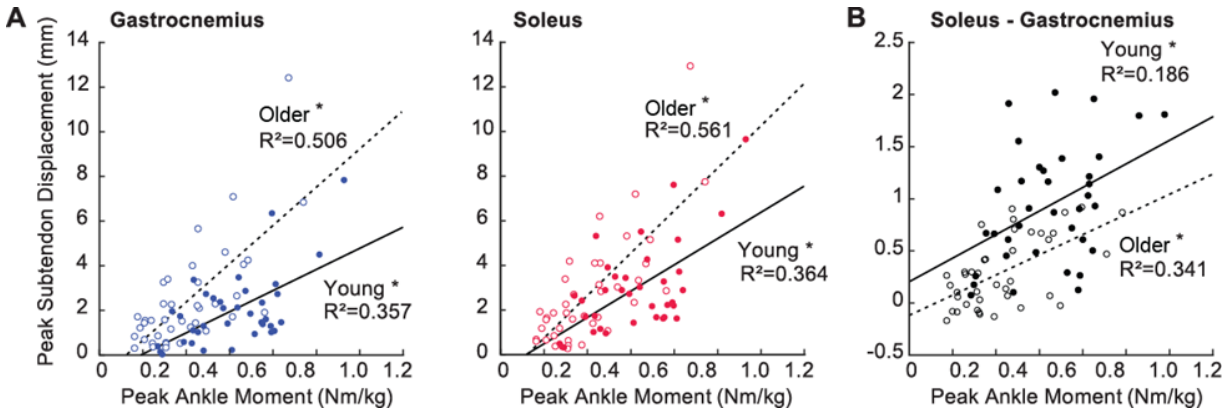

Figure 9: (A) Correlations between peak GAS subtendon displacement or peak SOL subtendon displacement and normalized peak ankle moment for young (solid line) and older (dashed line) adults. (B) Correlations between Achilles tendon non-uniformity (differences between peak SOL subtendon displacement and peak GAS subtendon displacement) and normalized peak ankle moment. Asterisks (*) represent significant differences between young and older adults (p<0.05).

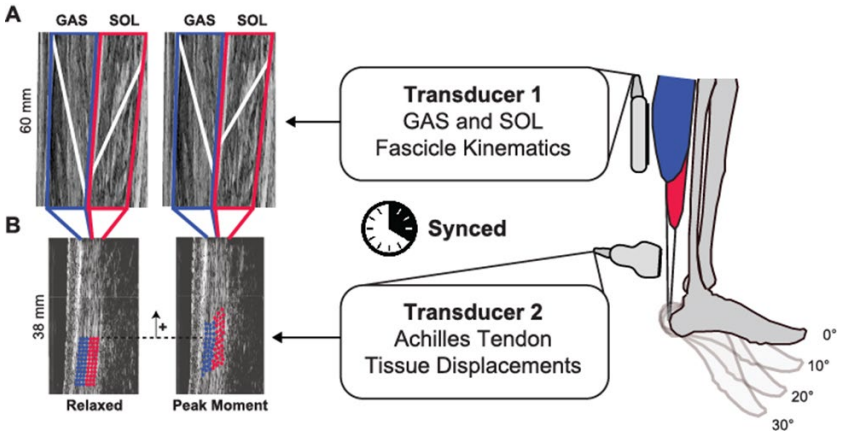

Supplementary Figure 1: We utilized a dual-probe ultrasound imaging approach to simultaneous assess medial gastrocnemius (GAS) and soleus (SOL) muscle length change and tissue displacement in their associated subtendons of the free Achilles tendon at 4 different ankle angles. (A) An open source MATLAB routine quantified time series of GAS and SOL fascicle lengths and pennation angles from cine B-mode images. (B) A custom 2-dimensional speckle tracking technique estimated GAS (blue) and SOL (red) subtendon tissue displacements.

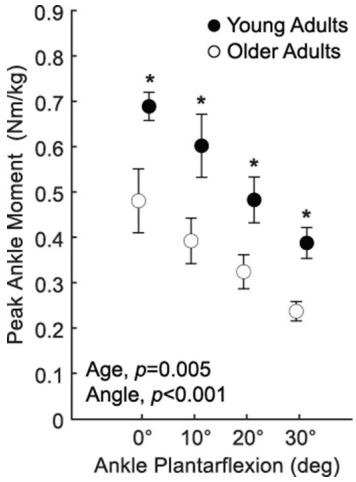

Supplementary Figure 2: Group mean peak ankle moment at each ankle angle (plantarflexion, positive) for young and older adults. Older adults are shifted to the right for clarity. Compared to young adults, older adults' peak ankle moment was significantly lower at each ankle angle (*, *p*-values<0.05) and averaged 34% lower when pooled across all conditions ($p<0.001$). Bars represent standard error.

DISCUSSION

In this study, we investigated the effect of aging on triceps surae muscle-subtendon interaction during a series of ramped maximum isometric voluntary contractions. Our data fully supported our primary hypothesis that age-related effects on Achilles subtendon tissue displacement patterns would be mirrored by anatomically consistent effects on triceps surae muscle contractile behavior. Specifically, compared to young adults, older adults had more uniform Achilles subtendon tissue displacements that extended to smaller differences between gastrocnemius and soleus muscle shortening. Likewise, our data supported our secondary hypothesis; compared to those in young adults, older adult subtendons were significantly more sensitive to changes in force transmission that followed from changes in ankle joint position. As we describe in more detail below, these results may provide a biomechanical basis for previously reported correlations between more uniform subtendon tissue displacements and reduced ankle moment generation during walking in older adults (Franz & Thelen, 2015).

Overall, our findings for peak GAS and peak SOL subtendon displacements, as well as the differences between the two, are consistent with prior studies (Arndt et al., 2012; Bojsen-Moller & Magnusson, 2015). Studies investigating the effect of aging on Achilles tendon non-uniformity have revealed more uniform free Achilles subtendon tissue displacements in animal models (Thorpe et al., 2013), middle-aged humans (Slane & Thelen, 2015), and in older humans (Franz & Thelen, 2015). Moreover, our findings for GAS and SOL fascicle length, pennation angle, and longitudinal muscle length change are generally consistent with prior literature on isolated contractions (Kawakami et al., 1998; Maganaris et al., 1998). Age-associated differences in triceps surae muscle contractile behavior have been extensively studied and have revealed lower triceps

surae muscle volume (Macaluso et al., 2002), force-generating capacity (Narici, Maganaris, Reeves, & Capodaglio, 2003), and specific tension (i.e., maximum voluntary force divided by cross-sectional area) with increasing age (Kent-Braun & Ng, 1999). Consistent with these findings, our older adult subjects exerted, on average, 34% smaller peak ankle moments than young adults. However, we found no significant difference in peak GAS or peak SOL muscle shortening between young and older adults, consistent with some (Karamanidis & Arampatzis, 2006) but not all (Narici et al., 2003) studies. Indeed, some studies have reported an association between reduced muscle mass and smaller muscle length change during isolated triceps surae contractions in older adults (Morse, Thom, Birch, & Narici, 2005; Narici et al., 2003). Those studies also report an age-related decrease in pennation angle (Morse et al., 2005; Narici et al., 2003), which we neither observed at rest (p's$\geq$0.080) nor at peak ankle moment (p's$\geq$0.205).

Compared to those in young adults, more uniform Achilles subtendon tissue displacements in older adults may reflect a proliferation of collagen cross-linking and interfascicle adhesions. Indeed, using equine models of the Achilles tendon, Thorpe et al. (2013) revealed an age-related reduction in interfascicular sliding (Thorpe et al., 2013). They also suggest older tendon fascicles experience age-related alterations in viscoelastic and quasi-static properties (e.g., stress relaxation, stiffness, structural alignment). One plausible explanation for reduced interfascicular sliding in older tendon is variation in its underlying structure at the cellular level compared to younger tendon. The interfascicular matrix of the Achilles tendon contains a mixture of particular proteoglycans and glycoproteins that facilitate sliding and, compared to the collagen fibers themselves, is uniquely altered by aging (Thorpe, Riley, Birch, Clegg, & Screen, 2017). However, we focus on non-uniform behavior at the subtendon level, and it is unclear how sliding at each

hierarchical level of the Achilles tendon (e.g., subtendon, fascicle, fiber) manifests its influence on gross triceps surae muscle-subtendon interaction.

Age-related changes in the gross mechanical behavior of the Achilles tendon, and more specifically in sliding between adjacent subtendons, allude to the potential for functional consequences on triceps surae muscle contractile behavior in older adults. We previously posited that one such functional consequence could be coupling between individual muscles of the triceps surae, thereby compromising their ability to operate as independent actuators. Indeed, our findings may provide a biomechanical basis for the previously reported correlation between age-related decreases in Achilles subtendon non-uniformity and reduced peak ankle moment during walking (Franz & Thelen, 2015). Specifically, our findings are the first to suggest that a reduction in sliding between adjacent subtendons in the Achilles are accompanied by smaller differences in muscle shortening between GAS and SOL in older adults. It is unclear from our measurements if there are disparate functional effects between the individual triceps surae muscles. Here, aging disproportionately affected peak shortening of SOL across the range of motion tested, thereby contributing to its contractile behavior more resembling that of GAS in older than in young adults. Similarly, it is possible that coupling between the GAS and SOL subtendons, and thus interactions between the individual triceps surae muscles, explains the absence of a significant positive correlation in older adults between peak GAS muscle shortening and peak GAS subtendon displacement. However, the isolated contractions tested here may not be representative of the effects that would emerge during functional activity; incorporating age-associated subtendon adhesions in musculoskeletal simulations of walking revealed declines in muscle-tendon unit force output for GAS but not SOL (Franz & Thelen, 2016). Nevertheless, smaller differences between GAS and SOL length change in older adults could negatively affect those muscle's ability to

independently contribute to forward propulsion and trunk support – distinct biomechanical tasks attributed to these muscles during walking (McGowan et al., 2008).

Thus far, our position has been that age-related changes in Achilles subtendon tissue displacements negatively affect triceps surae muscle contractile behavior in older adults (i.e., 'tendon-up' theory). However, we cannot exclude the alternative hypothesis; aging may independently affect triceps surae muscle contractile behavior and thereby yield more uniform Achilles subtendon displacements (i.e., 'muscle-down' theory). Aging is widely known to deleteriously affect muscle contractile behavior through changes in myofilament protein biology, muscle coordination, and loss of viable motor units (Miller et al., 2014). Reduced triceps surae muscle force generation in aging, even if homogenous across the triceps surae muscles, could itself diminish non-uniform Achilles subtendon tissue displacements. Indeed, peak ankle moment in this study positively correlated with tendon non-uniformity across our study cohort. Our mechanistic understanding of these causal relations may be further compounded by increased Achilles tendon tissue compliance due to aging (Narici, Maffulli, & Maganaris, 2008). Consistent with most human studies, our data revealed that older subtendons were significantly more sensitive to changes in tendon force than those in young adults. Similarly, peak GAS and peak SOL subtendon displacements were unaffected by age, despite lower ankle moments in older than young adults. We are currently trying to distinguish between these 'tendon-up' and 'muscle-down' theories through a combination of musculoskeletal modeling, dual-probe ultrasound imaging during walking, and electrical stimulation.

We previously outlined the limitations of the experimental techniques applied in this study (Clark & Franz, 2018b), but briefly: first, we interpreted our data using a generalized anatomical approximation of the muscles of the triceps surae and their associated subtendons (Edama et al.,

2015; Gils et al., 1996; Szaro et al., 2009). Two-dimensional ultrasound imaging may not fully capture the complex architecture of three-dimensional structures (Chow et al., 2000). Likewise, between-subject variability in anthropometrics may influence the precision of ultrasound probe placement. However, we note that there was no significant difference in subject height (p=0.312) nor leg length (p=0.192) between young and older adults. Second, UltraTrack uses semi-automated fascicle tracking that has inherent limitations in reliability and determination (Farris & Lichtwark, 2016). Third, two-dimensional speckle tracking of the Achilles tendon is subject to out of plane motion (Franz et al., 2015). Fourth, we did not attempt to estimate Achilles tendon force transmission (Bojsen-Moller & Magnusson, 2015). Finally, we report negligible but present ankle rotation that likely influences subtendon tissue displacements (Handsfield et al., 2017). Here, we add limitations associated with uncovering aging effects. As previously noted, we cannot definitively attribute our observations to aging effects on sliding between adjacent subtendon versus those on muscle contractile behavior. Moreover, we only included self-reported healthy young and older adults, however, physical activity status most likely impacts the mechanical properties of the triceps surae muscle tendon unit (Joseph et al., 2014).

CONCLUSION

In summary, we reveal that more uniform Achilles subtendon tissue displacements in older versus young adults extend to anatomically consistent and potentially unfavorable changes in muscle contractile behavior – evidenced by smaller differences between GAS and SOL peak shortening during isometric force generation. Foremost, these findings provide an important biomechanical basis for previously reported correlations between more uniform Achilles subtendon behavior and reduced ankle moment generation during waking in older adults.

Additional mechanistic insight into the causal relations underlying these changes are required before advocating for any specific clinical countermeasure. For example, conventional therapies prompting changes from the muscle down may be designed to promote independent actuation of individual triceps surae muscles. Alternatively, to promote changes from the tendon up, there is some support for the use of hyaluronic acid and/or lubricin injection to maintain and restore tendon homeostasis during the aging process (Kaux, Samson, & Crielaard, 2015).

CHAPTER 4: IMAGING AND SIMULATION OF INTER-MUSCULAR DIFFERENCES IN TRICEPS SURAE CONTRIBUTIONS TO FORWARD PROPULSION DURING WALKING[3]

INTRODUCTION

Forward propulsion during the push-off phase of walking is largely governed by differential neuromechanical contributions from the biarticular medial (MG) and lateral gastrocnemius (LG) and the uniarticular soleus (SOL) spanning the ankle (Gottschall & Kram, 2003). Indeed, although they share a common Achilles tendon, some evidence suggests these muscles can act as relatively independent actuators while producing a net plantarflexion moment during late stance (Clark & Franz, 2018a; Handsfield et al., 2017; Szaro et al., 2009). However, the relative contribution of these individual muscles to forward propulsion remains equivocal. Characterizing these contributions has far reaching implications for the design and control of wearable assistive devices and for targeted therapeutics that attempt to overcome deficits in forward propulsion - for example, those due to age or gait pathology.

Historically, contributions from MG, LG, and SOL to forward propulsion in walking have been estimated by combining *in vivo* measurements (e.g., electromyography [EMG] and ultrasound imaging) with experimental manipulations. For example, one may consider changing

[3] This chapter previously appeared as an article in the *Annals of Biomedical Engineering*. The original citation is as follows: Clark WH, Pimentel RE, and Franz JR. (2020). Imaging and Simulation of Inter-Muscular Differences in Triceps Surae Contributions to Forward Propulsion During Walking. *Annals of Biomedical Engineering* (2020). doi:10.1007/s10439-020-02594-x

the mechanical demand for forward propulsion by altering walking speed alone. However, walking speed affects both forward propulsion and vertical support, confounding conclusions made regarding inter-muscular differences (Francis et al., 2013; Lai et al., 2015). Many studies have overcome this challenge by more directly manipulating the mechanical demand for forward propulsion at a fixed walking speed. Building off a paradigm introduced by Chang & Kram (Chang & Kram, 1999), Gottschall & Kram (2003) measured MG versus SOL differences in muscle activation in subjects responding to horizontal aiding and impeding forces applied to the body's center of mass (Gottschall & Kram, 2003). Their findings revealed that MG activation exhibited larger changes than the SOL in response to those targeted changes in the demand for forward propulsion. Similarly, Miyoshi et al. (2006) recorded triceps surae activation in a reduced gravity environment and suggested that MG activation was more dependent on speed-related changes to forward propulsion, while SOL activation was more dependent on changes to vertical support (Miyoshi et al., 2006). In a third experimental manipulation, Francis et al. (2013) prescribed muscle activation during the stance phase at a fixed walking speed using electrical surface stimulation of the MG and SOL (Francis et al., 2013). Consistent with the prevailing empirical data, their results showed that MG stimulation elicited larger anterior shifts in stance phase center of pressure than that elicited by SOL stimulation. However, not all experimental studies yield a consistent interpretation; McGowen et al. (2008) manipulated trunk load and weight support and determined from EMG measurements that the SOL was the primary contributor to forward propulsion (McGowan et al., 2008).

EMG provides important information regarding the timing and magnitude of triceps surae muscle activity. However, EMG alone can yield inconsistent or incorrect interpretations of underlying muscle force and work – themselves highly dependent on muscle fascicle length and

length change (Disselhorst-Klug, Schmitz-Rode, & Rau, 2009; Roberts & Gabaldon, 2008). Advances in ultrasound imaging have catalyzed efforts to quantify triceps surae contractile behavior during functional activities such as walking, including the characterization of inter-muscular differences in fascicle length change. Despite considerable improvements in image collection and processing, there is wide variation regarding triceps surae contractile behavior in terms of absolute length change and type of contraction (i.e., shortening, isometric, lengthening) at different phases of the gait cycle (Cronin et al., 2013; Leitner et al., 2019). Moreover, studies that have compared MG, LG, and/or SOL fascicle behavior during walking use methodological paradigms that manipulate speed (Cronin & Finni, 2013; Farris & Sawicki, 2012b; Lai et al., 2015), walking duration (Cronin et al., 2013; Cronin, Peltonen, Sinkjaer, & Avela, 2011), or slope (Hoffman, Cresswell, Carroll, & Lichtwark, 2014; Lichtwark & Wilson, 2006). Although these studies are appropriately designed to answer their respective research questions, none have directly manipulated the mechanical demand for forward propulsion in isolation. Moreover, similar to those drawn from patterns of muscle activation, conclusions about inter-muscular differences in function drawn from estimates of muscle fascicle length change are incomplete (Dick, Biewener, & Wakeling, 2017; Gottschall & Kram, 2003).

Thus, to reconcile the prevailing literature on this scientifically and translationally important question, a combined empirical and computational simulation framework is warranted. Advances in musculoskeletal modeling provide the opportunity to complement patterns of muscle activation and fascicle length changes with estimated differences between MG, LG, and SOL force and positive mechanical work *in silico*. Of course, although empirically driven, biological complexity of musculoskeletal modeling is often exchanged for computational performance, potentially yielding reduced specificity to fully characterize inter-muscular differences (Hicks,

Uchida, Seth, Rajagopal, & Delp, 2015). Despite these limitations, several studies have directly or indirectly compared the biomechanical function of the MG, LG, and SOL during walking. Some modeling studies suggest that the SOL is the primary contributor to forward propulsion. Neptune et al. (2001) used a musculoskeletal modeling and optimization framework and concluded that the SOL accelerates the trunk, whereas the MG and LG initiate leg swing (Neptune, Kautz, & Zajac, 2001). Those authors later added (2008) that the SOL contributes more than the MG and LG to forward propulsion in order to meet the demands of increased walking speeds (Neptune et al., 2008). In a different modeling study, Lenhart et al. (2014) concluded that SOL activity induced greater anterior pelvic tilt and ankle plantarflexion than that of the MG during the push-off phase of walking (Lenhart et al., 2014). Nonetheless, other modeling studies have concluded that the gastrocnemius muscles are more responsible for forward propulsion. For example, using an induced acceleration analysis, Liu et al. (2006) suggested that the MG induced greater forward center of mass acceleration, while the SOL induced greater vertical acceleration (M. Q. Liu, Anderson, Pandy, & Delp, 2006).

Electromyography, ultrasound imaging, and musculoskeletal modeling, when used alone, provide a valuable but incomplete representation of the relative contributions of the MG, LG, and SOL to forward propulsion during walking. Moreover, no study to date has combined these measurements while systematically manipulating both walking speed and the mechanical demand for forward propulsion at a fixed speed – namely, through the use of horizontal aiding and impeding forces. The aim of this study was to quantify inter-muscular differences in the response of the gastrocnemius and soleus muscles to changes in forward propulsion by assessing muscle activation, contractile behavior, and model-predicted estimates of force and positive mechanical work. We tested the null hypothesis that conclusions based on muscle-specific responses derived

from empirical measurements would be consistent with those derived from musculoskeletal simulations over a range of tasks that alter the demand for forward propulsion.

METHODS

Subjects and Protocol

An *a priori* power analysis revealed that we would need n=6 and n=5 subjects to detect ($p<0.05$) speed effects (Nilsson & Thorstensson, 1989) and horizontal force effects (Gottschall & Kram, 2003), respectively, on peak anterior force – a limb-level measure of forward propulsion we use in this study to establish task efficacy. We increase our sample size to n=10 to better approximate that used in those aforementioned studies. We recruited healthy young adults between the ages of 18 and 35. We excluded subjects based on the following criteria: lower extremity injury in the last 6 months, medication that causes dizziness, having a leg prosthesis, or needing an assistive walking device. Ten young adults (age: 24.1±3.6 years, height: 1.77±0.08 m, mass: 76.7 ± 10.0 kg, 6M/4F) participated. All subjects provided written informed consent in compliance with the UNC Biomedical Sciences Institutional Review Board.

Figure 10 summarizes our experimental protocol, measurements, and *in vivo* and *in silico* analyses. Based on a previous study in our lab, young adults have an average overground preferred walking speed of 1.3 m/s (Conway, Bissette, & Franz, 2018). Malatesta et al. (2017) revealed that the overground preferred walking speed in younger adults averages 0.12 m/s faster than the treadmill preferred walking speed (Malatesta, Canepa, & Menendez Fernandez, 2017). As such, we chose 1.2 m/s to represent our "normal" treadmill walking speed. Prior to data collection, subjects walked on an instrumented treadmill (Bertec Corp., Columbus, Ohio, USA) for 6 minutes at 1.2 m/s to precondition their triceps surae muscle-tendon units and to acclimate to treadmill

walking (Hawkins et al., 2009). Subjects then walked for 1 min each at a range of speeds (0.8, 1.2, and 1.6 m/s) and again at 1.2 m/s with: (*i*) a 5% body weight (BW) horizontal aiding force (designed to decrease the mechanical demand for forward propulsion) and (*ii*) a 5% BW horizontal impeding force (designed to increase the mechanical demand for forward propulsion). We applied horizontal aiding and impeding forces using a custom, feedback-controlled, motor-driven horizontal force system described in detail previously (Figure 10**)** (Conway et al., 2018; Conway & Franz, 2019, 2020). Briefly, in real-time, a LabVIEW interface (cRIO-9064, National Instruments, Austin, TX, USA) controlled a servo motor (Kollmorgen, Radford, VA, USA) in series with a horizontal cable affixed to a waist belt worn by the subject. During trials with horizontal forces, subjects received verbal encouragement to maintain upright posture (i.e., to avoid excess trunk lean and lumbar bending). All data was collected as part of a larger study that incorporated a second ultrasound probe, secured distal to the right soleus muscle-tendon junction. We removed the second probe at speeds greater than 1.2 m/s to ensure subject comfort and range of motion. As such, trials were block randomized. The first block contained 5 walking conditions (speed ≤ 1.2 m/s), 4 reported in this study (0.8 m/s, 1.2 m/s, 5% BW aiding force at 1.2 m/s, and 5% BW impeding force at 1.2 m/s). The second block contained 4 walking conditions (speed ≥ 1.2 m/s), 1 reported in this study (1.6 m/s). All trials were 1 min long and were separated by 2 min of rest.

Experimental Measurements and Analysis

For all trials, we collected ground reaction forces from the instrumented treadmill at 1000 Hz. Simultaneously, twelve cameras (Motion Analysis Corporation, Santa Rosa, CA, USA) operating at 100 Hz recorded the three-dimensional positions of 34 retroreflective markers. Specifically, we attached anatomical markers to subject's sacrum and bilateral anterior and

posterior superior iliac spines, lateral femoral condyles, lateral malleoli, 1st and 5th metatarsal heads, and calcanei. We also secured right and left leg thigh and shank clusters to improve segment tracking. We filtered ground reaction force and marker data using a 4th order low-pass Butterworth filter with cutoff frequencies of 100 Hz and 6 Hz, respectively (Winter, 1990). For electromyographic (EMG) measurements, prior to sensor placement, we prepped the skin by shaving and using an alcohol wipe. We then placed differential wireless recording electrodes (Trigno, Delsys Inc., Natick, MA, USA) with 10 mm inter-electrode distance over the right leg soleus (SOL) and lateral gastrocnemius (LG) using published recommendations (Hermens, Freriks, Disselhorst-Klug, & Rau, 2000). Specifically, we placed the SOL recording electrode approximately two-thirds distal to the lateral femoral condyles along a line projecting to the lateral malleolus. We placed the LG recording electrode approximately one-third distal to the head of the fibula along a line projecting to the calcaneus. Post collection, we demeaned, full-wave rectified, bandpass filtered (4th order Butterworth, 20-450 Hz), and normalized each EMG signal to its mean value during the 1.2 m/s condition (Figure 10B**)**. We then averaged GRF and EMG measurements over 10 strides, with the first stride corresponding to the first heel strike captured by ultrasound data, detailed below.

For individual muscle fascicle measurements, a 60 mm ultrasound transducer (LV7.5/60/128Z-2, UAB Telemed, Vilnius, Lithuania) recorded cine B-mode images through the right medial gastrocnemius (MG) and SOL at 76 frames per second using an image depth of 50 mm (Figure 10C). A 1000 Hz binary analog synchronization signal indicated the start and stop of each ultrasound video using a wave form generator (SDG1025, SIGLENT, Shenzhen). We co-registered ultrasound signals with ground reaction forces and determined the frames corresponding to each heel strike for strides coincident with the B-mode collection. The same investigator

processed all ultrasound data to minimize inter-investigator variability. Ultrasound data was collected after the subject reached their prescribed walking speed and their movement pattern had stabilized. At the first co-registered heel strike, we defined a static region of interest surrounding the MG and SOL muscle bellies and aponeuroses. We then defined one MG and one SOL muscle fascicle for each muscle. An affine extension to an optic flow algorithm (UltraTrack) quantified time series of MG and SOL fascicle lengths from 2 strides per condition (Farris & Lichtwark, 2016). We visually confirmed tracking results and manually corrected fascicle endpoints when necessary. Fascicle length change measurements were normalized by their length at heel strike. We filtered the manually corrected tracking results using a 4^{th} order low-pass Butterworth filter with a cutoff frequency of 6 Hz and then averaged the results over 2 strides.

Musculoskeletal Modeling and Simulation

For each subject, we scaled a three-dimensional, 23-degree-of-freedom musculoskeletal model with 92 Hill-type musculotendon units (Gait 2392, OpenSim 4.0) (Delp et al., 2007) to a standing calibration trial (Figure 10D**)**. For all subsequent processing, and consistent with published approaches, (Rajagopal et al., 2016) we locked the subtalar and metatarsophalangeal joints and assessed model-predicted outcomes from the first stride analyzed for ultrasound and EMG outcomes. For those, we also locked the lumbar joints to overcome our lack of trunk kinematic data. As recommended by Arnold et al. (2013), we set tendon strain at maximum isometric force (i.e., "FmaxTendonStrain") for each muscle to 4%, except the MG, LG, and SOL, which we set to 10% to account for Achilles tendon compliance (Arnold, Hamner, Seth, Millard, & Delp, 2013; Farris & Sawicki, 2012a). Likewise, we increased the maximum isometric force of all muscles to 2.0 times default (Arnold et al., 2013). The Inverse Kinematics (IK) Tool determined generalized joint angles for each time step (marker root mean square [RMS] < 1.0 cm) (Delp et

al., 2007; Hicks et al., 2015). Driven by IK results and measured ground reaction forces, the Residual Reduction Algorithm (RRA) Tool updated segment masses, marker trajectories, and center of mass (CoM) location to minimize required compensatory forces. We continued reducing residuals (average uses of RRA per trial: 2.08±0.27) until recommended thresholds were satisfied in all cases (total mass adjustment < 0.5 kg, ΔCoM < 2.0 cm, RMS residual force < 5 N, RMS Residual Moment < 30 Nm) (Delp et al., 2007; Hicks et al., 2015). Using RRA-adjusted kinematics and segmental mass properties, the Static Optimization Tool resolved net joint moments into individual muscle forces by minimizing the sum of cubed muscle activations (Monaco, Coscia, & Micera, 2011; Zargham, Afschrift, De Schutter, Jonkers, & De Groote, 2019). Finally, the Analysis Tool estimated MG, LG, and SOL positive mechanical work (i.e., positive area under the respective force-velocity curves) and, to provide context for muscle fascicle length measurements, muscle-tendon unit (MTU) lengths. Similar to fascicle length measurements, MTU length change results were normalized by their length at heel strike.

Statistical Analysis

For each muscle, we defined the "push-off" phase of the gait cycle from midstance to the offset of respective model-predicted muscle force generation (threshold = 10% peak force) (Gottschall & Kram, 2003). For experimental outcomes, two repeated-measures ANOVAs tested for significant main effects of speed (0.8, 1.2, 1.6 m/s) or horizontal forces (5% BW aiding force, 1.2 m/s, 5% BW impeding force) on MG and SOL average fascicle length and peak fascicle shortening and, during the push-off phase of walking, average LG and SOL activation. Similarly, for model-predicted outcomes, two repeated-measures ANOVAs tested for significant main effects of speed and horizontal forces on peak MG, LG and SOL MTU shortening and, during the push-off phase of walking, average muscle force and positive mechanical work. Mauchly's test of

sphericity evaluated the homogeneity of variance; when the assumption was violated, Greenhouse-Geisser adjustments were applied. When significant main effects were identified, post-hoc Tukey's t-tests identified significant differences versus "normal" walking (i.e., 1.2 m/s). All statistical tests used an alpha level of 0.05. Effect sizes are reported as η_p^2 and Cohen's d for main effects and pairwise comparisons, respectively.

RESULTS

Experimental Outcomes

Throughout our results narrative, we report pairwise comparisons that support the presence of inter-muscular differences in response to task demand. Where indicated, main effects were driven by increases in said outcome with faster walking speeds, with pairwise comparisons disclosed in their respective figures. Our experimental manipulations successfully altered the mechanical demand for forward propulsion; peak anterior ground reaction force systematically changed in response to changes in speed (main effect, $p<0.001$, $\eta_p^2=0.902$) and applied horizontal forces (main effect, $p<0.001$, $\eta_p^2=0.824$). LG and SOL muscle activations during push-off were significantly affected by speed (main effect, p-values<0.001, $\eta_p^2\geq0.732$, Figure 11A) and horizontal forces (main effect, p-values<0.001, $\eta_p^2\geq0.772$, Figure 11B). However, pairwise comparisons revealed that only LG activation was affected by both aiding (decreased) and impeding (increased) forces (p-values≤0.001, $d\geq1.171$). Similarly, MG and SOL peak fascicle shortening and average lengths were significantly affected by speed (main effect, p-values≤0.003, $\eta_p^2\geq0.473$, Figure 12A) and horizontal forces (main effect, p-values≤0.004, $\eta_p^2\geq0.461$, Figure 12B). However, compared to walking normally, increased push-off demand (i.e., walking with impeding

forces) elicited greater peak shortening in MG (p=0.006, d=0.874) but not SOL (p=0.15, d=0.714). Moreover, this effect on MG was not explained by changes in joint posture. Indeed, only SOL peak MTU shortening was significantly affected by horizontal forces (main effect, p-values=0.004, η_p^2=0.458); MG peak MTU shortening was unaffected (main effect, p-values=0.637, η_p^2=0.049). Compared to walking normally, both aiding and impeding forces resulted in significant differences in average fascicle length for MG (p-values≤0.021, d≥0.362, Figure 13B) but not SOL (p-values≥0.078, d≤0.33). Neither MG nor SOL average MTU length was affected by horizontal forces (main effect, p-values≥0.139, η_p^2≤0.197).

Musculoskeletal Modeling Outcomes

Model-predicted MG, LG, and SOL muscle forces averaged during push-off were similarly affected by walking speed (main effect, p-values≤0.042, η_p^2≥0.297, Figure 14A). Conversely, only average MG and LG muscle forces were significantly affected by horizontal forces (main effect, p-values<0.001, η_p^2≥0.575, Figure 14B). Specifically, compared to walking normally, average MG and LG muscles forces decreased in response to aiding forces (p-values≤0.005, d≥1.085). Changes in walking speed did not affect model-predicted MG, LG, and SOL positive mechanical work (main effect, p-values≥0.331, η_p^2≤0.116, Figure 15A). However, only MG and LG positive mechanical work were significantly affected by horizontal forces (main effect, p-values<0.001, η_p^2≥0.662, Figure 15B); SOL positive mechanical work was unaffected (main effect, p=0.236, η_p^2=0.148). Specifically, compared to walking normally, MG and LG positive mechanical work decreased in response to aiding forces (p-values≤0.045, d≥0.357) and increased in response to impeding forces (p-values≤0.014, d≥0.287). Finally, model-predicted estimates of MG, LG, and SOL activation averaged during push-off were significantly affected by changes in speed (main

effect, p-values≤0.001, η_p^2≥0.828, Figure 16A) and horizontal forces (main effect, p-values≤0.008, η_p^2≥0.413 Figure 16B). However, compared to walking normally, only MG and LG activation significantly decreased in response to aiding forces (p-values≤0.001, d≥1.156).

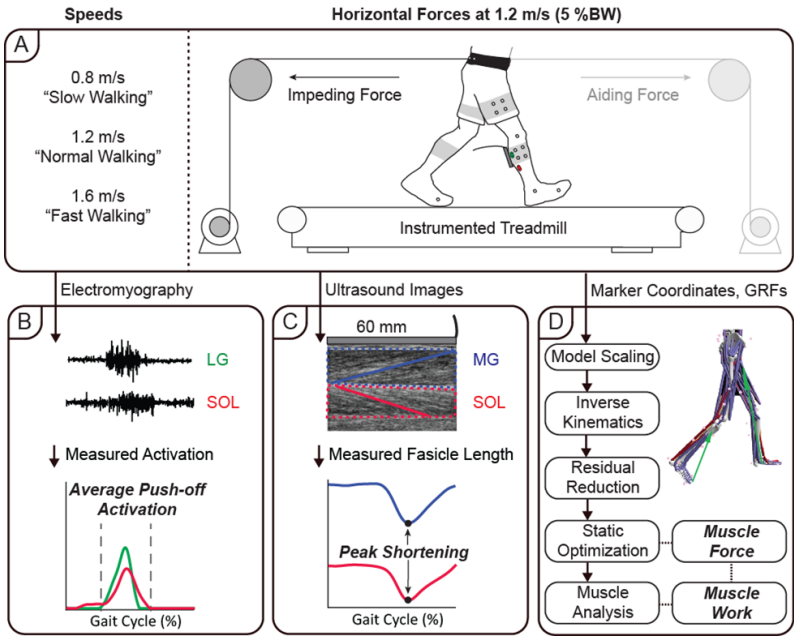

Figure 10: Summary of our experimental protocol, measurements, and *in vivo* and *in silico* analyses. A) Subjects walked for 1 minute on an instrumented treadmill at a range of speeds (0.8, 1.2, and 1.6 m/s) and again at 1.2 m/s with a 5% body weight (BW) horizontal aiding force and a 5% BW horizontal impeding force. B) We recorded EMG activity of the lateral gastrocnemius (LG) and soleus (SOL) and determined the average activation during the push-off phase of walking. C) We collected ultrasound data of the medial gastrocnemius (MG) and SOL and quantified time series of fascicle lengths from 2 strides per condition. D) Subject-specific, scaled musculoskeletal models, driven by marker coordinates and ground reaction forces (GRFs), estimated MG, LG and SOL excitation, force, and positive mechanical work using static optimization.

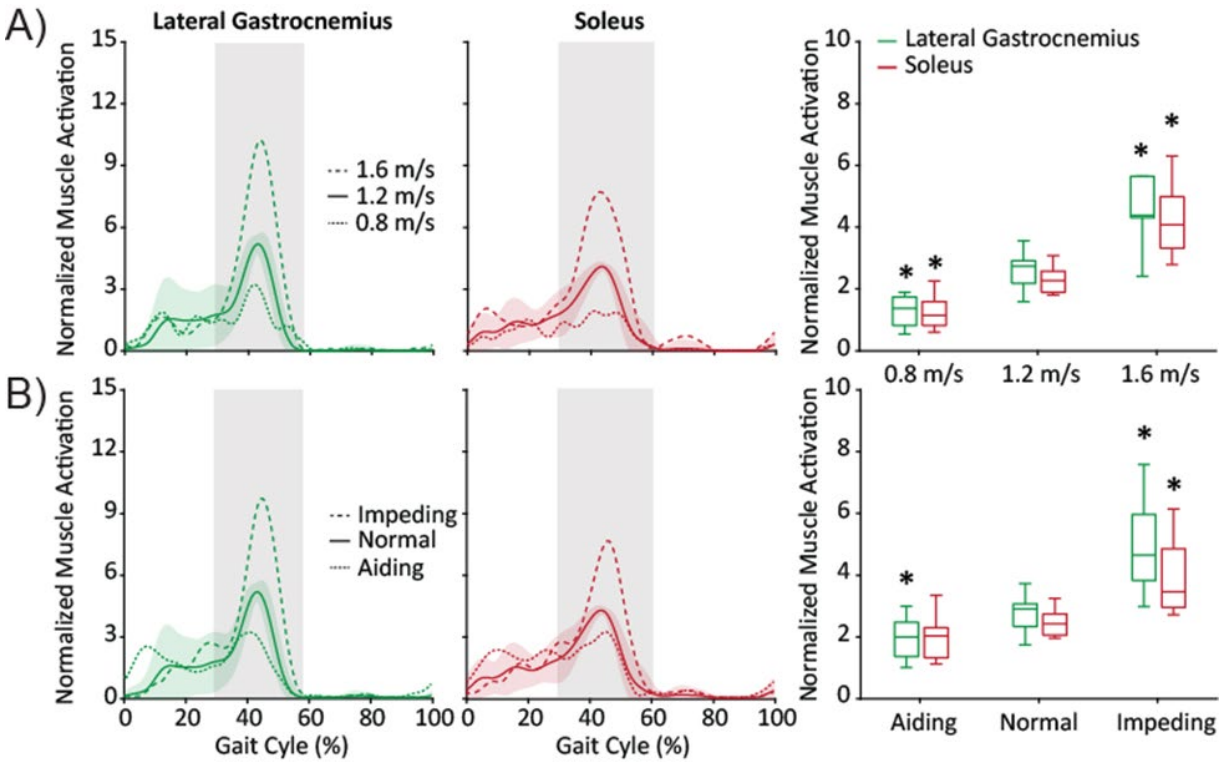

Figure 11: A) Lateral gastrocnemius (LG-green) and soleus (SOL-red) average muscle activation during push-off were similarly affected by changes in speed. B) In response to horizontal forces only LG activation was affected by both aiding and impeding forces. Shaded rectangular area represents the push-off phase of walking. Shaded (LG-green, SOL-red) represents standard error during normal walking (1.2 m/s). Boxplots show average muscle activation during push-off. Pairwise comparison vs. normal walking (1.2 m/s) represented by asterisks.

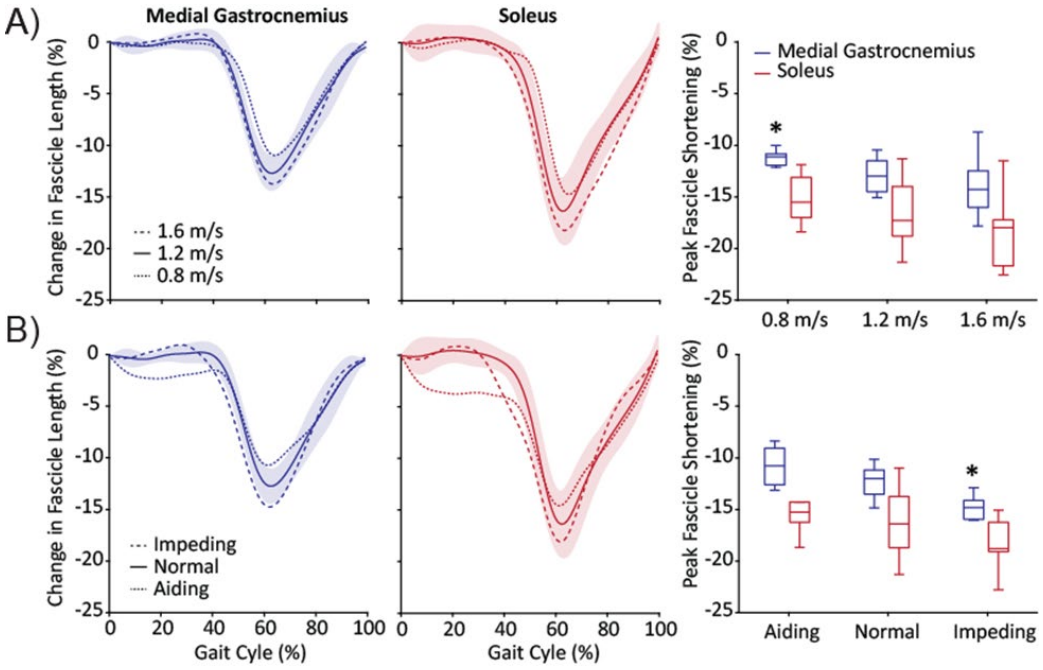

Figure 12: Time series of medial gastrocnemius (MG-blue) and soleus (SOL-red) fascicle shortening during changes in speed (A) and horizontal forces (B). Fascicle length change measurements were normalized by their length at heel strike. Shaded area represents standard error during normal walking (1.2 m/s). Boxplots show peak fascicle shortening. Significant ($p<0.05$) pairwise comparisons vs. normal walking (1.2 m/s) represented by asterisks.

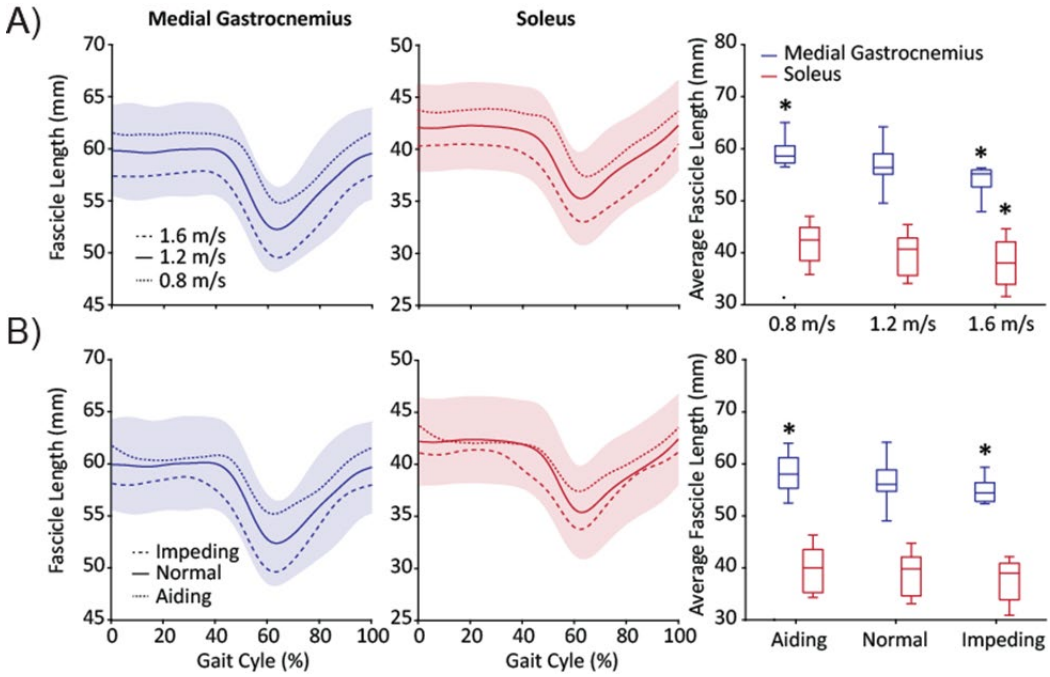

Figure 13: Time series of medial gastrocnemius (MG-blue) and soleus (SOL-red) fascicle length during changes in speed (A) and horizontal forces (B). Shaded area represents standard error during normal walking (1.2 m/s). Boxplots show average fascicle length over the entire gait cycle. Significant ($p<0.05$) pairwise comparisons vs. normal walking (1.2 m/s) represented by asterisks.

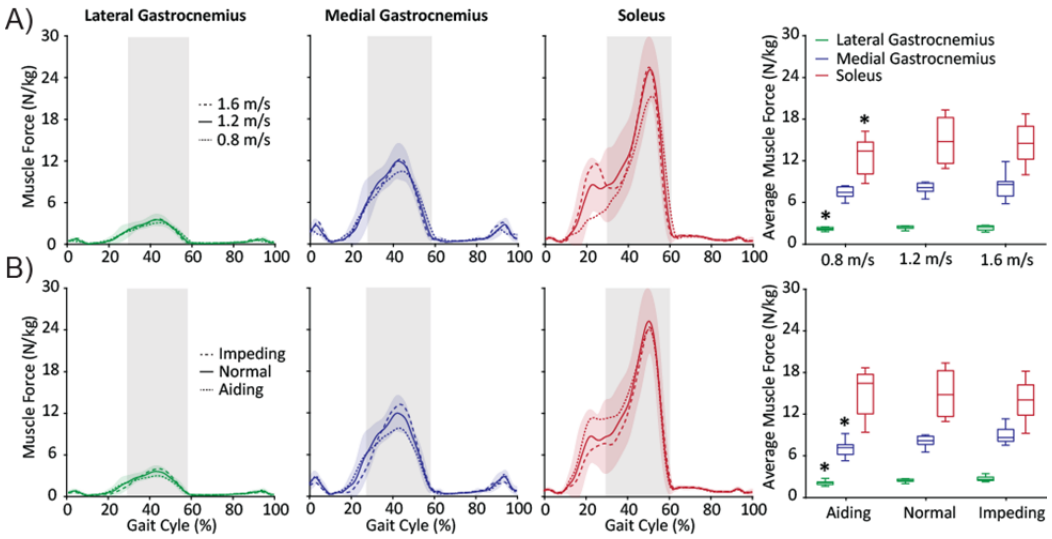

Figure 14: A) Model-predicted LG (green), MG (blue), and SOL (red) muscle forces averaged during push-off were similarly affected by walking speed. B) Conversely, only average LG and MG muscle forces were significantly affected by horizontal forces. Shaded grey rectangular area represents the push-off phase of walking. Shaded (LG-green, MG-blue, SOL-red) represents standard error during normal walking (1.2 m/s). Boxplots show average muscle force during push-off. Significant ($p<0.05$) pairwise comparisons vs. normal walking (1.2 m/s) represented by asterisks.

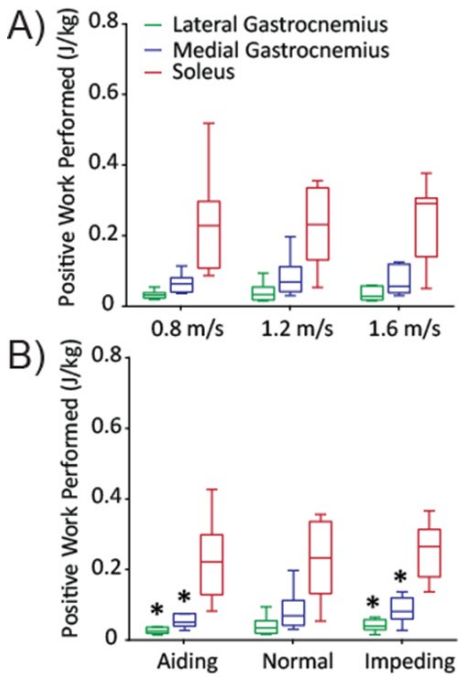

Figure 15: A) Model-predicted LG (green), MG (blue), and SOL (red) positive work during push-off were unaffected by changes in walking speed. B) Conversely, only LG and MG positive work were significantly affected by horizontal forces. Boxplots show positive work performed during push-off. Significant ($p<0.05$) pairwise comparisons vs. normal walking (1.2 m/s) represented by asterisks.

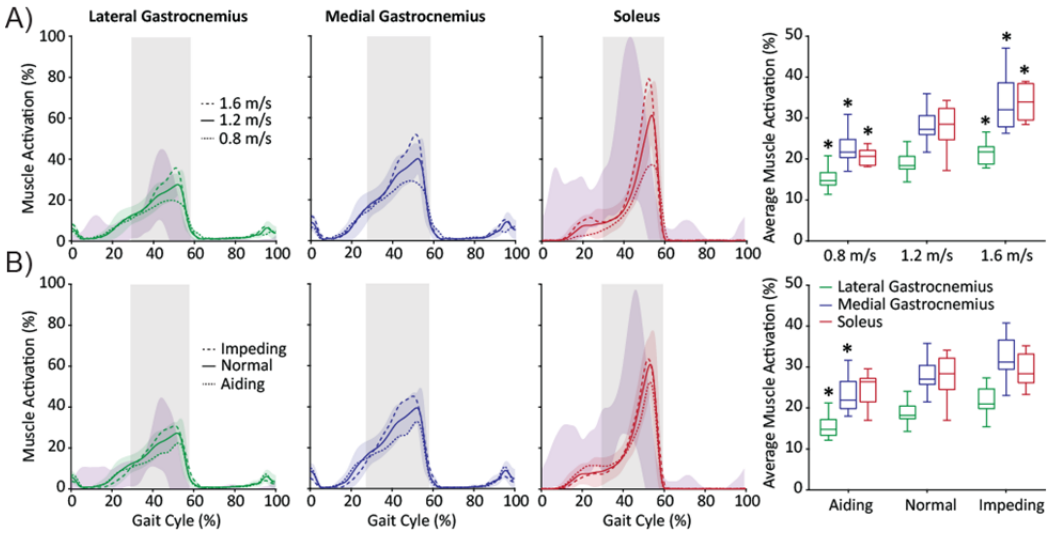

Figure 16: A) Model-predicted LG (green), MG (blue), and SOL muscle forces averaged during push-off were similarly affected by walking speed. B) Compared to walking normally, only LG and MG activation significantly decreased in response to aiding forces (-19% and -19.3%, respectively). Shaded grey rectangular area represents the push-off phase of walking. Shaded (LG-green, MG-blue, SOL-red) represents standard error during normal walking (1.2 m/s). Shaded purple area represents the standard deviation of all associated experimental trials for the LG and SOL, normalized to peak model-predicted activation during normal walking. Boxplots show average muscle activation during push-off. Significant ($p<0.05$) pairwise comparisons vs. normal walking (1.2 m/s) represented by asterisks.

DISCUSSION

The overarching goal of this study was to quantify inter-muscular differences between the medial gastrocnemius (MG), lateral gastrocnemius (LG), and soleus (SOL) in response to changes in forward propulsion during walking. Although many studies have added significant value to this ongoing scientific discussion, the wide array of *in vivo* measurements, *in silico* estimates, and experimental manipulations have led to considerable differences in inter-muscular conclusions. Here, toward a more complete understanding of triceps surae behavior, we combined electromyography, ultrasound imaging, and musculoskeletal modeling during conditions that systematically manipulated either walking speed or the mechanical demand for forward propulsion at a fixed speed. We interpreted our results in the context that the muscle that was more sensitive to altered demands for forward propulsion would therefore contribute more. In support of our null hypothesis, we found that muscle-specific responses derived from experimental measurements (i.e., activation and fascicle behavior) were consistent with those derived from musculoskeletal simulations (i.e., muscle force and positive mechanical work) within the same subjects. As we discuss in more detail below, our cumulative findings suggest that the biarticular gastrocnemius muscles play a more significant role than the uniarticular soleus in governing changes in forward propulsion during the mid to late stance phase of walking. Reconciling these inter-muscular differences, and the relatively disparate literature on this topic to date, is critical for the design and control of wearable assistive devices and for targeted therapeutics that attempt to mitigate deficits in forward propulsion.

Our *in vivo* and *in silico* results are within the range of values shown in prior literature. First, the amplitude and timing of our measured LG and SOL muscle activations agree well with previous studies, both in response to changes in walking speed (Lai et al., 2015) and the application

of horizontal forces (Gottschall & Kram, 2003). Moreover, our model-predicted estimates of LG and SOL activation generally well-replicated our *in vivo* measurements, with one notable difference. Specifically, similar to other studies, (M. Q. Liu et al., 2006) model-predicted activations were delayed compared to their respective *in vivo* measurement; however, both model-predicted and *in vivo* activations exhibited characteristic bursts within our analyzed region of interest (i.e., push-off). This comparison is shown for each main effect (i.e., speed [Figure 16A] and horizontal forces [Figure 16B]), with the purple shaded region representing the standard deviation of all associated experimental trials for the LG and SOL, normalized by peak model-predicted activation during normal walking. Second, our ultrasound measurements for the MG and SOL were generally consistent with the majority of previous studies in terms of length at heel-strike, average length, and absolute length change (Cronin et al., 2013; Farris & Sawicki, 2012a; Lai et al., 2015; Panizzolo et al., 2013). Similar those studies, in all conditions except those with aiding forces, both muscles maintained nearly isometric behavior during early to mid-stance before undergoing characteristic shortening that peaked just after toe-off. During the aiding force condition, both muscles shortened during early stance, likely due to exaggerated dorsiflexion from heel-strike to foot flat. Although not completely analogous in terms experimental manipulations, this behavior is comparable to that shown for the MG during downhill walking (Lichtwark & Wilson, 2006). Finally, our model-predicted estimates of muscle force and positive work generally agree with prior studies (Anderson & Pandy, 2003; Blazkiewicz, Wiszomirska, Kaczmarczyk, Naemi, & Wit, 2017; Neptune & Sasaki, 2005; Neptune et al., 2008).

Compared to walking at 1.2 m/s, MG, LG, and SOL experimental and model-predicted results were almost uniformly affected by changes in walking speed. During push-off, each muscle's activation significantly increased with increasing walking speed. This phenomenon has

been widely reported since it was first proposed in the seminal works by Hill (1953) and Winter (1983), who suggested the triceps surae contributes to forward propulsion (Hill, 1953; Winter, 1983). Here, in agreement with Hill and Winters, LG and SOL average force produced during push-off significantly increased (+13.4% and +21.1%, respectively) from slow walking (i.e., 0.8 m/s) to normal walking, but not from normal walking to fast walking (i.e., 1.6 m/s). Riley et al. (2001) found nearly identical results when measuring propulsive adaptations to changes in walking speed (Riley, Della Croce, & Kerrigan, 2001). Their findings suggest that the contribution from muscles spanning the ankle to forward propulsion was more sensitive to changes at slower walking speeds due to an increased utilization of hip flexors and extensors at higher speeds. Increased use of hip flexors and extensors could also explain why our model-predictions for positive work performed by the MG, LG, and SOL during push-off was invariant between walking speeds. Conversely, Neptune et al. (2009) found both the MG and SOL increase fiber positive work in response to increasing walking speeds (Neptune et al., 2008). However, their work estimates were not isolated to the mid to late stance phase of walking and only incorporated sagittal plane motion. Although our findings for activation, force, and work were similar for each muscle tested across changes in walking speed, inter-muscular differences existed at the fascicle level. Compared to walking normally, in our study only MG peak fascicle shortening decreased with slower speed (-13.5%). This behavior is very similar to the findings of Farris & Sawicki (2012), who found a reduction in MG peak shortening at walking speeds slower than normal, but consistent peak shortening at speeds faster than normal (Farris & Sawicki, 2012a). Their results suggest that average positive power produced by the biarticular MG MTU increases with walking speed until reaching self-selected speeds (~1.2 m/s). On the other hand, the uniarticular SOL may have consistent fascicle behavior over the range of speeds due to a large demand for vertical support

that spans both slow and fast walking (Orendurff et al., 2004). Indeed, some studies have suggested the SOL is primarily responsible for vertical support and secondarily responsible for forward propulsion (M. Q. Liu et al., 2006; Miyoshi et al., 2006).

Unfortunately, changes in walking speed influence the demand for both forward propulsion and vertical support, thereby likely confounding our interpretations of inter-muscular differences in activation, fascicle behavior, force, and mechanical work (Francis et al., 2013; Lai et al., 2015). Thus, results derived from conditions using horizontal forces provide more clear estimates of inter-muscular contributions to forward propulsion alone. In agreement with our findings for activation, although they measured a different head of the gastrocnemius, Gottschall & Kram (2003) also found that while both gastrocnemius and soleus activation during push-off increased significantly in response to impeding forces, only gastrocnemius activation decreased significantly in response to aiding forces (-30.4%) (Gottschall & Kram, 2003). As noted by those authors, these findings suggest that the gastrocnemius muscles play a more important role in modulating forward propulsion, but the SOL may act synergistically when the demand for forward propulsion is great. Similar to our findings for activation, MG peak fascicle shortening and average fascicle length were much more sensitive to altered demands for forward propulsion than those for the SOL. Despite the architectural differences between these muscles (i.e., uniarticular SOL vs. biarticular MG), we saw no evidence that changes in MTU length could explain muscle-level differences in the response to our experimental manipulations. Compared to walking normally, greater MG fascicle shortening during the impeding force condition (+17.4%) could be elicited by greater muscle activation in order to meet the demand for greater force transmission. Indeed, compared to the SOL, the MG has a greater percentage of Type II fiber physiological cross sectional area

(PCSA), which produces more force than Type I fibers, more commonly represented in the SOL (Gollnick, Sjodin, Karlsson, Jansson, & Saltin, 1974).

MG muscle activation and fascicle shortening were both more sensitive to the application of horizontal forces than those for SOL, consistency that we interpret in support of the gastrocnemius' role in governing changes in forward propulsion. However, some studies would suggest that the preservation of muscle contractile behavior in the presence of horizontal forces would be more indicative of that muscle's functional role during walking. Indeed, greater fascicle shortening could lead to a force deficit due to a leftward shift on the length-tension curve and faster shortening velocities (Fukunaga et al., 2001). Cronin et al. (2013) found that SOL fascicle behavior, not MG fascicle behavior, was preserved over the course of a 60 min prolong walk (Cronin et al., 2013). They argued that the preservation of SOL behavior is due to an energetically favorable recruitment of shorter fascicles with slower shortening velocities and greater relative Type I fiber PCSA. In our study, compared to walking normally, greater MG fascicle shortening during the impeding force condition, driven more by greater activation than by effects on joint posture, may be energetically unfavorable but necessary to meet the demand for greater push-off. The average fascicle length of the MG increased with aiding forces (+2.5%) and decreased with impeding forces (-3.5%), with potential consequences for the economy of force generation (i.e., force per unit activation). On the other hand, the average operating length of the SOL remained unchanged across horizontal force conditions. In agreement, Rubenson et al. (2012) reported that SOL operating length is mostly gait-independent and consistently operates on the ascending limb of the force-length curve, thereby providing stable but suboptimal force production (Rubenson et al., 2012).

Despite some disagreement in the interpretation of fascicle behavior, increased MG fascicle shortening and muscle activation were accompanied by greater MG force and positive work during mid to late stance - complimentary *in silico* evidence that the gastrocnemius muscles are more responsible for forward propulsion than the SOL. Due to its larger size and thus force-generating capacity, (Sutherland, Cooper, & Daniel, 1980) the SOL accounted for the greatest percentage of average force and positive work among the triceps surae muscles. However, compared to walking normally, SOL kinetics were invariable in response to horizontal forces. Indeed, only MG and LG average force and positive work were significantly affected by the application of horizontal forces. Specifically, MG and LG force (-15.5% and -15.6%, respectively) and positive work (-21.9% and -21.3%, respectively) decreased in response to aiding forces. Additionally, MG and LG positive work increased (+19.5% and +19.9%, respectively) in response to impeding forces. One interpretation of these findings is that the SOL provides a large, but invariant contribution to forward propulsion while the gastrocnemius muscles provide a smaller, but task-dependent contribution that increases to meet the demand for forward propulsion. Similarly, though in response to changes in walking speed, Liu et al. (2008) suggested the SOL provides a task-dependent contribution to vertical support, while the gastrocnemius muscles' contribution to vertical support was invariant (M. Q. Liu, Anderson, Schwartz, & Delp, 2008).

There is considerable evidence that forces produced and work performed by the MG, LG, and SOL contribute significantly to forward propulsion. This is translationally important, as those forces and that work is reduced by aging and gait pathology (DeVita & Hortobagyi, 2000; Fukashiro et al., 2006; Goldberg & Stanhope, 2013). Accordingly, many training programs have been designed to overcome reductions in triceps surae muscle strength or power capacity, albeit with limited success (DeVita & Hortobagyi, 2000; Foure et al., 2011). Our results suggest that

rehabilitation techniques that preferentially strengthen the gastrocnemius muscles, perhaps through targeted biofeedback, may result in more beneficial neuromechanical strategies during push-off that could translate into improvements in gait performance. As an additional translational implication, many studies have disproportionately targeted uniarticular SOL function through the design and prescription of ankle exoskeletons (Farris, Robertson, & Sawicki, 2013; Nuckols, Dick, Beck, & Sawicki, 2020; Zhang et al., 2017). On the other hand, at least one study has shown that exoskeleton configurations that mimic the biarticular gastrocnemius muscles yield greater reductions in metabolic cost during walking than those that mimic the uniarticular soleus (Malcolm, Galle, Derave, & De Clercq, 2018).

There are several limitations and assumptions in this study. First, the three-dimensional architecture of the MG, LG, and SOL is complex and contains multiple regions that may vary in activation, fascicle length, and force development. For example, we only imaged the posteromedial aspect of the SOL, which may differ substantially from other compartments (Chow et al., 2000). Second, we cannot be certain that the same representative fascicle was selected for all conditions for each participant. To mitigate variation in fascicle selection, for each subject, we overlaid the fascicle identified at initial contact for the 1.2 m/s condition and updated the endpoints to the correct positions before continuing the tracking procedure. Third, using automated tracking routines, several studies report standard errors between 5% and 10% of absolute length (Aeles et al., 2017; Gillett, Barrett, & Lichtwark, 2013; Kwah, Pinto, Diong, & Herbert, 2013). More recently, using UltraTrack, Drazan et al. (2019) revealed MG fascicle length root mean square error values were near 7% when the ankle is rotating at 30 °/s and surpassed 10% when the ankle is rotating ≥ 120 °/s (Drazan, Hullfish, & Baxter, 2019). To mitigate these errors and improve our scientific rigor, we recorded our ultrasound images at a higher frame rate (76 fps) to account for

faster shortening velocities and we performed frame-by-frame manual corrections of the automated tracking results. Fourth, our study used three fixed walking speeds which themselves were not prescribed as a function of each subject's preferred walking speed. However, this is a common methodological approach in the biomechanics literature and is unlikely to influence of overarching conclusions. Fifth, the horizontal forces were applied to the subject's waist, and thus subjects necessarily recruited proximal muscle groups (e.g., muscles spanning the hip) in addition to the triceps surae (Conway et al., 2018). Sixth, although we consistently encouraged subjects to maintain upright posture, we did not measure trunk kinematics and therefore locked lumbar coordinates in our musculoskeletal simulations. Finally, despite using the Residual Reduction Algorithm tool, lower limb reserve torque actuators were needed to account for ignored passive structures and insufficient muscle force generating capacity, but were controlled to recommended thresholds (Hicks et al., 2015).

CONCLUSION

By combining electromyography, ultrasound imaging, and musculoskeletal modeling in the same subjects, this study provides the most complete report to date of the relative contributions of the gastrocnemius and soleus muscles to forward propulsion during walking. Based on consistent evidence from empirical measurements and musculoskeletal simulations, we conclude that the biarticular gastrocnemius muscles play a more significant role than the uniarticular soleus in governing changes in forward propulsion during the push-off phase of walking. Our results may have important implications for the prescription of targeted therapeutics and for the design and control of wearable assistive devices.

CHAPTER 5: AGE-RELATED CHANGES TO TRICEPS SURAE MUSCLE-SUBTENDON INTERACTION DYNAMICS DURING WALKING

INTRODUCTION

Mechanical output at the ankle during push-off is an important determinant of walking performance and is significantly reduced with advancing age (Hardy et al., 2007; Purser et al., 2005). More specifically, net ankle joint moment and mechanical power (i.e., push-off intensity) is largely governed by the forces generated by the lateral and medial gastrocnemius (GAS) and soleus (SOL) muscles that make up the triceps surae (Fukashiro et al., 2006; Orselli et al., 2017; Zajac, 1989). Despite collectively transferring their force through a common distal tendon, the triceps surae muscles undergo different fascicle shortening behaviors during walking and, biomechanically, contribute differently to forward propulsion and vertical support (Clark, Pimentel, & Franz, 2020; Francis et al., 2013; Gottschall & Kram, 2003; M. Q. Liu et al., 2006; Miyoshi et al., 2006). These muscle-level differences may be facilitated by the architectural complexity of the Achilles tendon, which itself is comprised of three distinct bundles of tendon fascicles, known as subtendons, that originate from GAS and SOL muscles (Cummins, Anson, & et al., 1946; Del Buono et al., 2013; Doral et al., 2010; Edama et al., 2015; Pekala et al., 2017; Szaro et al., 2009). Comparative work and our own *in vivo* evidence suggest that sliding between adjacent subtendons has the potential to allow differences in GAS vs. SOL contractile behavior (Clark & Franz, 2018b; Gains et al., 2020; Thorpe et al., 2013). Unfortunately, animal models of the aging tendon present with a proliferation of collagen cross-linking and prominent reductions

in sliding between subtendons (Thorpe et al., 2012, 2013). In agreement with those finds, we have observed more uniform Achilles tendon tissue displacement patterns in older adults that have the potential to disrupt the potential for muscle contractile independence (Clark & Franz, 2020). These results, at least at the tendon level, appear to be clinically meaningful; during walking, more uniform subtendon displacements within the human Achilles tendon correlate with reduced push-off intensity in older adults (Franz & Thelen, 2015). These observations allude to a fundamental change in the interaction between triceps surae muscles and the Achilles tendon as a determinant for reduced mechanical output – a finding that currently lacks direct empirical data during walking and has far reaching implications for the design and control of wearable assistive devices that attempt to overcome age-related deficits of forward propulsion.

The presence of subtendon sliding is mediated by the interfascicular matrix of the Achilles tendon and has been commonly observed in rat and equine tendons (e.g., (Gains et al., 2020; Thorpe et al., 2013)). In young adult humans, evidence for sliding is generally attributed to observations of differential tissue displacements at different depths of the Achilles tendon (i.e., significant differences in tissue displacements attributed to the gastrocnemius and soleus subtendons) and has been shown during passive ankle rotation (Arndt et al., 2012), eccentric loading (Slane & Thelen, 2014, 2015), and walking (Franz et al., 2015). Studies in humans using advanced musculoskeletal modeling (Handsfield et al., 2017) and studies in rats using electrical stimulation (Finni et al., 2018; Maas et al., 2020) suggest non-uniform tissue displacements are likely a result of differential force transmission from the triceps surae muscles. Recently, to empirically characterize the origins of non-uniform tissue displacement patterns in the human Achilles tendon, we introduced a dual-probe ultrasound imaging approach that enables simultaneous assessment of GAS vs. SOL muscle contractile behavior and tissue displacements in

their associated regions of the Achilles tendon (Clark & Franz, 2018a). Using this approach during fixed-end contractions, we found that differences between GAS and SOL muscle shortening gave rise to anatomically consistent differences in subtendon tissue displacements (Clark & Franz, 2018a). As a logical extension of our dual-probe imaging work in younger adults, we more recently observed that more uniform Achilles tendon tissue displacements in older adults during fixed-end contractions were accompanied by smaller differences between peak GAS and SOL muscle shortening (Clark & Franz, 2020).

If triceps surae muscle dynamics can precipitate anatomically consistent patterns of localized tissue displacements within the architecturally complex Achilles tendon, would an age-related reduction in the capacity for sliding between adjacent subtendons negatively influence muscle contractile behavior during walking? Although the answer is unclear, any change therein would likely influence the triceps surae muscles' relative contribution to forward propulsion – an outcome that is consistently reduced in older adults (Franz & Kram, 2013). In young adults, the majority of empirical studies suggest the GAS muscles are primarily responsible for governing changes in forward propulsion while the SOL is primarily responsible for governing changes in vertical support (e.g., (Clark et al., 2020; Francis et al., 2013; Gottschall & Kram, 2003; M. Q. Liu et al., 2006; Miyoshi et al., 2006), though see (McGowan et al., 2008; Neptune et al., 2001; Neptune et al., 2008) for alternative theories). However, experimental manipulations of walking speed affect both walking subtasks, thus confounding our interpretations in the specific context of forward propulsion (Francis et al., 2013; Lai et al., 2015). Fortunately, the application of horizontal aiding and impeding forces at fixed speeds has provided a more direct means in the literature to manipulate the mechanical demand for forward propulsion (Chang & Kram, 1999; Gottschall & Kram, 2003). Using horizontal forces in young adults, we recently revealed that compared to

walking normally, increased mechanical demand for forward propulsion elicits larger peak GAS fascicle shortening than that of the SOL (Clark et al., 2020). Therefore, it is likely that disruption of GAS fascicle behavior via a reduction in the capacity for sliding between adjacent subtendons could deleteriously impact contributions to forward propulsion.

The purpose of this study was to investigate differences in GAS vs. SOL muscle length-change behavior as a determinant of previously observed correlations between more uniform Achilles tendon tissue displacements and reduced ankle joint mechanical output in older adults. To accomplish this, we used dual-probe dynamic ultrasound imaging during conditions that systematically altered the mechanical demand for forward propulsion via changes in speed and the application of horizontal aiding and impeding forces. First, we hypothesized that, compared to young adults, older adults would have (*i*) more uniform Achilles tendon tissue displacements during the stance phase of walking that (*ii*) would be accompanied by smaller differences between GAS and SOL muscle length change behavior. Second, we hypothesized that the magnitude of differences between GAS and SOL muscle length change behavior would correlate with net ankle joint moment, power, and work performed during push-off. Finally, based on previous studies that suggest GAS muscles are more responsible than the SOL in governing changes in forward propulsion, we tested the secondary hypotheses that increases in the demand for forward propulsion would elicit larger differences in muscle- and tendon-level behavior in young, but not older adults. We would interpret our secondary hypothesis in the context of the overarching premise that a larger capacity for sliding between adjacent Achilles subtendons facilitates independent GAS vs. SOL muscle actuation and thus biomechanical function during walking – a phenomenon that is fundamentally altered by age.

METHODS

Subjects and Protocol

We recruited healthy young adults between 18 and 35 years of age and healthy older adults between 65 and 80 years of age. We screened and excluded subjects who reported a lower extremity injury in the last 6 months, used a leg prosthesis, needed an assistive walking device, or were taking medication that causes dizziness. We report data for 9 young (24±4 yrs, 74.3±9.9 kg, 1.8±0.1 m, 5M/4F) and 9 older (74±4 yrs, 66.8±5.9 kg, 1.7±0.1 m, 6M/3F) adults. All subjects provided written informed consent in compliance with the University of North Carolina Biomedical Sciences Institutional Review Board.

Before data collection, we determined each subject's preferred walking speed as the average of three times taken to walk the middle 2 m of a 10 m walkway. Subjects then walked on an instrumented treadmill (Bertec Corp., Columbus, Ohio, USA) for 6 minutes at their preferred walking speed (above 1.0 m/s) to precondition their triceps surae and Achilles tendon units and acclimate to treadmill walking (Hawkins et al., 2009). Subjects then walked for 1 min each at a range of speeds (0.8, 1.0, and 1.2 m/s) and again at 1.2 m/s ("Normal") with: (*i*) a 5% body weight horizontal aiding force and (*ii*) a 5% body weight horizontal impeding force, as shown in Figure 17. A feedback-controlled, motor-driven horizontal force system applied horizontal aiding and impeding forces, as described previously (Conway et al., 2018; Conway & Franz, 2019, 2020). Briefly, in real-time, a custom LabVIEW interface (cRIO-9064, National Instruments, Austin, TX, USA) controlled a servo motor (Kollmorgen, Radford, VA, USA) in series with a horizontal cable attached to a waist belt worn by the subject. During trials with horizontal impeding or aiding forces, we consistently encouraged subjects to maintain upright posture (i.e., avoid excess trunk leaning). We fully randomized by walking condition and provided 2 min of rest between conditions.

Subjects were barefoot throughout all walking trials to facilitate proper placement of ultrasound transducers. We collected all ensuing data after each subject reached their targeted walking speed and their movement pattern stabilized.

Experimental Measurements and Analysis

For all trials, twelve cameras (Motion Analysis Corporation, Santa Rose, CA, USA) recorded the 3-D positions of retroreflective markers attached to each subject's sacrum and bilateral anterior and posterior superior iliac spines, lateral femoral condyles, lateral malleoli, 1st and 5th metatarsal heads, and calcanei. To improve segment tracking, we secured right and left leg thigh and shank marker clusters. We filtered marker position and ground reaction force (GRF) data using a 4th order low-pass Butterworth filter with cutoff frequencies of 6 Hz and 100 Hz, respectively. We scaled a 7-segment, 18 degree of freedom model of each subject's pelvis and lower limbs using marker position data from a standing trial (Arnold, Ward, Lieber, & Delp, 2010)and then updated the model to include functional hip joint centers (Piazza, Okita, & Cavanagh, 2001). A global optimization technique calculated ankle joint moment, power, and positive ankle push-off work for each stride corresponding to ultrasound data as detailed in the following section (Silder et al., 2008).

Ultrasound Measurements

A 7 MHz, 60 mm ultrasound transducer (LV7.5/60/128Z-2, UAB Telemed, Vilnius, Lithuania) placed over the mid-belly of the right leg medial gastrocnemius (GAS) recorded cine B-mode images at 76 frames per second using an image depth of 50 mm. This transducer placement and depth enabled synchronized assessment of GAS and soleus (SOL) fascicle behavior in the same imaging plane. We secured the ultrasound probe using a custom 3-D printed probe holder made of a flexible filament (NinjaFlex, Fenner Inc., Manheim, PA, USA) and wrapped in

Coban (3M, St. Paul, MN, USA). Simultaneously, a 10 MHz, 38 mm ultrasound transducer (L14-5W/38, Ultrasonix Corp., Richmond, BC) placed over the right leg free Achilles tendon (AT), approximately 6 cm distal to the SOL muscle-tendon junction, recorded 128 lines of ultrasound radiofrequency data at 155 frames per second using an image depth of 20 mm. This transducer placement and depth enabled synchronized assessment of two equally sized tendon depths – superficial and deep – corresponding to subtendon tissue thought to arise from the GAS and SOL, respectively. This characterization represents the most prevalent anatomical arrangement in cadaveric studies (Anson & McVay, 1971; Edama et al., 2015; Szaro et al., 2009; van Gils, Steed, & Page, 1996). We secured the second ultrasound probe using a custom probe holder made of a layered plastazote foam and wrapped in Coban.

For each ultrasound transducer, a 1000 Hz binary analog synchronization signal indicated the start and stop of each ultrasound video using a wave form generator (SDG1025, SIGLENT, Shenzhen). We co-registered ultrasound data with GRF data and detected heel-strike and toe-off gait events using a 10 N vertical GRF threshold. Finally, we quantified time series of GAS and SOL fascicle behavior (i.e., length and pennation angle) and superficial and deep Achilles tendon tissue behavior (i.e., subtendon displacements), from the same 2 strides per condition, as described in detail below. The same investigator processed all ultrasound data to minimize inter-investigator variability.

Triceps Surae Muscle Kinematics

At the first co-registered heel-strike, we defined a static polygon region of interest surrounding the GAS and SOL muscle bellies and corresponding superficial and deep aponeuroses. For each muscle, we defined one fascicle from superficial to deep aponeurosis that most represented the muscle belly. An open source MATLAB routine, UltraTrack (Farris & Lichtwark,

2016), based on an affine extension to an optic flow algorithm, quantified time series GAS and SOL fascicle length and pennation angle. UltraTrack defines pennation angle relative to the horizontal axis of the image. Thus, to more accurately define pennation angle, for each muscle, we quantified the angle of the deep aponeurosis relative to the horizontal axis of the image and then subsequently applied a frame by frame correction to fascicle pennation angle. For fascicle tracking and superficial aponeurosis pennation angle corrections, we visually confirmed the results and applied manual corrections when necessary. We filtered all manually corrected tracking results using a 4^{th} order low-pass Butterworth filter with a cutoff frequency of 6 Hz and then averaged the results over 2 strides (heel-strike to heel-strike). For fascicle behavior, we report time series GAS and SOL average fascicle operating length and velocity (i.e., derivative of fascicle length with respect to time). For a more direct comparison of longitudinal tissue displacements, we multiplied muscle fascicle length by the cosine of the pennation angle to compute longitudinal muscle length along the Achilles tendon line of action. Then, to place our results in the context of distal to proximal subtendon displacement, we normalized muscle length change results by their length at toe-off. Finally, for muscle behavior, we report stance-phase peak differences in longitudinal muscle length change (i.e., GAS – SOL).

Achilles Subtendon Tissue Kinematics

A 2-D speckle tracking algorithm quantified localized Achilles subtendon tissue displacements using previously published techniques (Chernak Slane & Thelen, 2014). Although muscle fascicle data during gait is usually represented from heel-strike to heel-strike to fully characterize the stretch shortening cycle, 2-D elastography speckle tracking is more accurate when the initial frame corresponds to an instant of negligible tendon force (i.e., toe-off) (Chernak & Thelen, 2012; Chernak Slane & Thelen, 2014). As such, at the first co-registered toe-off, we

created a rectangular region of interest (~15 x 3 mm grid of nodes with 1 x 0.5 mm spacing, encompassing only Achilles tendon tissue) on a reconstructed B-mode image using the raw radiofrequency data. A 2 x 1 mm kernel centered at each nodal position contained up-sampled (4x) radiofrequency data and acted as a search window for successive 2-D normalized cross-correlation functions. Second order polynomials then regularized frame-to-frame nodal displacements that maximized the 2-D cross correlations, using a threshold of r=0.7 (Korstanje, Selles, Stam, Hovius, & Bosch, 2010). In rare cases when correlations fell below threshold, we determined new displacements for the relative frames based on a cubic interpolation of neighboring, highly correlated frames, and in the subsequent frame we added the median-filtered (3 x 3 nodes) nodal displacement. For each stride (toe-off to subsequent toe-off), we averaged the forward and backward tracking results. The resultant cumulative displacements represented the longitudinal displacements of superficial (i.e., originating from the GAS) and deep (i.e., originating from the SOL) subtendon tissue. We filtered all subtendon tracking results using a 4^{th} order low-pass Butterworth filter with a cutoff frequency of 6 Hz and then averaged the results over 2 strides (toe-off to toe-off). Finally, we report Achilles tendon non-uniformity as the stance-phase peak differences in longitudinal displacements (i.e., superficial – deep).

Statistical Analysis

For each outcome measure, Mauchly's test of sphericity assessed normal distributions for each outcome measure. When the assumption of normality was violated, Greenhouse-Geisser adjustments were applied. Mixed factorial ANOVAs tested for the effect of age (young vs. older adults) and speed (i.e., 0.8, 1.0, and 1.2 m/s) or horizontal pulling force (i.e., 1.2 m/s, aiding, and impeding) on ankle joint kinematics (i.e., range of motion) and kinetics (i.e., peak ankle moment, peak ankle power, and positive ankle push-off work during stance), GAS and SOL fascicle

kinematics (i.e., peak fascicle shortening velocity, average fascicle length), peak Achilles tendon non-uniformity during stance, and peak GAS-SOL longitudinal muscle length change at the instant of peak tendon non-uniformity. When significant main effects were found, two-tailed independent samples *t* tests identified age-related differences. Two-tailed paired samples *t* tests identified differences in muscle behavior (i.e., GAS vs. SOL) and subtendon behavior (i.e., superficial vs. deep). Finally, for young and older adults, we calculated Pearson's correlation coefficients between peak Achilles tendon non-uniformity, GAS-SOL longitudinal muscle length change, and ankle joint kinetic outcomes. We report effect sizes as η_p^2 and Cohen's d for main effects and pairwise comparisons, respectively. All statistical tests used an alpha level of 0.05.

RESULTS

Average ± standard deviation results and age-related post hoc comparisons for each outcome measure are summarized in Table 2. Results for GAS and SOL average fascicle operating length and peak shortening velocity are reported in the appendix. Here, we focus on the main effects of speed, horizontal forces, and age. We report age×speed or age×horizontal force interaction effects when significant.

Average preferred overground walking speed was not significantly different between young (1.3±0.1 m/s) and older (1.2±0.2 m/s) adults (P = 0.19, d = 0.65). Ankle range of motion increased with increased speed (P < 0.05, η_p^2 = 0.309) and horizontal force (P < 0.05, η_p^2 = 0.274). Compared to young, older adults walked with 3.2±0.8° less ankle joint range of motion across our study protocol (Speed: P < 0.05, η_p^2 = 0.313; Force: P < 0.05, η_p^2 = 0.332; Figure 18). Peak ankle moment, peak ankle power, and positive ankle push-off work increased with increasing speed (P-

values < 0.05, $\eta_p^2 \geq 0.602$) and horizontal force (P-values < 0.05, $\eta_p^2 \geq 0.696$), as shown in Figure 19. Although we did not observe a significant main effect of age on peak ankle moment (Speed: P = 0.34, $\eta_p^2 = 0.057$; Force: P = 0.18, $\eta_p^2 = 0.112$), older adults did walk with significantly smaller peak ankle power than young (Speed: P = 0.07, $\eta_p^2 = 0.188$; Force: P < 0.05, $\eta_p^2 = 0.247$). In addition, although we did not observe a significant main effect of age on positive ankle push-off work during conditions that changed speed (P = 0.58, $\eta_p^2 = 0.020$), older adults tended to perform less positive ankle push-off work than young during conditions that altered horizontal forces (P = 0.06, $\eta_p^2 = 0.202$). The purpose of this study was to investigate muscle-level behavior as a determinant of previously observed correlations between tendon-level behavior and reduced mechanical output at the ankle in older adults. As such, we first report tendon-level outcomes, followed by muscle-level outcomes at the instant of peak tendon non-uniformity. For each, box plots with individual data points are shown in Figure 20 and time normalized kinematic profiles are shown in Figure 21.

Tendon-Level Outcomes: Subtendon Displacement and Tendon Non-Uniformity

Peak superficial and deep subtendon tissue displacements increased with increasing speed (P-values < 0.05, $\eta_p^2 \geq 0.454$) and horizontal force (P-values < 0.05, $\eta_p^2 \geq 0.443$). Peak superficial subtendon tissue displacements in older adults were significantly smaller than in young adults (Speed: P < 0.05, $\eta_p^2 = 0.538$; Force: P < 0.05, $\eta_p^2 = 0.495$). Conversely, we did not observe a significant main effect of age on peak deep subtendon tissue displacements (Speed: P = 0.21, $\eta_p^2 = 0.098$; Force: P = 0.41, $\eta_p^2 = 0.043$). Peak Achilles tendon non-uniformity (i.e., superficial – deep subtendon displacement) increased with increasing speed (P < 0.05, $\eta_p^2 = 0.540$) and horizontal force (P = 0.05, $\eta_p^2 = 0.373$). Moreover, older adult peak Achilles tendon non-uniformity was, on

average across our study protocol, 49±9% smaller than those in young (Speed: $P < 0.05$, $\eta_p^2 = 0.721$; Force: $P < 0.05$, $\eta_p^2 = 0.820$). Finally, compared to that in young adults, significant interactions revealed that older adult peak Achilles tendon non-uniformity was less sensitive to changes in speed (age×speed, $P < 0.05$, $\eta_p^2 = 0.218$) and horizontal forces (age×horizontal force, $P = 0.05$, $\eta_p^2 = 0.294$).

We observed a significant, positive correlation between peak Achilles tendon non-uniformity and positive ankle push-off work in young adults (Speed: $P < 0.05$, $R = 0.397$; Force: $P < 0.05$, $R = 0.525$; Figure 22). However, we did not observe a significant correlation between tendon-level behavior and ankle joint kinetics for any other condition or age group.

Muscle-Level Outcomes: Muscle Length Change and GAS vs. SOL Differences

At the instant of peak Achilles tendon non-uniformity, GAS and SOL longitudinal muscle length change relative to toe-off increased with increasing speed (P-values < 0.05, $\eta_p^2 > 0.261$) and horizontal force (P-values < 0.05, $\eta_p^2 \geq 0.529$). Older adult GAS longitudinal muscle length changes were significantly smaller than those in young adults (Speed: $P = 0.05$, $\eta_p^2 = 0.219$; Force: $P < 0.05$, $\eta_p^2 = 0.421$). Moreover, compared to those in young adults, significant interactions revealed that older adult GAS longitudinal muscle length changes were less sensitive to changes in horizontal force (age×horizontal force, $P < 0.05$, $\eta_p^2 = 0.410$). Conversely, we did not observe a significant main effect of age on SOL longitudinal muscle length change (Speed: $P = 0.45$, $\eta_p^2 = 0.036$; Force: $P = 0.33$, $\eta_p^2 = 0.060$). These disparate effects on GAS versus SOL longitudinal muscle length change are likely complicated by changes in joint posture. However, at the instant of peak Achilles tendon non-uniformity, both older adult GAS and SOL muscle-tendon unit length

change relative to toe-off were significantly smaller than those in young adults (Speed: P-values < 0.05, $\eta_p^2 \geq 0.283$; Force: P-values < 0.05, $\eta_p^2 \geq 0.272$).

At the instant of peak Achilles tendon non-uniformity, GAS – SOL differences in longitudinal muscle length were unaffected by changes in speed (P = 0.638, η_p^2 = 0.028) and horizontal force (P = 0.16, η_p^2 = 0.108). Older adult muscle-level differences were, on average across our protocol, 17% smaller than those in younger adults (Speed: P < 0.05, η_p^2 = 0.275; Force: P < 0.05, η_p^2 = 0.630), but with high variability (e.g., 39% smaller during impeding force condition and 5% larger during the aiding force condition). Moreover, compared to those in young adults, significant interactions revealed that older adult muscle-level differences were less sensitive to changes in speed (age×speed, P < 0.05, η_p^2 = 0.174) and horizontal forces (age×horizontal force, P < 0.05, η_p^2 = 0.272).

We did not observe a significant correlation between GAS – SOL differences in longitudinal muscle length change behavior and Achilles tendon non-uniformity during conditions that altered speed for young or older adults (P-values ≥ 0.46, R-values ≤ 0.149). However, muscle-level differences positively correlated with Achilles tendon non-uniformity in young (P < 0.05, R = 0.502) but not older adults (P = 0.41, R = 0.165) during conditions that altered horizontal force (Figure 23). For conditions that altered speed, we only observed a significant correlation between young adult muscle-level differences and peak ankle moment (P < 0.05, R = 0.487). Conversely, during conditions that altered horizontal force, GAS – SOL differences in longitudinal muscle length behavior positively correlated with peak ankle moment (P < 0.05, R = 532), peak ankle power (P < 0.05, R = 0.420), and positive ankle push-off work in young (P < 0.05, R = 0.600). In older adults, correlations were either non-significant (peak ankle moment: P = 0.54, R = -0.122;

positive ankle push-off work: $P = 0.07$, $R = -0.350$) or negative (peak ankle power: $P < 0.05$, $R = -0.425$).

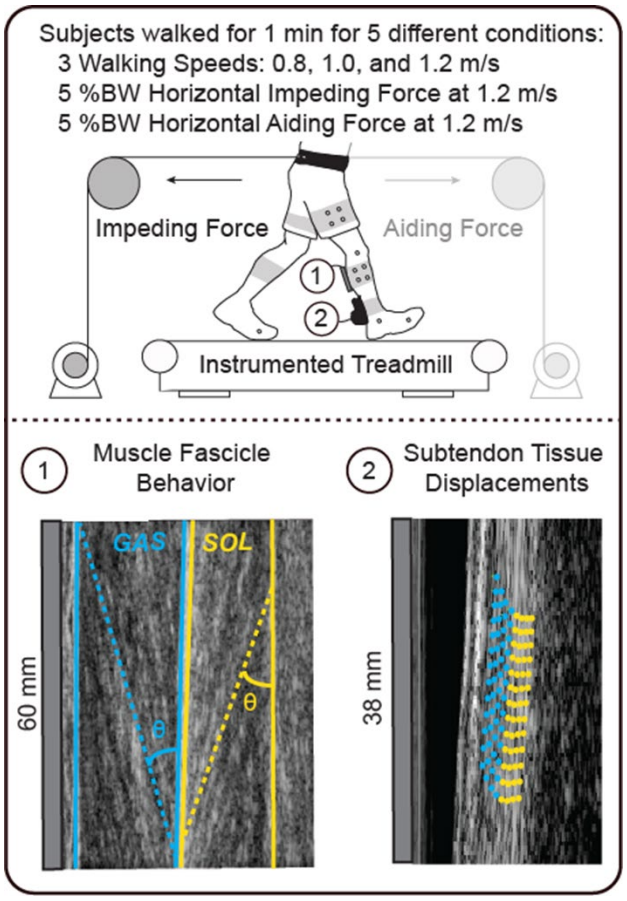

Figure 17: Schematic showing experimental manipulations and the application of dual-probe ultrasound imaging of (1) medial gastrocnemius (GAS-blue) and soleus (SOL-yellow) muscle contractile behavior and (2) Achilles subtendon tissue displacements.

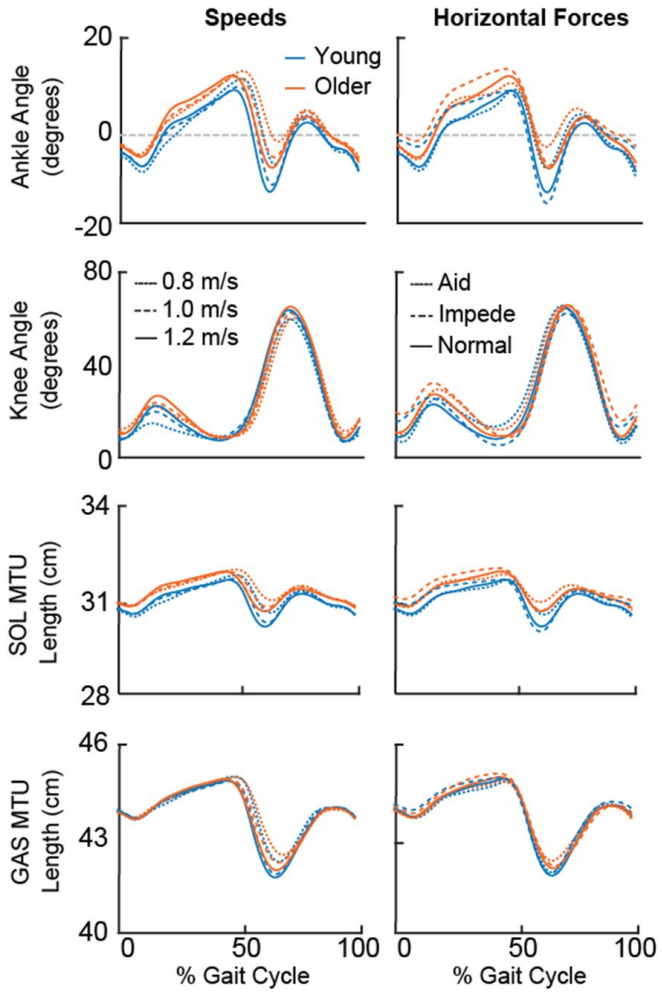

Figure 18: Group average profiles for ankle angle, knee angle, soleus (SOL), and medial gastrocnemius (GAS) muscle-tendon unit (MTU) length for young (blue) and older (orange) adults during conditions that altered speed (left) and horizontal force (right).

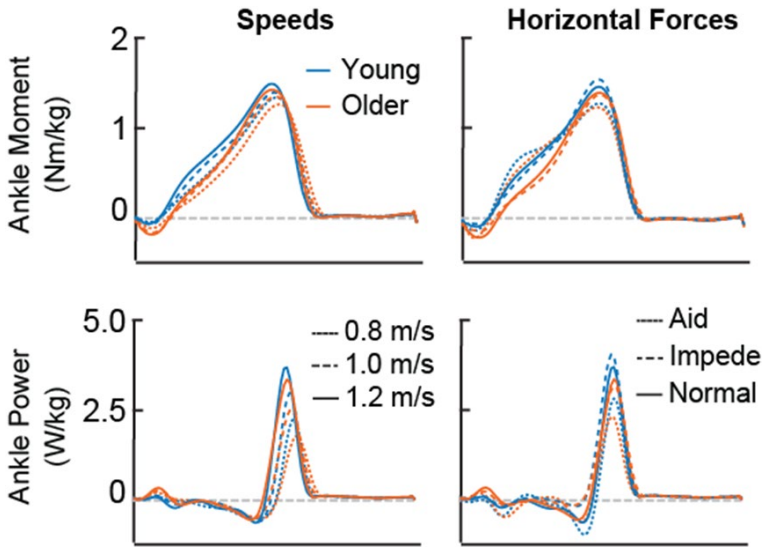

Figure 19: Group average profiles for ankle moment and ankle power curves for young (blue) and older (orange) adults during conditions that alter speed (left) and horizontal force (right).

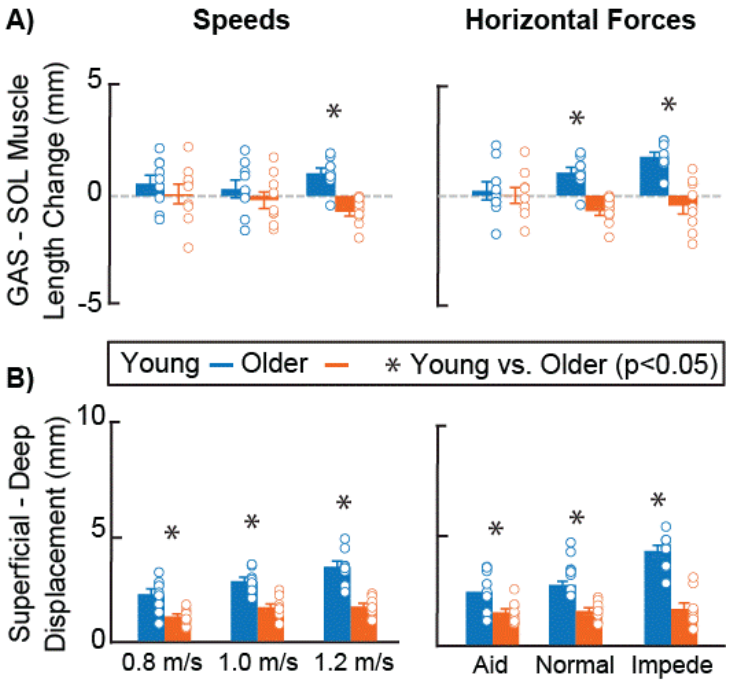

Figure 20: (A) Bar plots representing group average peak medial gastrocnemius (GAS) – soleus (SOL) longitudinal muscle length change relative to toe-off. (B) Bar plots representing peak superficial – deep Achilles tendon tissue displacements relative to toe-off. Single asterisks (*) represent significant differences between young (blue) and older (orange) adults ($P < 0.05$). Open circles represent individual data points. Error bars represent standard error.

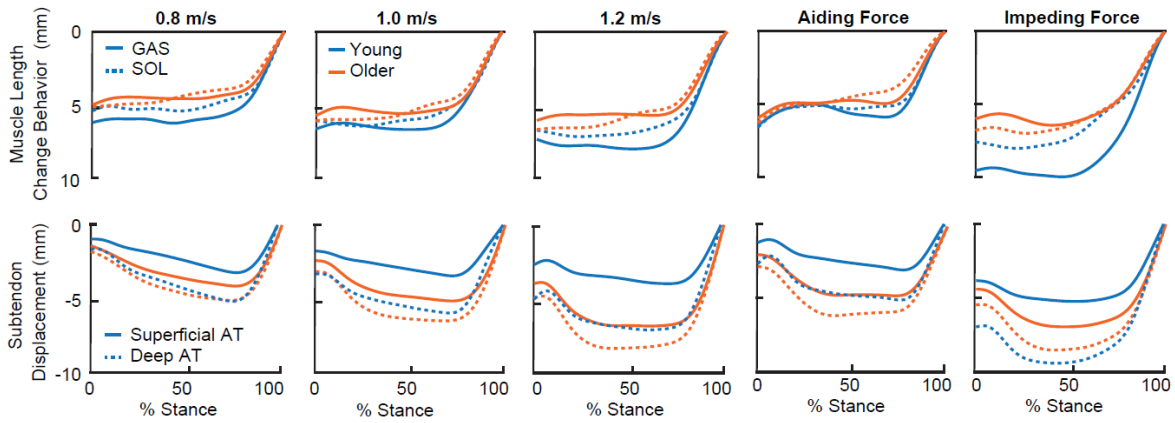

Figure 21: Time normalized, group average profiles for medial gastrocnemius (GAS) and soleus (SOL) longitudinal muscle length change (above) and superficial and deep Achilles tendon displacement (below) relative to toe-off for young (blue) and older (orange) adults.

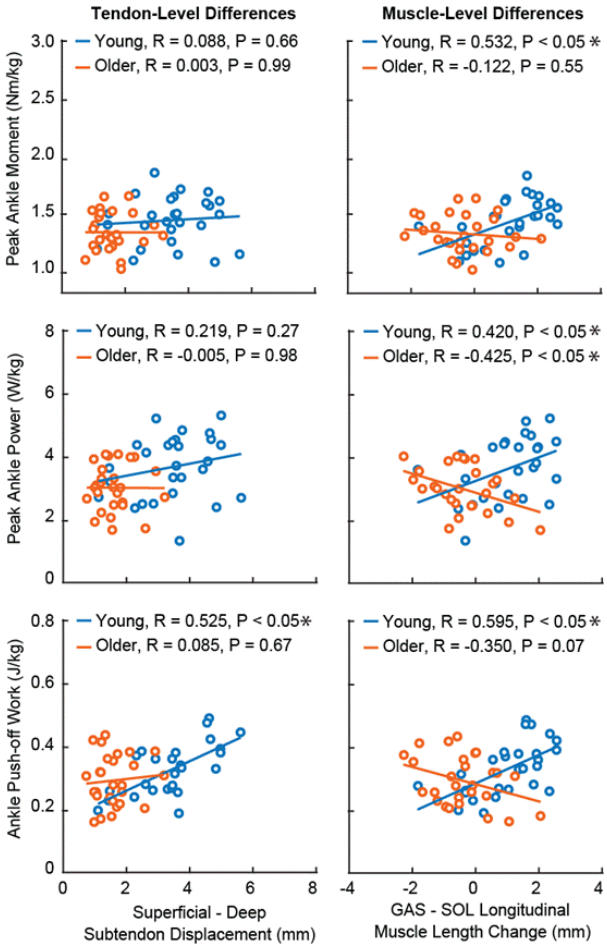

Figure 22: Correlations between push-off intensity (i.e., peak ankle moment, peak ankle power, and ankle push-off work) and (left) Achilles tendon non-uniformity (superficial – deep subtendon tissue displacement) and (right) medial gastrocnemius (GAS) – soleus (SOL) longitudinal muscle length changes during conditions that alter the mechanical demand for forward propulsion via horizontal forces. Individual data points for young and older adults represented by blue and orange open circles, respectively. Single asterisks (*) represent significant correlations ($P < 0.05$).

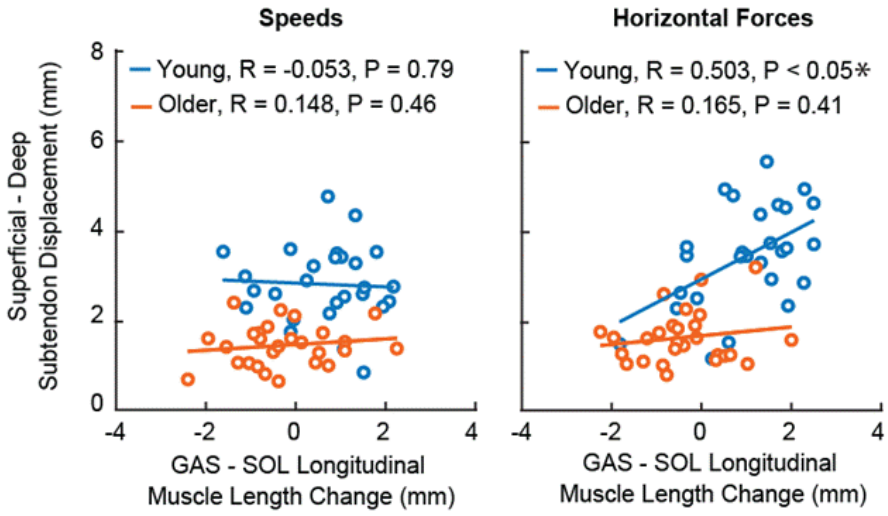

Figure 23: Correlations between Achilles tendon non-uniformity (superficial – deep subtendon tissue displacements) and medial gastrocnemius (GAS) – soleus (SOL) longitudinal muscle length changes during conditions that alter speed (left) and horizontal force (right). Individual data points for young and older adults represented by blue and orange open circles, respectively. Single asterisks (*) represent significant correlations ($P < 0.05$).

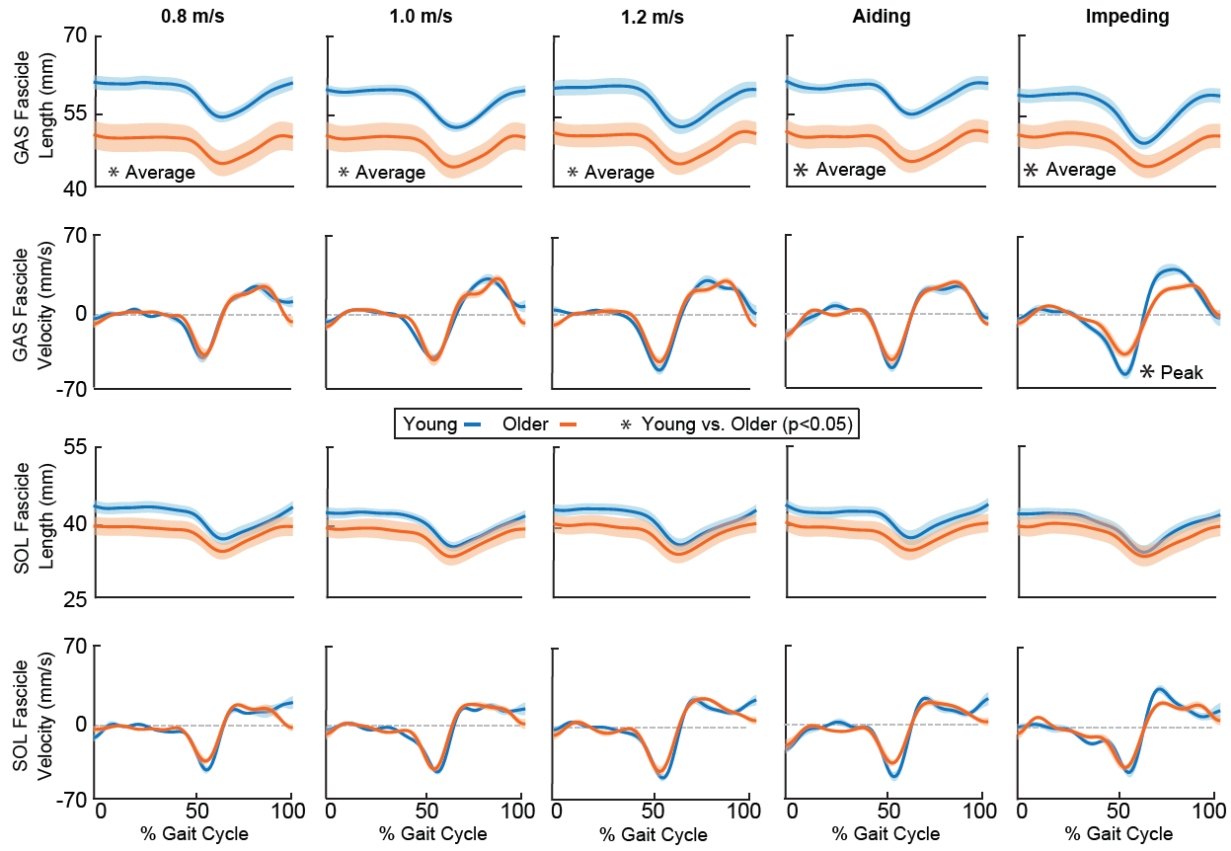

Supplementary Figure 3: Group average (standard error) fascicle length and velocity profiles for the medial gastrocnemius (GAS) and soleus (SOL) muscles. Single asterisks (*) represent significant differences between young (blue) and older (orange) adults ($P < 0.05$).

Table 2.
Summary statistics and effect sizes for pairwise comparisons across conditions.

	0.8 m/s			1.0 m/s			1.2 m/s ("Normal")			5 %BW Aiding			5 %BW Impeding		
	Young	Older	*p* (*d*)	Young	Older	*p* (*d*)	Young	Older	*p* (*d*)	Young	Older	*p* (*d*)	Young	Older	*p* (*d*)
Plantarflexor Mechanical Output															
Moment	1.32±0.18*	1.24±0.10*	0.26 (0.546)	1.38±0.14*	1.33±0.13*	0.41 (0.398)	1.47±0.19	1.40±0.19	0.43 (0.382)	1.32±0.17*	1.24±0.10*	0.25 (0.568)	1.59±0.21*	1.41±0.17	0.07 (0.913)
Power	2.25±0.47*	1.88±0.31*	0.06 (0.945)	3.10±0.52*	2.68±0.39*	0.07 (0.916)	3.92±0.78	3.44±0.66	0.18 (0.662)	2.95±0.88*	2.39±0.55*	0.13 (0.762)	**4.43±0.89***	**3.44±0.53**	**0.01 (1.356)**
Work	0.20±0.03*	0.18±0.04*	0.30 (0.510)	0.27±0.06*	0.26±0.06*	0.71 (0.179)	0.34±0.05	0.33±0.07	0.77 (0.141)	0.26±0.05*	0.22±0.04*	0.09 (0.855)	**0.43±0.06***	**0.35±0.07**	**0.02 (1.254)**
Peak Achilles Subtendon Displacement (mm)															
Superficial	**3.04±1.18**	**4.20±0.98***	**0.04 (1.071)**	**3.30±1.36**	**5.10±1.77***	**0.03 (1.141)**	**4.01±1.32**	**6.90±1.10**	**0.00 (2.389)**	**2.73±1.09***	**4.78±1.13***	**0.00 (1.850)**	5.12±1.91	7.09±2.91	0.11 (0.801)
Deep	5.22±1.36*^	5.34±1.15*^	0.84 (0.095)	6.09±1.21*^	6.67±1.49*^	0.38 (0.426)	7.47±1.50^	8.51±0.91^	0.10 (0.836)	5.20±1.46*^	6.28±1.03*^	0.09 (0.859)	9.50±1.53*^	8.76±2.67^	0.48 (0.340)
Difference	**2.18±0.75***	**1.14±0.37***	**0.00 (1.751)**	**2.79±0.53***	**1.57±0.48**	**0.00 (2.424)**	**3.47±0.77**	**1.61±0.43**	**0.00 (2.997)**	**2.47±0.98***	**1.50±0.52**	**0.02 (1.242)**	**4.38±0.81***	**1.67±0.82**	**0.00 (3.332)**
Peak Muscle Longitudinal Muscle Length Change (mm)															
MG	5.59±1.79*	4.56±2.11	0.28 (0.527)	6.08±1.34*	5.56±2.08	0.54 (0.296)	**7.79±1.38**	**5.49±1.42**	**0.00 (1.641)**	4.72±0.77*	4.97±1.52	0.66 (0.213)	**9.84±2.49***	**6.04±1.61**	**0.00 (1.812)**
SOL	5.01±1.59*	4.47±1.32*	0.45 (0.367)	5.75±0.78	5.74±1.45	0.99 (0.005)	6.74±1.00^	6.20±1.24^	0.33 (0.473)	4.49±1.52*	4.96±1.50*	0.52 (0.310)	8.06±1.92^	6.49±1.95	0.10 (0.810)
Difference	0.59±1.12	0.09±1.34	0.41 (0.399)	0.33±1.20	0.18±1.13*	0.36 (0.127)	**1.05±0.70**	**0.71±0.61**	**0.00 (0.520)**	0.23±1.25	0.01±1.08	0.71 (0.181)	**1.78±0.62***	**0.45±1.16**	**0.00 (1.431)**
Average Fascicle Operating length															
MG	**59.11±3.71**	**48.76±8.22**	**0.00 (1.622)**	**57.43±2.93**	**48.47±7.77**	**0.01 (1.525)**	**57.94±4.68**	**49.09±6.89**	**0.01 (1.502)**	**59.19±3.41**	**49.21±6.81**	**0.00 (1.853)**	**56.05±4.16**	**48.64±7.29**	**0.02 (1.248)**
SOL	40.92±3.48	37.62±5.35	0.14 (0.729)	39.59±2.82	36.94±5.59	0.22 (0.599)	40.26±3.48	37.66±5.61	0.25 (0.557)	40.87±3.65	37.74±5.70	0.18 (0.656)	39.24±3.50	37.29±6.10	0.42 (0.393)
Fascicle Shortening Velocity															
MG	46.64±10.70	45.06±14.52	0.80 (0.124)	43.79±7.18*	48.27±17.49	0.49 (0.335)	56.08±12.43	48.76±10.57	0.20 (0.634)	52.17±11.47	48.10±11.31	0.46 (0.357)	**63.05±12.54**	**45.92±11.77**	**0.01 (1.409)**
SOL	43.46±8.77	38.28±8.79*^	0.23 (0.591)	46.31±7.78	43.90±7.90	0.52 (0.308)	51.01±9.46	45.42±12.20	0.29 (0.512)	48.73±12.95	39.25±5.53^	0.06 (0.953)	46.54±13.73^	43.17±11.56	0.58 (0.266)

Summary statistics shown are mean±SD, significant age group differences are shown in **bold** ($p<0.05$), *indicates a within-group speed/force difference compared to walking at 1.2 m/s ($p<0.05$), ^ indicates a within group MG/SOL or superficial/deep difference ($p<0.05$).

DISCUSSION

In this study, we investigated differences in medial gastrocnemius (GAS) vs. soleus (SOL) muscle length change behavior as a determinant of previously observed correlations between more uniform Achilles tendon tissue displacements and reduced ankle joint mechanical output in older adults. We used dual-probe ultrasound imaging to simultaneously quantify muscle length change behavior and subtendon tissue displacements during conditions that systematically altered the mechanical demand for forward propulsion via changes in speed and the application of horizontal aiding and impeding forces. In support of our hypotheses, older adults walked with a significant reduction in Achilles tendon non-uniformity that was accompanied by smaller differences between GAS and SOL longitudinal muscle length change behavior. Moreover, we observed between-group differences in the extent to which muscle length change behavior and push-off intensity (i.e., moment, power, and positive push-off work) are correlated. As we elaborate in more detail below, these findings suggest that age-related changes to the interaction between triceps surae muscles and the Achilles tendon appears to negatively impact ankle joint mechanical output.

In our study, despite walking with identical experimental manipulations, older adults exhibited hallmark deficits in push-off intensity that were evident via conventional biomechanical analysis of joint-level kinematics and kinetics. Here, in agreement with the prevailing literature, older adults walked with a characteristic reduction in ankle angle range of motion (Boyer, Andriacchi, & Beaupre, 2012). Moreover, in response to increased mechanical demand for forward propulsion, older adults walked with significantly smaller peak ankle power than young adults (e.g., -22% with impeding forces). Likewise, older adults tended to walk with a reduction in positive ankle push-off work (e.g., -18% with impeding forces). However, contrary to several prior studies, we did not observe an effect of age on peak ankle moment generation during walking,

likely as a result of our relatively slow range of walking speeds (Buddhadev & Martin, 2016). Yet, similar to our findings, Knaus et al. (2020) revealed that older adults who walked with similar ankle moment generation to younger adults presented with deleterious changes in Achilles tendon structure-function relations that are not uncovered using conventional biomechanical analyses alone (Knaus et al., 2020).

Our results for Achilles tendon tissue displacements agree well with previous findings in terms of age-related differences and changes in response to increased mechanical demand. Our research group previously revealed that the magnitude of Achilles tendon non-uniformity increased with faster speeds and, when pooling young and older adults together, positively correlated with push-off intensity (non-uniformity vs. moment: $R = 0.63$; vs. power: $R = 0.39$; vs. positive work: $R = 0.44$; P-values < 0.05) (Franz & Thelen, 2015). Moreover, this prior work showed more uniform Achilles tendon tissue displacements in older adults (age-related differences up to 41% at 1.25 m/s), consistent with animal models of aging tendon and a reduced capacity for sliding (Thorpe et al., 2012, 2013). Here, we report similar age-related reductions in Achilles subtendon non-uniformity that increased at faster walking speeds (up to 53% smaller in older adults at 1.20 m/s). We also add that those age-related differences are even larger in response to impeding forces designed to increase the mechanical demands for propulsion (age-related differences up to 63% during the impeding force condition). However, unlike our previous work which pooled young and older adults together, we believe separating age groups will better elucidate changes in the interaction between muscle and tendon and the resultant implications on ankle joint mechanical output.

In young adults, across changes in horizontal force, the magnitude of Achilles tendon non-uniformity positively correlated with larger differences in GAS vs. SOL muscle length change

behavior. However, these correlations were absent in older adults. Consistent with our previous results during fixed-end contractions (Clark & Franz, 2020), more uniform Achilles tendon tissue displacements in older adults coincided with a reduction in GAS vs. SOL muscle length change behavior. Moreover, we add that older adult muscle- and tendon-level behavior were significantly less sensitive to changes in horizontal force. We interpret these cumulative findings to suggest that the Achilles tendon facilitates independent triceps surae muscle actuation in young adults and restricts that actuation in older adults – likely through decreased capacity for sliding between adjacent subtendons. Indeed, compared to younger tendons, older tendons present with a proliferation of interfascicle adhesions which may underly prominent reductions in the capacity for sliding between adjacent subtendons (Thorpe et al., 2012, 2013). If more uniform Achilles tendon tissue behavior restricts triceps surae contractile behavior, our results suggests this primarily affects the GAS muscle-subtendon unit. In response to horizontal forces, GAS muscle length change behavior and superficial subtendon displacement (i.e., tissue associated with the GAS) was significantly reduced in older adults, while SOL muscle-subtendon behavior remained unchanged. Moreover, older adult GAS operating lengths were shorter than those of young adults, while SOL operating lengths were preserved (see Supplementary Information).

The mechanisms underlying age-related deficits in push-off intensity appear to be strongly influenced by triceps surae muscle-Achilles subtendon interaction. In young adults, the magnitude of GAS vs. SOL muscle length change behavior positively correlated with each measure of push-off intensity (i.e., peak ankle moment, power, and positive push-off work). In our view, these findings provide a mechanistic link for previously observed correlations between the magnitude of Achilles tendon tissue non-uniformity and ankle joint mechanical output. Consistent with our overarching hypothesis that more uniform Achilles tendon tissue displacements disrupts triceps

surae contractile behavior and thus ankle joint mechanical output, we did not observe any significant positive correlations between GAS vs. SOL muscle length change behavior and push-off intensity in older adults. Recently, we combined electromyography, ultrasound imaging, and musculoskeletal modeling in the same subjects and revealed that the biarticular gastrocnemius muscles play a more significant role than the uniarticular SOL in governing changes in forward propulsion in young adults (Clark et al., 2020). It follows that any disruption in muscle contractile behavior would deleteriously impact their relative contribution to forward propulsion, thereby affecting push-off intensity. Indeed, length is a critical determinant of muscle force production, and by extension, moment and power generation (Rubenson et al., 2012). However, it is important to note that conclusions based on muscle lengths alone are fundamentally incomplete as they relate to muscle-tendon force estimates (Dick et al., 2017; Gottschall & Kram, 2003). For example, the stretch and recoil of the Achilles tendon can produce substantial forces during the push-off phase of walking and likely governs the speed of ankle rotation as energy is returned, thus significantly impacting ankle moment and power generation (Lichtwark & Wilson, 2006; Orselli et al., 2017).

Our results may have important implications for the design and control of wearable assistive devices that attempt to overcome age-related deficits of forward propulsion. Our study suggests more uniform Achilles tendon tissue behavior may primarily affect the GAS muscle-subtendon unit. To date, the majority of studies disproportionate target the uniarticular SOL through the design and prescription of ankle exoskeletons (e.g., (Farris et al., 2013; Nuckols et al., 2020; Zhang et al., 2017)). At least one study has shown that exoskeleton configurations that mimic the biarticular GAS yield larger reductions in metabolic cost during walking than those that mimic the uniarticular SOL (Malcolm et al., 2018). Finally, our results may have implications on therapeutic techniques (e.g., hyaluronic acid injections (Abate, Schiavone, & Salini, 2014; Kaux

et al., 2015)), rehabilitation strategies (e.g., preferentially strengthen the GAS), or surgical techniques that seek to maintain or restore tendon function due to injury or the aging process (Pedowitz & Kirwan, 2013).

Cumulatively, our results suggest advancing age deleteriously impacts triceps surae muscle-Achilles tendon interaction, thereby reducing plantarflexor mechanical output. However, age-related changes to the neural drive may compound our mechanistic understanding of muscle-tendon interaction. In our study, with increasing ankle power, we observed a positive slope in young adults (i.e., GAS > SOL longitudinal length change) and a negative slope in older adults (i.e., GAS < SOL longitudinal length change). This difference may suggest that older adults utilize a different neural control strategy than young adults to meet the demand for greater push-off intensity, potentially with greater relative reliance on soleus muscle output. With age, Type II fiber physiological cross-sectional area, more commonly represented in the GAS, is reduced more than that of Type I fibers, more commonly represented in the SOL (Ishihara, Naitoh, & Katsuta, 1987; Larsson & Edstrom, 1986). Moreover, compared to young adults, older adults exhibit impaired muscle coordination and a loss of viable motor units (Miller et al., 2014). Together, these findings necessarily impact triceps surae muscle force generation in older adults, and even if homogenous across the triceps surae muscles, could themselves diminish non-uniform Achilles subtendon tissue displacements. Finally, we add that increased Achilles tendon tissue compliance due to aging may further diminish force transmission from the triceps surae muscles (Narici et al., 2008).

There are several important limitations to this study. First, this study uses a generalized approximation of triceps surae muscle-Achilles tendon anatomy that may not be fully captured using two-dimensional ultrasound imaging. For example, we only imaged the posteromedial SOL, which may differ from the anterior, posterior, medial, and lateral components (Chow et al., 2000).

Second, we have previously outlined limitations in our muscle (Clark et al., 2020) and tendon tracking techniques (Clark & Franz, 2018a; Franz & Thelen, 2015). For muscle, we attempted to mitigate errors in automated tracking by recording at a higher frame rate (76 fps) and performing frame-by-frame manual corrections of automated results (Aeles et al., 2017; Gillett et al., 2013; Kwah et al., 2013). For tendon, we attempted to mitigate motion artifacts by limiting our maximum walking speed to 1.2 m/s. Third, we only report subtendon tissue displacements, an outcome we can measure with a higher level of confidence than subtendon elongation. Estimating subtendon tissue elongation relative to the tendon insertion point on the calcaneus can be prone to errors (Csapo et al., 2013; Matijevich et al., 2018). Fourth, we made no attempt to estimate forces transmitted from individual muscles through individual subtendons, which are likely heterogeneous and highly complex (Bojsen-Moller & Magnusson, 2015). A future studying employing musculoskeletal simulations of muscle forces is warranted, although it is unclear if traditional modeling approaches (e.g., OpenSim (Delp et al., 2007)) have the biological complexity required to fully characterize inter-muscular and inter-subtendon differences. Finally, the majority of our conclusions are based on correlations that cannot definitively convey causal links.

CONCLUSION

In this study, we provide *in vivo* evidence that, during walking, older adults present with a significant reduction in Achilles tendon non-uniformity that is accompanied by smaller differences between medial gastrocnemius and soleus longitudinal muscle length change behavior. Moreover, we observed between-group differences in the extent to which muscle length change behavior and push-off intensity (i.e., moment, power, and positive push-off work) are correlated. Overall, we interpret our findings to suggest that the capacity for sliding between adjacent subtendons

facilitates independent triceps surae muscle actuation in young adults but restricts that actuation in older adults. The resultant disruption in triceps surae muscle contractile behavior likely contributes to hallmark reductions in push-off intensity during walking in older adults.

APPENDIX

Fascicle Operating Length

Average GAS and SOL fascicle operating lengths were unaffected by changes in speed (P-values ≥ 0.26, $\eta_p^2 \leq 0.080$), but decreased in response to increases in horizontal force (P-values < 0.05, $\eta_p^2 \geq 0.313$). Older adults had significantly shorter average GAS fascicle operating lengths than young adults (Speed: P < 0.05, $\eta_p^2 = 0.418$; Force: P < 0.05, $\eta_p^2 = 0.400$). Moreover, significant interactions revealed older adult GAS fascicle operating lengths were less sensitive to changes in horizontal force than that of younger adults (age×horizontal force, P < 0.05, $\eta_p^2 = 0.322$). Conversely, we did not observe a significant main effect of age on average SOL fascicle operating length (Speed: P = 0.18, $\eta_p^2 = 0.112$; Force: P = 0.27, $\eta_p^2 = 0.075$).

Muscle Fascicle Velocity

The magnitudes of peak GAS and SOL fascicle shortening velocity increased with increasing speed (P-values < 0.05, $\eta_p^2 \geq 0.180$) but were unaffected by horizontal forces (P-values ≥ 0.34, $\eta_p^2 \leq 0.065$). We did not observe a significant main effect of age on the magnitudes of peak GAS or SOL fascicle shortening velocity during conditions that altered speed (P-values ≥ 0.22, $\eta_p^2 \leq 0.091$). However, older adult GAS fascicle shortening velocity was significantly slower than young adults during conditions that altered horizontal force (P < 0.05, $\eta_p^2 = 0.236$); SOL fascicle shortening velocity was unaffected by age (P = 0.15, $\eta_p^2 = 0.127$).

CHAPTER 6: THE EFFECTS OF TRICEPS SURAE MUSCLE STIMULATION ON LOCALIZED ACHILLES SUBTENDON TISSUE DISPLACEMENTS

INTRODUCTION

A significant portion of the mechanical power needed to walk is generated by the triceps surae (Farris & Sawicki, 2012b). Individual muscles of the triceps surae (*i.e.*, medial gastrocnemius [MG], lateral gastrocnemius [LG], and soleus [SOL]) transmit their power through the architecturally complex Achilles tendon (AT). The AT is comprised of three distinct bundles of tendon fascicles (i.e., "subtendons") originating from each triceps surae muscle that twist as they descend and attach to the calcaneus (Edama et al., 2015; Szaro et al., 2009; van Gils et al., 1996). We (Clark & Franz, 2018a; Franz et al., 2015; Franz & Thelen, 2016) and others (Crouzier, Lacourpaille, Nordez, Tucker, & Hug, 2018; Slane & Thelen, 2014) have suspected that the presence of distinct subtendons may allow for some level of independent actuation among the individual triceps surae muscles when generating an ankle moment during functional activity. Indeed, many studies have revealed different neuromechanical contributions and contractile behaviors between the uniarticular soleus and biarticular gastrocnemius muscles during walking (Francis et al., 2013; Gottschall & Kram, 2003; Lenhart et al., 2014). However, a clear mechanistic link between the activation patterns of individual muscles of the triceps surae and the resultant displacement patterns of individual subtendons of the Achilles tendon has yet to be clearly defined. Establishing the neuromechanical independence of individual triceps surae muscle-tendon units

(MTUs) in healthy young adults is vital in understanding deleterious changes due to age and/or pathology.

Using *in vivo* ultrasound imaging, researchers have revealed non-uniform displacement patterns (i.e., greater displacement of SOL subtendon tissue vs. the MG/LG subtendon tissue) in the human Achilles tendon during passive ankle rotation, eccentric loading, and walking (Arndt et al., 2012; Franz et al., 2015; Slane & Thelen, 2014). We recently added that triceps surae muscle dynamics themselves may play a role in precipitating those characteristic non-uniform Achilles subtendon displacements patterns (Clark & Franz, 2018a). Specifically, using dual-probe ultrasound imaging, we revealed that differences in the magnitude of shortening between the MG and SOL positively correlated with differences in tissue displacements in their associated subtendons of the Achilles tendon during maximum voluntary isometric contractions. However, complex inter-muscular patterns of volitional activation may confound the interpretation of emergent subtendon tissue displacements. Tian et al. (2012) observed a direct lateral force transmission between the SOL and MG during passive knee motion, evident by significant SOL fascicle elongation during MG fascicle shortening, despite the uniarticular nature of the SOL (Tian et al., 2012). As a result, equal force transmission by the MG and SOL is unlikely, requiring a specific level of unequal muscle activation to occur. Moreover, compared to the MG and LG, the SOL has greater muscle volume and force-generating capacity, possibly resulting in a disproportionate influence on Achilles subtendon tissue displacements (Albracht et al., 2008; Ogihara et al., 2017). Thus, to control for these potentially confounding factors and to improve the understanding of how triceps surae muscles precipitate non-uniform tendon tissue behavior, there is a clear need to control for muscle activation.

Electrical stimulation provides a non-invasive tool to bypass volitional muscle activation and establish mechanistic causal links between triceps surae force transmission and resultant Achilles subtendon tissue displacement. Using electrical muscle stimulation, Maas et al. (2020) demonstrated that Achilles subtendons have some ability to slide independently in Wistar rats (Maas et al., 2020). Their findings suggested that a combination of differential triceps surae muscle loading, ankle angle, and knee angle affected Achilles subtendon strain, magnitude of displacement, and the magnitude of non-uniformity. Despite these findings, the anatomical differences between rats and humans may confound our interpretation of emergent subtendon tissue displacements. In addition, the Wistar rats were partially dissected to allow for sutures to be placed within the Achilles tendon potentially disrupting the *in situ* behavior of the muscle-subtendon units which may affect the generalizability of the results. However, to our knowledge, no study to date has leveraged electrical muscle stimulation to regulate individual muscle activation while measuring the *in vivo* Achilles subtendon tissue response in human subjects.

The goal of this study was to leverage electrical muscle stimulation to quantify the effects of activation to individual triceps surae muscles on localized Achilles subtendon tissue displacements. Here, we controlled the magnitude of force transmission of individual triceps surae muscles during isometric contractions at various ankle angles and recorded the resultant Achilles subtendon displacements using cine B-mode ultrasound imaging. We hypothesized that electrical stimulation of individual triceps surae muscles would elicit larger displacements in their associated regions of the Achilles tendon. We also tested the secondary hypothesis that the relationship between individual and differential (SOL – MG) subtendon displacements would vary with ankle angle, which we would interpret in the context of muscle-tendon unit slack (Hug et al., 2013; C.

L. Liu et al., 2020) and posture-dependent changes in force transmission (Davis, Kaufman, & Lieber, 2003; Landin, Thompson, & Reid, 2015).

METHODS

Subjects

Sixteen healthy young subjects met our inclusion/exclusion criteria and provided written informed consent as per the University of North Carolina at Chapel Hill Institutional Review Board (16–0379). Participants had no musculoskeletal injuries over the previous six months and did not have a history of neuromuscular disease. We excluded six subjects during our quality control process for being unable to produce requisite peak ankle moments without discomfort elicited by electrical stimulation (n=2), protocol deviations which affected the prescribed torque or analog synchronization (n=2), or poor ultrasound image quality (n=2). Thus, we report data for 10 subjects (age: 22.5±2.2 years, mass: 67.8±9.21 kg, height: 1.72±0.08 m, 7 females).

Electrical Simulation Equipment and Protocol

Stimulating surface electrodes were place on subjects' right lower leg (Figure 24). Specifically, two DONECO stimulating electrodes (~50 x 50 mm with an interelectrode distance of 5 mm) were placed over the muscle bellies of the medial gastrocnemius (MG) and the posterolateral aspect of the soleus (SOL), nearest the site that elicited the largest twitch contraction under stimulation (Figure 24). We respectively aligned each pair of stimulating electrodes in the direction of the muscle fascicles (Hermens et al., 2000). Subjects first completed a 6-minute warm up walk on a treadmill (Bertec Corp., Columbus, OH) at 1.2 m/s to precondition muscle-tendon units spanning their ankles (Hawkins et al., 2009).

Thereafter, subjects sat in a dynamometer (Biodex System 4 Pro, Biodex Medical Systems, Shirly, NY) with their trunk flexed to ~85° and knee flexed to 20°, the latter replicating the joint posture during the push-off phase of walking (Chao, Laughman, Schneider, & Stauffer, 1983). Subjects first performed 3 maximum voluntary isometric contractions (MVIC) with their ankle at 20° plantarflexion. In pilot testing, this joint posture was determined to be the most uncomfortable during electrical stimulation, and thus ensured that subjects could accommodate the establish stimulus intensities for all conditions. At this joint posture, we determined the stimulation intensities (i.e., $Stim_{MG}$ and $Stim_{SOL}$) necessary for the MG or SOL to respectively produce 7.5% of the average peak net ankle moment generated from the three MVICs. We applied stimulation (Grass Instruments S48 Square Pulse Stimulator, A-M Systems, Carlsborg, WA) using 300 μs pulses at 33 Hz according to published recommendations (Merletti, Knaflitz, & DeLuca, 1992). We chose 7.5% MVIC since this value produced a measurable net ankle moment (≥4 Nm) without undue discomfort. We matched the desired ankle moment to preserve force transmission through the Achilles tendon across all conditions, thereby placing our interpretations in the context of constant force transition, despite known differences in muscle force-generating capacity (Bojsen-Moller, Schwartz, Kalliokoski, Finni, & Magnusson, 2010). In another condition, we prescribed simultaneous stimulation intensities (i.e., $Stim_{BOTH}$) that produced 15% MVIC peak net ankle moment (i.e., twice that of the individual muscles) using the same voltage ratio from the individual stimulation conditions and a potentiometer to resist the voltage applied to the muscle with the larger net ankle moment response. After all the trials were completed, the subjects then performed 3 MVICs again, which was later used to assess whether muscle fatigue occurred as a result of electrical stimulation.

After determining the voltages necessary to achieve 7.5% and 15% MVIC ankle moment, we maintained those voltages during all subsequent ankle joint postures. Specifically, at three ankle joint angles (i.e., 20° dorsiflexion, neutral [0°], and 20° plantarflexion), each subject underwent 2 sets of 3 electrical stimulation conditions: $Stim_{MG}$, $Stim_{SOL}$, and $Stim_{BOTH}$. In addition, subjects performed two volitional contractions (VOL) at each ankle joint posture using ankle moment biofeedback. Here, subjects volitionally matched the ankle moment generated by the dual stimulation condition using a screen positioned in front of the dynamometer that projected their instantaneous ankle moment and a target line representing the dual stimulation target moment (i.e., 15% MVIC). After a brief period of practice, subjects steadily increased their instantaneous ankle moment over 1 second, reached the target line, and then steadily returned to rest over 1 second. Between conditions, subjects rested for at least 1 minute. We block randomized ankle joint postures and experimental conditions as an additional measure to mitigate fatigue effects.

Electromyographic Measurements

We placed wireless Delsys Trigno recording electrodes over the lateral gastrocnemius (LG), MG, and SOL muscle bellies near the stimulating electrodes and closest to Seniam recommendations (Hermens et al., 2000). During stimulation, we were unable to measuring muscle activation via recording electrodes due to signal saturation, which occurred at ±2.5 V. Thus, we performed a low voltage sweep condition to estimate intermuscular excitation (e.g. $STIM_{MG}$ stimulating SOL muscle fibers) between the LG, MG, and SOL. Specifically, we applied a continuous 300 μs pulse train at 33 Hz that gradually increased from 0 V to 2.5 V. The low voltage sweep was applied to the MG and SOL at each ankle joint posture. We truncated and full wave rectified the measured LG, MG, and SOL muscle activations between 0.75±0.05 V to 2.25±0.05 V and segmented the ~30 second collection into 250 ms blocks. Within each block, we determined

the activation ratios between the LG, MG, and SOL by comparing peak EMG values. For each muscle being stimulated (i.e., MG and SOL), Pearson's correlation coefficients determined the relation between stimulation intensity (i.e., voltage) and measured activation ratios.

Ultrasound Measurements

A 7 MHz 38-mm linear array ultrasound transducer (L14-5W/38, Ultrasonix Corporation, Richmond, BC) operating at 155 frames/s recorded 128 lines of ultrasound radiofrequency (RF) data from subjects' right free Achilles tendon (AT). The transducer was placed ~6 cm distal to the SOL muscle tendon junction and was secured via a custom orthotic (Franz et al., 2015). A two-dimensional (2D) speckle tracking algorithm estimated localized displacements of AT tissue using previously published techniques (Chernak & Thelen, 2012; Chernak Slane & Thelen, 2014). In brief, we placed a rectangular region of interest (ROI) ~15 x 3 mm on a B-mode ultrasound image of the free AT at rest. The ROI contained a grid of nodes with 0.83 x 0.42 mm spacing defined to encompass only tendinous tissue. A 2 mm x 1 mm kernel containing up-sampled (4x) RF data, centered at each nodal position, provided a search window over which we defined 2D normalized cross-correlation functions between successive frames. We defined localized frame-to-frame nodal displacements that maximized these 2D cross-correlations, with the cumulative displacement representing the average of forward and backward tracking results. Subtendon tissue displacements were determined by averaging the displacements of nodes arising from two equally size tendon depths, superficial and deep, corresponding to the part of the Achilles anatomically considered to originate from the MG and SOL, respectively. Although many studies have acknowledged variation in AT architecture, our reported orientation, with equal sized MG and SOL subtendons, represents the majority of anatomical observations in cadaveric studies (Del Buono et al., 2013; Edama et al., 2015; Szaro et al., 2009; van Gils et al., 1996).

Data Reduction and Analysis

We filtered peak ankle moment and subtendon displacement data using a 4th order Butterworth filter with a cutoff frequency of 12 Hz. Binary analog signals originating from the ultrasound and Grass stimulator were used to synchronize ultrasound imaging with stimulation onset and torque generation. We analyzed all data between "key-frames" signifying the start and end of the trial. For the volitional condition, key-frames represented the onset and offset of ankle moment generation using a 5% threshold based on that conditions peak value. For the electrical stimulation conditions, the start key-frame represented the onset of stimulation and end key-frame used an analogous 5% threshold.

Statistical Analysis

Statistical analyses were performed using SPSS Statistics 26 (SPSS, Chicago, IL). We performed a two-way (condition×ankle posture) repeated measures analysis of variance (ANOVA) for each of the following primary outcome measures: peak ankle moment, peak SOL subtendon displacement, peak MG subtendon displacement, and Achilles tendon non-uniformity (i.e., peak SOL subtendon displacement – peak MG subtendon displacement). We also performed a one-way (ankle posture) repeated measures ANOVA on passive ankle moment. When a significant main effect or interaction was found, we performed Tukey's post-hoc pairwise comparisons to assess differences between condition and ankle joint posture. Effect sizes are reported as η_p^2 and Cohen's d for main effects and pairwise comparisons, respectively.

We used a combination of two mixed models to determine if generated ankle moment was a governing factor in measured tendon non-uniformity. We used a generalized linear mixed model with condition and ankle posture as fixed factors and generated moment as a random factor. In addition, we used a linear mixed model to estimate effect sizes of fixed and random factors. One-

sided paired student's t-tests were performed to determine if there was fatigue due to electrical stimulation by testing if subject's average post collection MVICs was less than their averaged pre collection MVICs. Paired student's t-test was also performed to determine if EMG activation ratios would be preserved across a range of stimulation voltages by comparing Pearson's correlation coefficients of activation ratios (MG/LG/SOL) to 0. For all comparisons, we defined significance using an alpha level of 0.05.

RESULTS

All results are reported as mean ± standard deviation. Tabulated descriptive statistics are provided in Table 3.

Peak Ankle Moment

We found no difference between baseline MVIC moments (81.3±21.8 Nm) and those measured at the end of the session (73.2±16.3 Nm) ($p=0.194$). Ankle posture had a significant main effect on passive ankle moment ($F_{2,18}=18.135$, $p<0.001$, $\eta_P^2=0.668$), with significant pairwise increases from 20° plantarflexion to 20° dorsiflexion (p-values≤0.012, d≥0.441, Figure 25). However, we found no significant main effect of ankle posture ($F_{2,16}=2.398$, $p=0.123$, $\eta_P^2=0.231$) or significant posture×condition interaction ($F_{2,16}=1.5$, $p=0.252$, $\eta_P^2=0.158$) on peak ankle moment. There was a main effect of condition ($F_{3,24}=18.283$, $p<0.001$, $\eta_P^2=0.696$) on peak ankle moment. However, as designed, pairwise comparisons revealed no significant differences between single muscle stimulation conditions (i.e., $STIM_{MG}$ vs. $STIM_{SOL}$) (p-values≥0.176, d≤0.456) nor between $STIM_{BOTH}$ and VOL (p-values≥0.081, d≤0.222) at any ankle posture (Figure 26A).

Individual Subtendon Tissue Displacements

Time normalized, group average subtendon displacement patterns are depicted in Supplementary Figure 4. We found significant main effects of ankle posture (MG: $F_{2,16}$=14.418, p<0.001 η_P^2=0.643; SOL: $F_{2,16}$=21.041, p<0.001, η_P^2=0.725) and condition (MG $F_{2,14}$=6.797, p=0.011, η_P^2=0.459, and SOL $F_{3,24}$=10.041, p<0.001, η_P^2=0.557) along with a significant interaction (MG: $F_{6,48}$=4.168, p=0.002, η_P^2=0.343; SOL: $F_{6,48}$=6.789, p<0.001, η_P^2=0.459) for individual (MG/SOL) subtendon tissue displacements. Pairwise comparisons revealed significantly larger subtendon displacements for $STIM_{BOTH}$ compared to all other experimental conditions (p-values≤0.029, d≥1.084) at 20° plantarflexion (20°) and a neutral ankle angle (0°) as shown in Figure 26B.

Subtendon Tissue Non-Uniformity

Time normalized, group average non-uniform displacement patterns are depicted in Supplementary Figure 5. Although we found no significant main effect of ankle posture ($F_{2,16}$=2.288, p=0.134, η_P^2=0.222) nor a significant condition×posture interaction ($F_{2,14}$=2.685, p=0.107, η_P^2=0.251) on subtendon non-uniformity, we found a significant main effect of condition ($F_{2,16}$=7.479, p=0.005, η_P^2=0.483). At 20° plantarflexion, pairwise comparisons revealed significantly larger subtendon non-uniformity arising from $STIM_{SOL}$ vs. $STIM_{MG}$ (p=0.004, d=0.869, Figure 26C). At neutral ankle angle, non-uniformity was significantly smaller for $STIM_{SOL}$ compared to VOL (p=0.039, d=0.608). In addition, non-uniformity arising from $STIM_{MG}$ was significant smaller than $STIM_{BOTH}$ and VOL conditions (p-values≤0.003, d≥0.925).

Using the generalized linear mixed model, we determined that peak moment had no significant effect on subtendon non-uniformity (p=0.092). Moreover, a linear mixed model yielded

larger estimated effect sizes for fixed factors (condition and ankle posture; 0.500±0.051; $p<0.001$) compared the random factor (peak moment; 0.310±0.040).

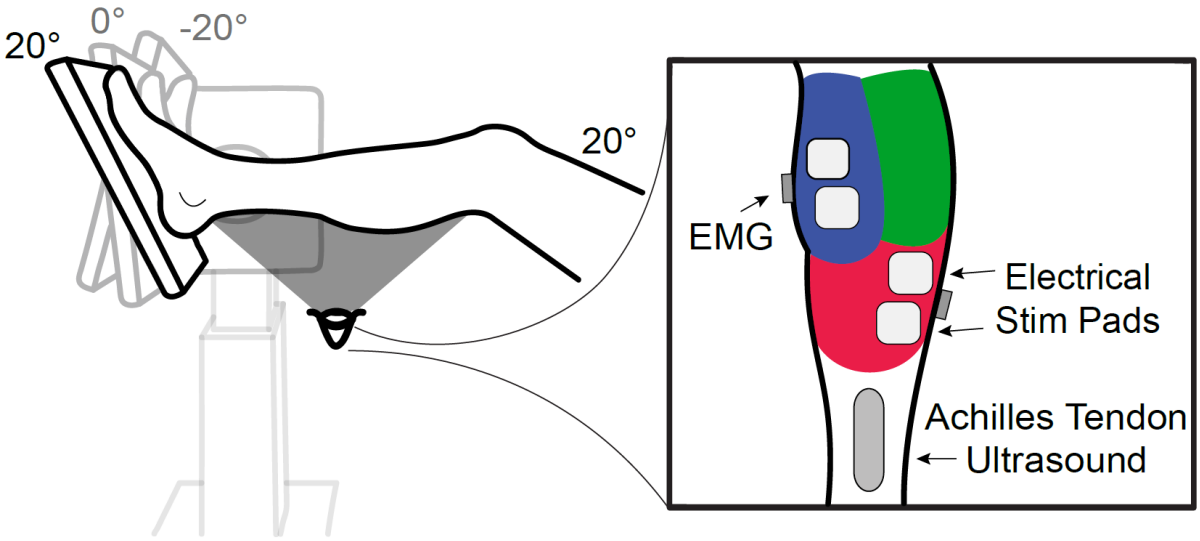

Figure 24: Depiction of experimental setup illustrating a typical subject's right medial gastrocnemius (MG-blue), lateral gastrocnemius (green), and soleus (SOL-red). With the knee flexed to 20°, surface electrodes stimulated the MG and/or SOL muscles at three different ankle postures (20° plantarflexion, 0°, and 20° dorsiflexion) while ultrasound recorded Achilles subtendon tissue displacements.

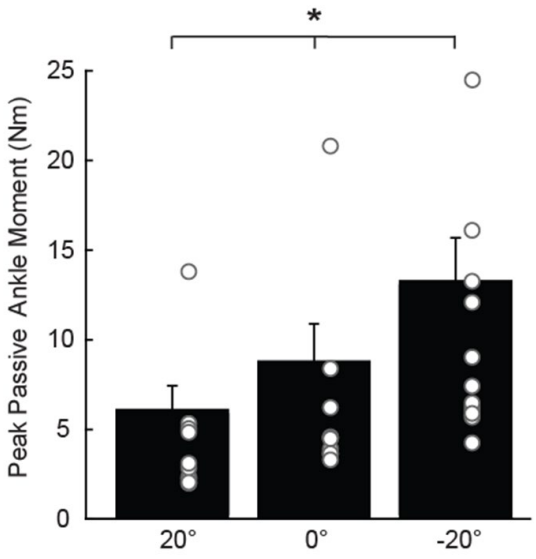

Figure 25: Group mean peak passive ankle moment (SD) for each ankle posture. Individual data points represented by open grey circles. Asterisks (*) represent significant differences between ankle postures ($p<0.05$).

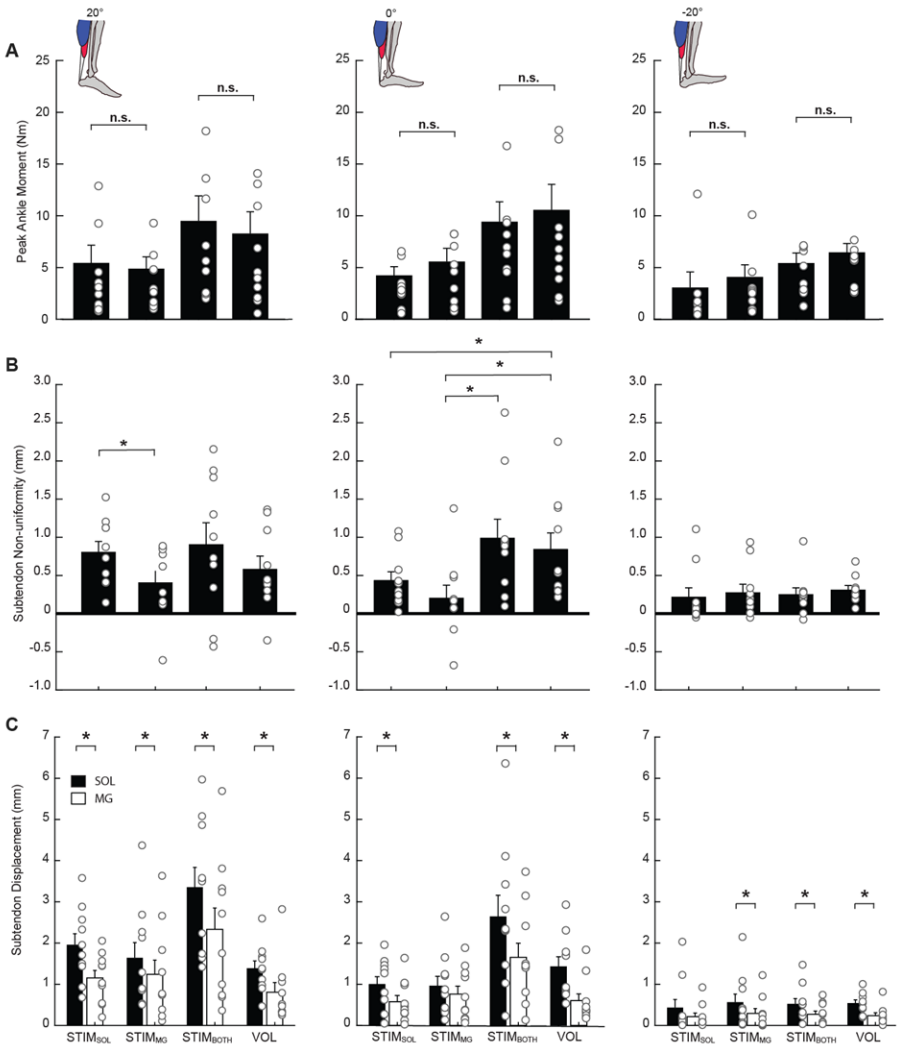

Figure 26: Mean (SD) of peak ankle moment (A), peak differential displacement (B), and peak individual subtendon displacement (C) for each experimental condition at each ankle posture. Individual data points represented by open grey circles. Consistent with our experimental design, non-significant differences between experimental conditions with similar torque targets ($STIM_{MG}$ vs. $STIM_{SOL}$ and $STIM_{BOTH}$ vs. VOL) are denoted n.s. ($p>0.05$). Asterisks (*) represent significant differences between ankle postures ($p<0.05$).

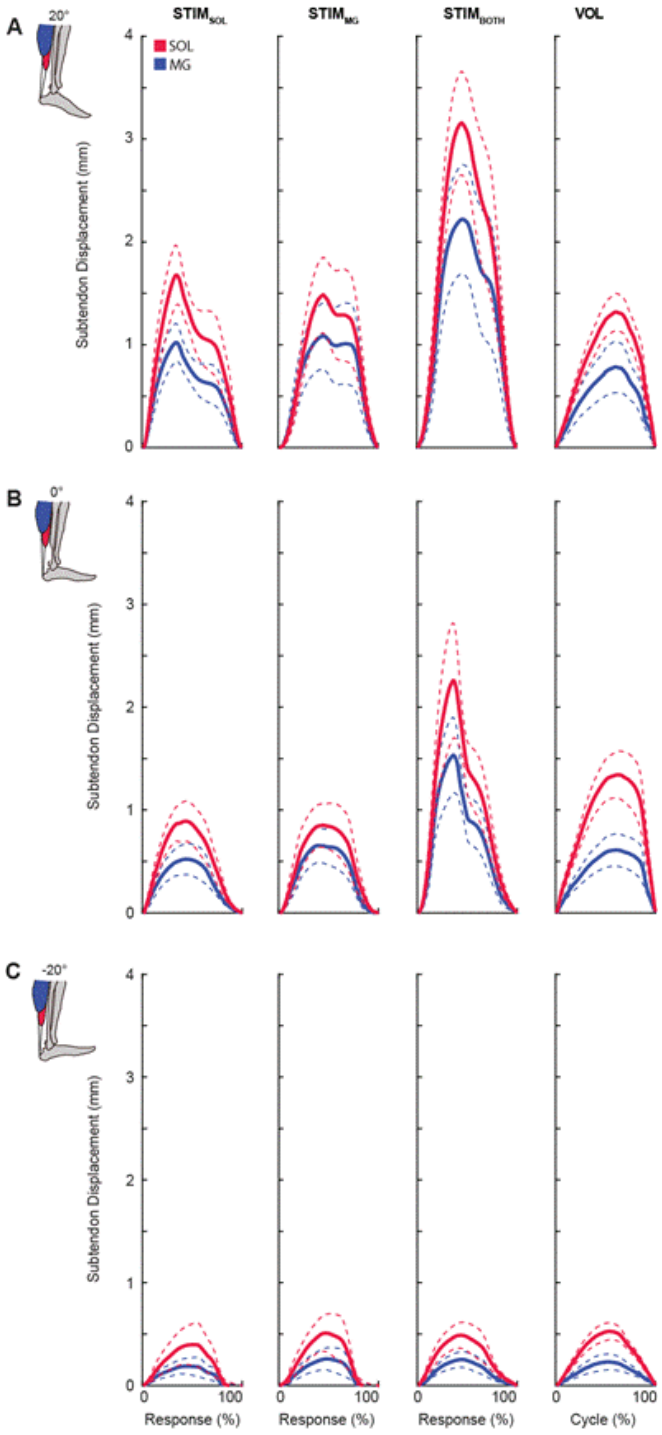

Supplementary Figure 4: Time normalized, group mean (SD) displacement patterns of the medial gastrocnemius subtendon (blue) and soleus subtendon (red) for each experimental condition at 20° plantarflexion (A), 0° neutral ankle angle (B), and 20° dorsiflexion (C).

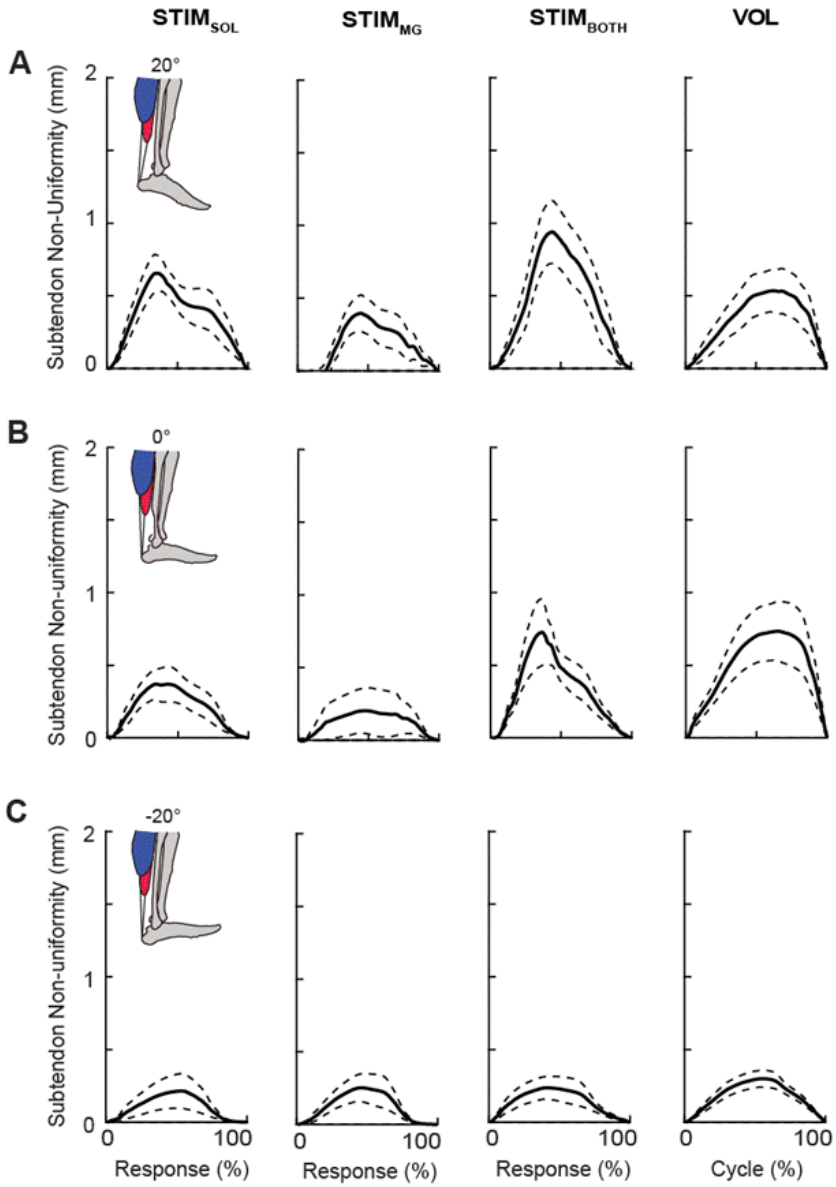

Supplementary Figure 5: Time normalized, group mean (SD) subtendon non-uniformity for each experimental condition at 20° plantarflexion (A), 0° neutral ankle angle (B), and 20° dorsiflexion (C).

Table 3.
Summary statistics for peak tendon non-uniformity and individual subtendon displacements across ankle angles and conditions.

	20°				0°				-20°			
	$STIM_{SOL}$	$STIM_{MG}$	$STIM_{BOTH}$	VOL	$STIM_{SOL}$	$STIM_{MG}$	$STIM_{BOTH}$	VOL	$STIM_{SOL}$	$STIM_{MG}$	$STIM_{BOTH}$	VOL
Non-Uniformity	0.81±0.44*	0.41±0.48†	0.91±0.90	0.58±0.54	0.44±0.36	0.21±0.53	0.99±0.78*	0.84±0.67*†	0.22±0.38	0.28±0.34	0.25±0.27	0.31±0.18
SOL	**1.96±0.89**	**1.64±1.23**	**3.36±1.59**	**1.39±0.59**	**1.00±0.61**	0.96±0.76	**2.64±1.72**	**1.43±0.78**	0.43±0.66	**0.56±0.66**	**0.52±0.43**	**0.54±0.26**
MG	**1.15±0.60**	**1.24±1.15**	**2.33±1.72**	**0.81±0.78**	**0.58±0.49**	0.76±0.64	**1.65±1.14**	**0.60±0.54**	0.21±0.28	**0.29±0.39**	**0.27±0.26**	**0.24±0.24**

Summary statistics shown are mean±SD, * indicates significant differences within ankle angle compared to $STIM_{MG}$, † indicates significant differences within ankle angle compared to $STIM_{SOL}$, significant differences between SOL and MG of the same ankle angle and conditions are **bold**
SOL: Soleus, MG: Medial Gastrocnemius, BOTH: SOL+MG, VOL: Volitional, Non-Uniformity: SOL-MG,

DISCUSSION

In this study, we quantified the effects of triceps surae muscle activation on localized Achilles subtendon displacement patterns using targeted electrical muscle stimulation and cine B-mode ultrasound imaging. Moreover, we controlled for peak ankle moment between analogous conditions (i.e., $STIM_{MG}$ vs. $STIM_{SOL}$ and $STIM_{BOTH}$ vs. VOL) to preserve force transmission through the Achilles tendon, thereby placing our interpretations in the context of constant force transmission despite known differences in muscle force-generating capacity (Crouzier et al., 2018; Fukunaga, Roy, Shellock, Hodgson, & Edgerton, 1996; Kinugasa, Kawakami, & Fukunaga, 2005). Together, this paradigm provides a first step toward establishing a mechanistic link between muscle activation and non-uniform displacement patterns within the Achilles tendon. In partial support of our first hypothesis, electrical stimulation of individual triceps surae muscles elicited larger relative displacements in their associated regions of the Achilles tendon, at least when the ankle was in plantarflexion. Moreover, in support of our second hypothesis, we found that the relationship Achilles tendon non-uniformity (SOL – MG subtendon tissue displacements) was sensitive to ankle joint posture. As we elaborate below, these findings point to at least some neuromechanical independence in actuation between the human triceps surae muscle-tendon units.

In this study, we sought empirical data associated with the relative independence of triceps surae muscle-subtendon units in response to muscle stimulation during fixed-end contractions. Interestingly, independent of posture or condition, SOL subtendon tissue displaced, on average, more than MG subtendon tissue. Larger relative tissue displacements in the SOL subtendon is most likely multifactorial in nature. For example, such behavior may arise from differences between gastrocnemius and SOL muscle- and/or subtendon tissue morphology or mechanical properties. At the muscle-level, the human SOL has far greater force-generating capacity than the MG and

LG (Albracht et al., 2008), and exhibits greater magnitudes of fascicle shortening and rotation during muscle action (Clark & Franz, 2018a). Likely as a result, in a similar study using electrical stimulation on rat muscle-tendon units at similar knee angles, Maas et al. (2020) only observed greater LG subtendon displacement than SOL subtendon displacement when both biarticular gastrocnemius muscles were stimulated (Maas et al., 2020) – a condition not tested in this study. Moreover, differences in mechanical properties (e.g., stiffness) are a plausible determinant for consistently larger displacements in the SOL subtendon. Using electrical stimulation in an animal model, Finni et al. (2018) found that the SOL subtendon undergoes greater strain during SOL muscle stimulation (8.4%) compared to the MG subtendon under equivalent MG muscle stimulation (4.7%). The authors attribute the differences in subtendon strain arising from isolated activation to differences in subtendon stiffness; namely, that the SOL subtendon is more compliant than its gastrocnemius counterparts (Finni et al., 2018). Similar to our findings, during MG stimulation, they observed equal displacements in SOL and MG subtendons. However, these differences are unlikely to fully explain our findings, particularly for conditions designed for isolated MG stimulation. Indeed, the interfascicular matrix of the Achilles tendon unevenly distributes forces between adjacent subtendons (Thorpe et al., 2015; Thorpe, Riley, Birch, Clegg, & Screen, 2016), with possible preference for the more compliant SOL subtendon in order to reduce the risk of injury.

Despite consistently larger tissue displacements in the SOL subtendon, variations in subtendon non-uniformity (i.e., SOL subtendon – MG subtendon) were sensitive to stimulation condition, particularly at 20° plantarflexion. Peak subtendon non-uniformity, on average, decreased (-60.9%) from plantarflexion to dorsiflexion. At 20° dorsiflexion, we did not observe significant differences between any stimulation conditions, likely due to an increase in passive

tension. Using shear wave elastography, Hug et al. (2013) reported larger triceps surae MTU passive tension with ankle dorsiflexion (Hug et al., 2013). Moreover, Liu et al. (2020) reported up to four-fold increase in triceps surae MTU stiffness as the ankle moves from plantarflexion to dorsiflexion (C. L. Liu et al., 2020). Perhaps accordingly, we found no $STIM_{MG}$ vs. SIM_{SOL} effects on subtendon non-uniformity at 0° (i.e., neutral) or 20° dorsiflexion. An increase in passive MTU tension would yield smaller subtendon tissue displacements for the same level of force transmission, consistent with our observations. Indeed, an increase in relative force transmission during the $STIM_{BOTH}$ and VOL condition, despite greater passive MTU tension, resulted in significantly greater levels of subtendon non-uniformity than $STIM_{MG}$ and SIM_{SOL} at our 0° neutral angle.

Conversely, when subtendon tissue displacements were largest and passive tension smallest (i.e., 20° plantarflexion), $STIM_{SOL}$ elicited significantly larger (+49.4%) tendon non-uniformity than that of $STIM_{MG}$. Although it was positive for all conditions, the magnitude of non-uniformity varied in anatomically consistent ways to individual triceps surae muscle activation. Moreover, these findings provide a mechanistic causal link between previously observed correlations between triceps surae muscle dynamics and non-uniform Achilles tendon tissue displacements during maximum isometric contractions (Clark & Franz, 2018a). Accordingly, this *in vivo* evidence points to at least some neuromechanical independence in actuation between the human triceps surae muscle-tendon units – with potentially implications on walking performance. Indeed, many studies have suggested the gastrocnemius and SOL muscles contribute differently to forward propulsion and vertical support during walking – evidenced by different changes in activation (e.g., (Clark et al., 2020; Gottschall & Kram, 2003; Miyoshi et al., 2006)) and fascicle length behavior (e.g., (Clark et al., 2020; Cronin et al., 2013)) in response to altered task demand.

Although necessary to abate subject discomfort, the prescribed ankle moment in our study of 7.5% and 15% of subjects' MVIC may not be representative of physiological loading during dynamic activity. Very recently, during volitional plantarflexion tasks, Wolfram et al. (2020) only observed subtendon non-uniformity after subjects reached 30% of their MVIC moment (Wolfram, Hodson-Tole, Morse, Winwood, & McEwan, 2020). However, it is important to note that Wolfram et al. used muscle-tendon junction (MTJ) kinematics which may not be representative of Achilles subtendon tissue displacements due to unaccounted for anatomical complexity distal to the MTJ (DeWall, Slane, Lee, & Thelen, 2014). Nevertheless, it is plausible that our study's prescription of force transmission, less than that generally expected during physiologically loading, may prevent definitive extrapolations to more functional activities such as walking. Indeed, peak moment values during walking average roughly 60 Nm to 166 Nm depending on walking speed (Hof, Van Zandwijk, & Bobbert, 2002), at least five times higher than our torque values (<11 Nm) during $STIM_{SOL}$ and $STIM_{MG}$ conditions. Compared to the relatively low peak ankle moments prescribed in our study design, we suspect that individual SOL versus MG stimulation would have larger disparate effects on tendon non-uniformity at higher levels of force generation, independent of ankle posture.

Establishing a baseline understanding of the relation between individual triceps surae muscle activation and resultant Achilles subtendon displacement patterns have important implications in the study of gait and mobility limitations. For example, we recently revealed that older adults have more uniform subtendon tissue displacements during MVIC tasks that extend to anatomically consistent and potentially unfavorable changes in muscle contractile behavior (Clark & Franz, 2020). An electrical stimulation protocol, ideally with greater force generation, could elucidate age-related mechanism by which (*i*) muscle-level behavior is restricted by tendon-level

behavior (via interfascicle adhesions and collagen crosslinking) (Narici et al., 2008) or (*ii*) tendon-level behavior is a result of changes in muscle-level behavior (via changes in protein biology, muscle coordination, and loss of viable motor units) (Miller et al., 2014). This research may be crucial in developing intervention techniques and diagnostic tools to help improve older adults' quality of life and well-being. As another example, these results could help inform procedures that surgically repair ruptured Achilles tendons or in response to other tendon injuries.

There are several limitations of this study. First, we only matched activation ratios between stimulation conditions at 20° plantarflexion. However, we did not observe any significant differences between peak moment of similar conditions (i.e., $STIM_{MG}$ vs. $STIM_{SOL}$ and $STIM_{BOTH}$ vs. VOL) at any ankle posture. Second, we only report isolated stimulation of the MG and SOL, along with a generalized anatomical approximation of the MG and SOL subtendons. Third, our 2D ultrasound imaging technique does not fully capture the complex 3D motion of the Achilles tendon which could lead to underestimating gross subtendon displacements. Likewise, we have previously described the limitations of the 2D speckle tracking estimates of Achilles subtendon displacements (Franz et al., 2015). Fourth, we cannot ensure isolated stimulation of the intended muscle (MG/SOL) due to nature of surface stimulating electrodes and EMG saturation. However, at voltages below EMG saturation we achieved large differential muscle activation (≥10:1). Fifth, researchers have demonstrated that force transmission occurs between adjacent triceps surae muscle bellies (Bojsen-Moller et al., 2010; Huijing, Maas, & Baan, 2003; Tian et al., 2012) and can increase with increased muscle activation (Finni et al., 2017; Tijs, van Dieen, Baan, & Maas, 2016). These complex mechanics of intermuscular force transmission may make drawing concrete conclusions difficult. However, with equal levels of force transmission between experimental conditions at the same ankle posture it is likely that the effect of force transmission would be also

be similar between conditions. Finally, we note that during experimental conditions, ankle posture may have shifted slightly (<3 degrees), which likely had a negligible effect on observed displacement patterns due to the low level of peak ankle moment during conditions (<11 Nm).

CONCLUSION

Our results suggest that localized tissue displacements within the architecturally complex Achilles tendon respond in anatomically consistent ways to different patterns of triceps surae muscle activation but are highly susceptible to changes in ankle joint posture. Accordingly, this *in vivo* evidence points to at least some neuromechanical independence in actuation between the human triceps surae muscle-subtendon units. Our research may be important in establishing a baseline of individual triceps surae muscle contributions to subtendon displacement patterns that will facilitate a deeper understanding of deleterious pathologies due to aging, tendon injury, or surgical intervention, which may have important implications in the design and implementation of clinical interventions to improve tendon health and preserve/restore mobility.

CHAPTER 7: CONCLUSIONS

The first purpose of this dissertation was to determine the role of triceps surae muscle contractile dynamics in governing non-uniform Achilles tendon displacement patterns in young and older adults. The second purpose of this proposal was to quantify the effects of aging on triceps surae muscle-Achilles tendon interaction and the resultant implications on ankle joint mechanical output during walking.

Study One

In my first study, we presented evidence that triceps surae muscle dynamics may precipitate non-uniform displacement patterns in the architecturally complex Achilles tendon. Moreover, we used a dual-probe imaging approach to empower simultaneous assessment of muscle and tendon toward an improved mechanistic understanding of triceps surae behavior. Our findings may be important for understanding age-associated changes in AT displacement patterns, which we suspect alter muscle contractile behavior in older adults.

Study Two

As an important step toward establishing mechanistic causal links, the purpose of this study was to investigate aging effects on the relation between non-uniform Achilles subtendon displacement patterns and triceps surae muscle contractile behavior using dual-probe ultrasound imaging during a series of ramped maximum isometric voluntary contractions. Here, we reveal that more uniform Achilles subtendon tissue displacements in older versus young adults extend to anatomically consistent and potentially unfavorable changes in muscle contractile behavior –

evidenced by smaller differences between GAS and SOL peak shortening during isometric force generation. Foremost, these findings provide an important biomechanical basis for previously reported correlations between more uniform Achilles subtendon behavior and reduced ankle moment generation during waking in older adults. Additional mechanistic insight into the causal relations underlying these changes are required before advocating for any specific clinical countermeasure. For example, conventional therapies prompting changes from the muscle down may be designed to promote independent actuation of individual triceps surae muscles. Alternatively, to promote changes from the tendon up, there is some support for the use of hyaluronic acid and/or lubricin injection to maintain and restore tendon homeostasis during the aging process (Kaux et al., 2015).

Study Three

In my third study, we sought to quantify inter-muscular differences in the response of the gastrocnemius and soleus muscles to changes in forward propulsion by assessing muscle activation, contractile behavior, and model-predicted estimates of force and positive mechanical work. By combining electromyography, ultrasound imaging, and musculoskeletal modeling in the same subjects, this study provides the most complete report to date of the relative contributions of the gastrocnemius and soleus muscles to forward propulsion during walking. Based on consistent evidence from empirical measurements and musculoskeletal simulations, we conclude that the biarticular gastrocnemius muscles play a more significant role than the uniarticular soleus in governing changes in forward propulsion during the push-off phase of walking. Our results may have important implications for the prescription of targeted therapeutics and for the design and control of wearable assistive devices.

Study Four

In this study, we provide *in vivo* evidence that, during walking, older adults present with a significant reduction in Achilles tendon non-uniformity that is accompanied by smaller differences between medial gastrocnemius and soleus longitudinal muscle length change behavior. Moreover, we observed between-group differences in the extent to which muscle length change behavior and push-off intensity (i.e., moment, power, and positive push-off work) are correlated. Overall, we interpret our findings to suggest that the capacity for sliding between adjacent subtendons facilitates differences in gastrocnemius versus soleus muscle shortening in young adults but restricts those differences in older adults. The resultant disruption in triceps surae muscle contractile behavior likely contributes to hallmark reductions in push-off intensity during walking in older adults.

Study Five

The goal of this final study was to leverage electrical muscle stimulation to quantify the effects of activation to individual triceps surae muscles on localized Achilles subtendon tissue displacements. Our results suggest that localized tissue displacements within the architecturally complex Achilles tendon respond in anatomically consistent ways to different patterns of triceps surae muscle activation but are highly susceptible to changes in ankle joint posture. Accordingly, this *in vivo* evidence points to at least some neuromechanical independence in actuation between the human triceps surae muscle-subtendon units. Our research may be important in establishing a baseline of individual triceps surae muscle contributions to subtendon displacement patterns that will facilitate a deeper understanding of deleterious pathologies due to aging, tendon injury, or surgical intervention, which may have important implications in the design and implementation of clinical interventions to improve tendon health and preserve/restore mobility.

APPENDIX 1: ACTIVATION-DEPENDENT CHANGES IN SOLEUS LENGTH-TENSION BEHAVIOR AUGMENT ANKLE JOINT QUASI-STIFFNESS[4]

The triceps surae muscle-tendon units are important in governing walking performance, acting to regulate mechanical behavior of the ankle through interaction between active muscle and passive elastic structures. Ankle joint quasi-stiffness (the slope of the relation between ankle moment and ankle rotation, k_A), is a useful aggregate measure of this mechanical behavior. However, the role of muscle activation and length-tension behavior in augmenting k_A remains unclear. Here, 10 subjects completed eccentric isokinetic contractions at rest and at two soleus activation levels (25% and 75% isometric voluntary contraction - IVC) prescribed using electromyographic biofeedback. Ultrasound imaging quantified activation-dependent modulation of soleus muscle length-tension behavior and its role in augmenting k_A. We found that soleus muscle stiffness (k_M) and k_A exhibit non-linear relations with muscle activation and were both more sensitive to the onset of activation than to subsequent increases in activation. Our findings also suggest that k_A can be modulated via activation through changes in soleus muscle length-tension behavior. However, this modulation is more complex than previously appreciated – reflecting interaction between active muscle and passive elastic tissues. Our findings may have implications for understanding normal and pathological ankle joint function and the design of impedance-based prostheses.

[4] Appendix 1 previously appeared as an article in the *Journal of Applied Biomechanics*. The original citation is as follows: Clark, W. H., & Franz, J. R. (2019). Activation-dependent changes in soleus length-tension behavior augment ankle joint quasi-stiffness. *J Appl Biomech* 35: 182-189, 2019. doi:10.1123/jab.2018-0297

APPENDIX 2: OLDER ADULTS OVERCOME REDUCED TRICEPS SURAE STRUCTURAL STIFFNESS TO PRESERVE ANKLE JOINT[5]

Ankle joint quasi-stiffness is an aggregate measure of the interaction between triceps surae muscle stiffness and Achilles tendon stiffness. This interaction may be altered due to age-related changes in the structural properties and functional behavior of the Achilles tendon and triceps surae muscles. We hypothesized that, due to a more compliant Achilles' tendon, older adults would exhibit lower ankle joint quasi-stiffness than young adults, during walking and during isolated contractions at matched triceps surae muscle activations. We also hypothesized that, independent of age, triceps surae muscle stiffness and ankle joint quasi-stiffness would increase with triceps surae muscle activation. We used conventional gait analysis in one experiment and, in another, electromyographic biofeedback and *in vivo* ultrasound imaging applied during isolated contractions. We found no difference in ankle joint quasi-stiffness between young and older adults during walking. Conversely, we found that: (*i*) young and older adults modulated ankle joint quasi-stiffness via activation-dependent changes in triceps surae muscle length-tension behavior, and (*ii*) at matched activation, older adults exhibited lower ankle joint quasi-stiffness than young adults. Despite age-related reductions during isolated contractions, ankle joint quasi-stiffness was maintained in older adults during walking – which may be governed via activation-mediated increases in muscle stiffness.

[5] Appendix 2 previously appeared as an article in the *Journal of Applied Biomechanics*. The original citation is as follows: Krupenevich, R. L., Clark, W. H., Sawicki, G. S., & Franz, J. R. (2020). Older adults overcome reduced triceps surae structural stiffness to preserve ankle joint quasi-stiffness during walking. *J Appl Biomech* 1-8, 2020. doi:10.1123/jab.2019-0340

REFERENCES

Abate, M., Schiavone, C., & Salini, V. (2014). The use of hyaluronic acid after tendon surgery and in tendinopathies. *Biomed Res Int, 2014*, 783632. doi:10.1155/2014/783632

Ackland, D. C., Lin, Y. C., & Pandy, M. G. (2012). Sensitivity of model predictions of muscle function to changes in moment arms and muscle-tendon properties: a Monte-Carlo analysis. *J Biomech, 45*(8), 1463-1471. doi:10.1016/j.jbiomech.2012.02.023

Aeles, J., Lichtwark, G. A., Lenchant, S., Vanlommel, L., Delabastita, T., & Vanwanseele, B. (2017). Information from dynamic length changes improves reliability of static ultrasound fascicle length measurements. *PeerJ, 5*, e4164. doi:10.7717/peerj.4164

Albracht, K., Arampatzis, A., & Baltzopoulos, V. (2008). Assessment of muscle volume and physiological cross-sectional area of the human triceps surae muscle in vivo. *J Biomech, 41*(10), 2211-2218. doi:10.1016/j.jbiomech.2008.04.020

Anderson, F. C., & Pandy, M. G. (2003). Individual muscle contributions to support in normal walking. *Gait Posture, 17*(2), 159-169. doi:10.1016/s0966-6362(02)00073-5

Anson, B. J., & McVay, C. B. (1971). Surgical Anatomy. *Leg. (5th ed.). W.B. Saunders Company, Philadelphia, London, Toronto (1971)*, 1186-1189.

Arndt, A., Bengtsson, A. S., Peolsson, M., Thorstensson, A., & Movin, T. (2012). Non-uniform displacement within the Achilles tendon during passive ankle joint motion. *Knee Surg Sports Traumatol Arthrosc, 20*(9), 1868-1874. doi:10.1007/s00167-011-1801-9

Arnold, E. M., Hamner, S. R., Seth, A., Millard, M., & Delp, S. L. (2013). How muscle fiber lengths and velocities affect muscle force generation as humans walk and run at different speeds. *J Exp Biol, 216*(Pt 11), 2150-2160. doi:10.1242/jeb.075697

Arnold, E. M., Ward, S. R., Lieber, R. L., & Delp, S. L. (2010). A model of the lower limb for analysis of human movement. *Ann Biomed Eng, 38*(2), 269-279. doi:10.1007/s10439-009-9852-5

Barber, L., Carty, C., Modenese, L., Walsh, J., Boyd, R., & Lichtwark, G. (2017). Medial gastrocnemius and soleus muscle-tendon unit, fascicle, and tendon interaction during walking in children with cerebral palsy. *Dev Med Child Neurol, 59*(8), 843-851. doi:10.1111/dmcn.13427

Barrett, R. S., & Lichtwark, G. A. (2008). Effect of altering neural, muscular and tendinous factors associated with aging on balance recovery using the ankle strategy: a simulation study. *J Theor Biol, 254*(3), 546-554. doi:10.1016/j.jtbi.2008.06.018

Beijersbergen, C. M., Granacher, U., Vandervoort, A. A., DeVita, P., & Hortobagyi, T. (2013). The biomechanical mechanism of how strength and power training improves walking

speed in old adults remains unknown. *Ageing Res Rev, 12*(2), 618-627. doi:10.1016/j.arr.2013.03.001

Blazkiewicz, M., Wiszomirska, I., Kaczmarczyk, K., Naemi, R., & Wit, A. (2017). Inter-individual similarities and variations in muscle forces acting on the ankle joint during gait. *Gait Posture, 58*, 166-170. doi:10.1016/j.gaitpost.2017.07.119

Bojsen-Moller, J., & Magnusson, S. P. (2015). Heterogeneous Loading of the Human Achilles Tendon In Vivo. *Exerc Sport Sci Rev, 43*(4), 190-197. doi:10.1249/JES.0000000000000062

Bojsen-Moller, J., Schwartz, S., Kalliokoski, K. K., Finni, T., & Magnusson, S. P. (2010). Intermuscular force transmission between human plantarflexor muscles in vivo. *J Appl Physiol (1985), 109*(6), 1608-1618. doi:10.1152/japplphysiol.01381.2009

Boyer, K. A., Andriacchi, T. P., & Beaupre, G. S. (2012). The role of physical activity in changes in walking mechanics with age. *Gait Posture, 36*(1), 149-153. doi:10.1016/j.gaitpost.2012.02.007

Browne, M. G., & Franz, J. R. (2017). The independent effects of speed and propulsive force on joint power generation in walking. *J Biomech, 55*, 48-55. doi:10.1016/j.jbiomech.2017.02.011

Buddhadev, H. H., & Martin, P. E. (2016). Effects of age and physical activity status on redistribution of joint work during walking. *Gait Posture, 50*, 131-136. doi:10.1016/j.gaitpost.2016.08.034

Chang, Y. H., & Kram, R. (1999). Metabolic cost of generating horizontal forces during human running. *J Appl Physiol (1985), 86*(5), 1657-1662. doi:10.1152/jappl.1999.86.5.1657

Chao, E. Y., Laughman, R. K., Schneider, E., & Stauffer, R. N. (1983). Normative data of knee joint motion and ground reaction forces in adult level walking. *J Biomech, 16*(3), 219-233. doi:10.1016/0021-9290(83)90129-x

Chernak, L. A., & Thelen, D. G. (2012). Tendon motion and strain patterns evaluated with two-dimensional ultrasound elastography. *J Biomech, 45*(15), 2618-2623. doi:10.1016/j.jbiomech.2012.08.001

Chernak Slane, L., & Thelen, D. G. (2014). The use of 2D ultrasound elastography for measuring tendon motion and strain. *J Biomech, 47*(3), 750-754. doi:10.1016/j.jbiomech.2013.11.023

Chow, R. S., Medri, M. K., Martin, D. C., Leekam, R. N., Agur, A. M., & McKee, N. H. (2000). Sonographic studies of human soleus and gastrocnemius muscle architecture: gender variability. *Eur J Appl Physiol, 82*(3), 236-244. doi:10.1007/s004210050677

Clark, W. H., & Franz, J. R. (2018a). Do triceps surae muscle dynamics govern non-uniform Achilles tendon deformations? *PeerJ, 6*, e5182. doi:10.7717/peerj.5182

Clark, W. H., & Franz, J. R. (2020). Triceps surae muscle-subtendon interaction differs between young and older adults. *Connect Tissue Res, 61*(1), 104-113. doi:10.1080/03008207.2019.1612384

Clark, W. H., Pimentel, R. E., & Franz, J. R. (2020). Imaging and Simulation of Inter-muscular Differences in Triceps Surae Contributions to Forward Propulsion During Walking. *Ann Biomed Eng*. doi:10.1007/s10439-020-02594-x

Conway, K. A., Bissette, R. G., & Franz, J. R. (2018). The Functional Utilization of Propulsive Capacity During Human Walking. *J Appl Biomech*, 1-31. doi:10.1123/jab.2017-0389

Conway, K. A., & Franz, J. R. (2019). Increasing the Propulsive Demands of Walking to their Maximum Elucidates Functionally Limiting Impairments in Older Adult Gait. *J Aging Phys Act*, 1-28. doi:10.1123/japa.2018-0327

Conway, K. A., & Franz, J. R. (2020). Shorter gastrocnemius fascicle lengths in older adults associate with worse capacity to enhance push-off intensity in walking. *Gait Posture, 77*, 89-94. doi:10.1016/j.gaitpost.2020.01.018

Cronin, N. J., af Klint, R., Grey, M. J., & Sinkjaer, T. (2011). Ultrasonography as a tool to study afferent feedback from the muscle-tendon complex during human walking. *J Electromyogr Kinesiol, 21*(2), 197-207. doi:10.1016/j.jelekin.2010.08.004

Cronin, N. J., Avela, J., Finni, T., & Peltonen, J. (2013). Differences in contractile behaviour between the soleus and medial gastrocnemius muscles during human walking. *J Exp Biol, 216*(Pt 5), 909-914. doi:10.1242/jeb.078196

Cronin, N. J., & Finni, T. (2013). Treadmill versus overground and barefoot versus shod comparisons of triceps surae fascicle behaviour in human walking and running. *Gait Posture, 38*(3), 528-533. doi:10.1016/j.gaitpost.2013.01.027

Cronin, N. J., Peltonen, J., Sinkjaer, T., & Avela, J. (2011). Neural compensation within the human triceps surae during prolonged walking. *J Neurophysiol, 105*(2), 548-553. doi:10.1152/jn.00967.2010

Crouzier, M., Lacourpaille, L., Nordez, A., Tucker, K., & Hug, F. (2018). Neuromechanical coupling within the human triceps surae and its consequence on individual force-sharing strategies. *J Exp Biol, 221*(Pt 21). doi:10.1242/jeb.187260

Csapo, R., Hodgson, J., Kinugasa, R., Edgerton, V. R., & Sinha, S. (2013). Ankle morphology amplifies calcaneus movement relative to triceps surae muscle shortening. *J Appl Physiol (1985), 115*(4), 468-473. doi:10.1152/japplphysiol.00395.2013

Cummins, E. J., Anson, B. J., & et al. (1946). The structure of the calcaneal tendon (of Achilles) in relation to orthopedic surgery, with additional observations on the plantaris muscle. *Surg Gynecol Obstet, 83*, 107-116.

Davis, J., Kaufman, K. R., & Lieber, R. L. (2003). Correlation between active and passive isometric force and intramuscular pressure in the isolated rabbit tibialis anterior muscle. *J Biomech, 36*(4), 505-512. doi:10.1016/s0021-9290(02)00430-x

Del Buono, A., Chan, O., & Maffulli, N. (2013). Achilles tendon: functional anatomy and novel emerging models of imaging classification. *Int Orthop, 37*(4), 715-721. doi:10.1007/s00264-012-1743-y

Delp, S. L., Anderson, F. C., Arnold, A. S., Loan, P., Habib, A., John, C. T., . . . Thelen, D. G. (2007). OpenSim: open-source software to create and analyze dynamic simulations of movement. *IEEE Trans Biomed Eng, 54*(11), 1940-1950. doi:10.1109/TBME.2007.901024

DeVita, P., & Hortobagyi, T. (2000). Age causes a redistribution of joint torques and powers during gait. *J Appl Physiol (1985), 88*(5), 1804-1811. doi:10.1152/jappl.2000.88.5.1804

DeWall, R. J., Slane, L. C., Lee, K. S., & Thelen, D. G. (2014). Spatial variations in Achilles tendon shear wave speed. *J Biomech, 47*(11), 2685-2692. doi:10.1016/j.jbiomech.2014.05.008

Dick, T. J. M., Biewener, A. A., & Wakeling, J. M. (2017). Comparison of human gastrocnemius forces predicted by Hill-type muscle models and estimated from ultrasound images. *J Exp Biol, 220*(Pt 9), 1643-1653. doi:10.1242/jeb.154807

Disselhorst-Klug, C., Schmitz-Rode, T., & Rau, G. (2009). Surface electromyography and muscle force: limits in sEMG-force relationship and new approaches for applications. *Clin Biomech (Bristol, Avon), 24*(3), 225-235. doi:10.1016/j.clinbiomech.2008.08.003

Doral, M. N., Alam, M., Bozkurt, M., Turhan, E., Atay, O. A., Donmez, G., & Maffulli, N. (2010). Functional anatomy of the Achilles tendon. *Knee Surg Sports Traumatol Arthrosc, 18*(5), 638-643. doi:10.1007/s00167-010-1083-7

Drazan, J. F., Hullfish, T. J., & Baxter, J. R. (2019). An automatic fascicle tracking algorithm quantifying gastrocnemius architecture during maximal effort contractions. *PeerJ, 7*, e7120. doi:10.7717/peerj.7120

Edama, M., Kubo, M., Onishi, H., Takabayashi, T., Inai, T., Yokoyama, E., . . . Kageyama, I. (2015). The twisted structure of the human Achilles tendon. *Scand J Med Sci Sports, 25*(5), e497-503. doi:10.1111/sms.12342

Edama, M., Kubo, M., Onishi, H., Takabayashi, T., Yokoyama, E., Inai, T., . . . Kageyama, I. (2016). Structure of the Achilles tendon at the insertion on the calcaneal tuberosity. *J Anat, 229*(5), 610-614. doi:10.1111/joa.12514

Farris, D. J., & Lichtwark, G. A. (2016). UltraTrack: Software for semi-automated tracking of muscle fascicles in sequences of B-mode ultrasound images. *Comput Methods Programs Biomed, 128*, 111-118. doi:10.1016/j.cmpb.2016.02.016

Farris, D. J., Robertson, B. D., & Sawicki, G. S. (2013). Elastic ankle exoskeletons reduce soleus muscle force but not work in human hopping. *J Appl Physiol (1985), 115*(5), 579-585. doi:10.1152/japplphysiol.00253.2013

Farris, D. J., & Sawicki, G. S. (2012a). Human medial gastrocnemius force-velocity behavior shifts with locomotion speed and gait. *Proc Natl Acad Sci U S A, 109*(3), 977-982. doi:10.1073/pnas.1107972109

Farris, D. J., & Sawicki, G. S. (2012b). The mechanics and energetics of human walking and running: a joint level perspective. *J R Soc Interface, 9*(66), 110-118. doi:10.1098/rsif.2011.0182

Finni, T., Bernabei, M., Baan, G. C., Noort, W., Tijs, C., & Maas, H. (2018). Non-uniform displacement and strain between the soleus and gastrocnemius subtendons of rat Achilles tendon. *Scand J Med Sci Sports, 28*(3), 1009-1017. doi:10.1111/sms.13001

Finni, T., Cronin, N. J., Mayfield, D., Lichtwark, G. A., & Cresswell, A. G. (2017). Effects of muscle activation on shear between human soleus and gastrocnemius muscles. *Scand J Med Sci Sports, 27*(1), 26-34. doi:10.1111/sms.12615

Foure, A., Nordez, A., McNair, P., & Cornu, C. (2011). Effects of plyometric training on both active and passive parts of the plantarflexors series elastic component stiffness of muscle-tendon complex. *Eur J Appl Physiol, 111*(3), 539-548. doi:10.1007/s00421-010-1667-4

Francis, C. A., Lenz, A. L., Lenhart, R. L., & Thelen, D. G. (2013). The modulation of forward propulsion, vertical support, and center of pressure by the plantarflexors during human walking. *Gait Posture, 38*(4), 993-997. doi:10.1016/j.gaitpost.2013.05.009

Franz, J. R., & Kram, R. (2013). Advanced age affects the individual leg mechanics of level, uphill, and downhill walking. *J Biomech, 46*(3), 535-540. doi:10.1016/j.jbiomech.2012.09.032

Franz, J. R., Slane, L. C., Rasske, K., & Thelen, D. G. (2015). Non-uniform in vivo deformations of the human Achilles tendon during walking. *Gait Posture, 41*(1), 192-197. doi:10.1016/j.gaitpost.2014.10.001

Franz, J. R., & Thelen, D. G. (2015). Depth-dependent variations in Achilles tendon deformations with age are associated with reduced plantarflexor performance during walking. *J Appl Physiol (1985), 119*(3), 242-249. doi:10.1152/japplphysiol.00114.2015

Franz, J. R., & Thelen, D. G. (2016). Imaging and simulation of Achilles tendon dynamics: Implications for walking performance in the elderly. *J Biomech, 49*(9), 1403-1410. doi:10.1016/j.jbiomech.2016.04.032

Fukashiro, S., Hay, D. C., & Nagano, A. (2006). Biomechanical behavior of muscle-tendon complex during dynamic human movements. *J Appl Biomech, 22*(2), 131-147. doi:10.1123/jab.22.2.131

Fukunaga, T., Kubo, K., Kawakami, Y., Fukashiro, S., Kanehisa, H., & Maganaris, C. N. (2001). In vivo behaviour of human muscle tendon during walking. *Proc Biol Sci, 268*(1464), 229-233. doi:10.1098/rspb.2000.1361

Fukunaga, T., Roy, R. R., Shellock, F. G., Hodgson, J. A., & Edgerton, V. R. (1996). Specific tension of human plantar flexors and dorsiflexors. *J Appl Physiol (1985), 80*(1), 158-165. doi:10.1152/jappl.1996.80.1.158

Gains, C. C., Correia, J. C., Baan, G. C., Noort, W., Screen, H. R. C., & Maas, H. (2020). Force Transmission Between the Gastrocnemius and Soleus Sub-Tendons of the Achilles Tendon in Rat. *Front Bioeng Biotechnol, 8*, 700. doi:10.3389/fbioe.2020.00700

Gillett, J. G., Barrett, R. S., & Lichtwark, G. A. (2013). Reliability and accuracy of an automated tracking algorithm to measure controlled passive and active muscle fascicle length changes from ultrasound. *Comput Methods Biomech Biomed Engin, 16*(6), 678-687. doi:10.1080/10255842.2011.633516

Gils, C. C., Steed, R. H., & Page, J. C. (1996). Torsion of the human Achilles tendon. *J Foot Ankle Surg, 35*(1), 41-48.

Goldberg, S. R., & Stanhope, S. J. (2013). Sensitivity of joint moments to changes in walking speed and body-weight-support are interdependent and vary across joints. *J Biomech, 46*(6), 1176-1183. doi:10.1016/j.jbiomech.2013.01.001

Gollnick, P. D., Sjodin, B., Karlsson, J., Jansson, E., & Saltin, B. (1974). Human soleus muscle: a comparison of fiber composition and enzyme activities with other leg muscles. *Pflugers Arch, 348*(3), 247-255. doi:10.1007/bf00587415

Gottschall, J. S., & Kram, R. (2003). Energy cost and muscular activity required for propulsion during walking. *J Appl Physiol (1985), 94*(5), 1766-1772. doi:10.1152/japplphysiol.00670.2002

Handsfield, G. G., Inouye, J. M., Slane, L. C., Thelen, D. G., Miller, G. W., & Blemker, S. S. (2017). A 3D model of the Achilles tendon to determine the mechanisms underlying nonuniform tendon displacements. *J Biomech, 51*, 17-25. doi:10.1016/j.jbiomech.2016.11.062

Hardy, S. E., Perera, S., Roumani, Y. F., Chandler, J. M., & Studenski, S. A. (2007). Improvement in usual gait speed predicts better survival in older adults. *J Am Geriatr Soc, 55*(11), 1727-1734. doi:10.1111/j.1532-5415.2007.01413.x

Hawkins, D., Lum, C., Gaydos, D., & Dunning, R. (2009). Dynamic creep and pre-conditioning of the Achilles tendon in-vivo. *J Biomech, 42*(16), 2813-2817. doi:10.1016/j.jbiomech.2009.08.023

Herbert, R. D., Clarke, J., Kwah, L. K., Diong, J., Martin, J., Clarke, E. C., . . . Gandevia, S. C. (2011). In vivo passive mechanical behaviour of muscle fascicles and tendons in human

gastrocnemius muscle-tendon units. *J Physiol, 589*(Pt 21), 5257-5267. doi:10.1113/jphysiol.2011.212175

Hermens, H. J., Freriks, B., Disselhorst-Klug, C., & Rau, G. (2000). Development of recommendations for SEMG sensors and sensor placement procedures. *J Electromyogr Kinesiol, 10*(5), 361-374. doi:10.1016/s1050-6411(00)00027-4

Hicks, J. L., Uchida, T. K., Seth, A., Rajagopal, A., & Delp, S. L. (2015). Is my model good enough? Best practices for verification and validation of musculoskeletal models and simulations of movement. *J Biomech Eng, 137*(2), 020905. doi:10.1115/1.4029304

Hill, A. V. (1953). The mechanics of active muscle. *Proc R Soc Lond B Biol Sci, 141*(902), 104-117. doi:10.1098/rspb.1953.0027

Hoang, P. D., Herbert, R. D., Todd, G., Gorman, R. B., & Gandevia, S. C. (2007). Passive mechanical properties of human gastrocnemius muscle tendon units, muscle fascicles and tendons in vivo. *J Exp Biol, 210*(Pt 23), 4159-4168. doi:10.1242/jeb.002204

Hof, A. L., Van Zandwijk, J. P., & Bobbert, M. F. (2002). Mechanics of human triceps surae muscle in walking, running and jumping. *Acta Physiol Scand, 174*(1), 17-30. doi:10.1046/j.1365-201x.2002.00917.x

Hoffman, B. W., Cresswell, A. G., Carroll, T. J., & Lichtwark, G. A. (2014). Muscle fascicle strains in human gastrocnemius during backward downhill walking. *J Appl Physiol (1985), 116*(11), 1455-1462. doi:10.1152/japplphysiol.01431.2012

Hug, F., Lacourpaille, L., Maisetti, O., & Nordez, A. (2013). Slack length of gastrocnemius medialis and Achilles tendon occurs at different ankle angles. *J Biomech, 46*(14), 2534-2538. doi:10.1016/j.jbiomech.2013.07.015

Huijing, P. A., Maas, H., & Baan, G. C. (2003). Compartmental fasciotomy and isolating a muscle from neighboring muscles interfere with myofascial force transmission within the rat anterior crural compartment. *J Morphol, 256*(3), 306-321. doi:10.1002/jmor.10097

Huijing, P. A., Yaman, A., Ozturk, C., & Yucesoy, C. A. (2011). Effects of knee joint angle on global and local strains within human triceps surae muscle: MRI analysis indicating in vivo myofascial force transmission between synergistic muscles. *Surg Radiol Anat, 33*(10), 869-879. doi:10.1007/s00276-011-0863-1

Ishihara, A., Naitoh, H., & Katsuta, S. (1987). Effects of ageing on the total number of muscle fibers and motoneurons of the tibialis anterior and soleus muscles in the rat. *Brain Res, 435*(1-2), 355-358. doi:10.1016/0006-8993(87)91624-6

Ishikawa, M., & Komi, P. V. (2008). Muscle fascicle and tendon behavior during human locomotion revisited. *Exerc Sport Sci Rev, 36*(4), 193-199. doi:10.1097/JES.0b013e3181878417

Ishikawa, M., Komi, P. V., Grey, M. J., Lepola, V., & Bruggemann, G. P. (2005). Muscle-tendon interaction and elastic energy usage in human walking. *J Appl Physiol (1985), 99*(2), 603-608. doi:10.1152/japplphysiol.00189.2005

Ishikawa, M., Niemela, E., & Komi, P. V. (2005). Interaction between fascicle and tendinous tissues in short-contact stretch-shortening cycle exercise with varying eccentric intensities. *J Appl Physiol (1985), 99*(1), 217-223. doi:10.1152/japplphysiol.01352.2004

Joseph, M. F., Lillie, K. R., Bergeron, D. J., Cota, K. C., Yoon, J. S., Kraemer, W. J., & Denegar, C. R. (2014). Achilles tendon biomechanics in response to acute intense exercise. *J Strength Cond Res, 28*(5), 1181-1186. doi:10.1519/JSC.0000000000000361

Karamanidis, K., & Arampatzis, A. (2006). Mechanical and morphological properties of human quadriceps femoris and triceps surae muscle-tendon unit in relation to aging and running. *J Biomech, 39*(3), 406-417. doi:10.1016/j.jbiomech.2004.12.017

Kaux, J. F., Samson, A., & Crielaard, J. M. (2015). Hyaluronic acid and tendon lesions. *Muscles Ligaments Tendons J, 5*(4), 264-269. doi:10.11138/mltj/2015.5.4.264

Kawakami, Y., Ichinose, Y., & Fukunaga, T. (1998). Architectural and functional features of human triceps surae muscles during contraction. *J Appl Physiol (1985), 85*(2), 398-404.

Kent-Braun, J. A., & Ng, A. V. (1999). Specific strength and voluntary muscle activation in young and elderly women and men. *J Appl Physiol (1985), 87*(1), 22-29. doi:10.1152/jappl.1999.87.1.22

Kinugasa, R., Kawakami, Y., & Fukunaga, T. (2005). Muscle activation and its distribution within human triceps surae muscles. *J Appl Physiol (1985), 99*(3), 1149-1156. doi:10.1152/japplphysiol.01160.2004

Kinugasa, R., Oda, T., Komatsu, T., Edgerton, V. R., & Sinha, S. (2013). Interaponeurosis shear strain modulates behavior of myotendinous junction of the human triceps surae. *Physiol Rep, 1*(6), e00147. doi:10.1002/phy2.147

Knaus, K. R., Ebrahimi, A., Martin, J. A., Loegering, I. F., Thelen, D. G., & Blemker, S. S. (2020). Achilles Tendon Morphology Is Related to Triceps Surae Muscle Size and Peak Plantarflexion Torques During Walking in Young but Not Older Adults. *Frontiers in Sports and Active Living, 2*(88). doi:10.3389/fspor.2020.00088

Korstanje, J. W., Selles, R. W., Stam, H. J., Hovius, S. E., & Bosch, J. G. (2010). Development and validation of ultrasound speckle tracking to quantify tendon displacement. *J Biomech, 43*(7), 1373-1379. doi:10.1016/j.jbiomech.2010.01.001

Kwah, L. K., Pinto, R. Z., Diong, J., & Herbert, R. D. (2013). Reliability and validity of ultrasound measurements of muscle fascicle length and pennation in humans: a systematic review. *J Appl Physiol (1985), 114*(6), 761-769. doi:10.1152/japplphysiol.01430.2011

Lai, A., Lichtwark, G. A., Schache, A. G., Lin, Y. C., Brown, N. A., & Pandy, M. G. (2015). In vivo behavior of the human soleus muscle with increasing walking and running speeds. *J Appl Physiol (1985), 118*(10), 1266-1275. doi:10.1152/japplphysiol.00128.2015

Landin, D., Thompson, M., & Reid, M. (2015). Knee and Ankle Joint Angles Influence the Plantarflexion Torque of the Gastrocnemius. *J Clin Med Res, 7*(8), 602-606. doi:10.14740/jocmr2107w

Larsson, L., & Edstrom, L. (1986). Effects of age on enzyme-histochemical fibre spectra and contractile properties of fast- and slow-twitch skeletal muscles in the rat. *J Neurol Sci, 76*(1), 69-89. doi:10.1016/0022-510x(86)90143-7

Lauber, B., Lichtwark, G. A., & Cresswell, A. G. (2014). Reciprocal activation of gastrocnemius and soleus motor units is associated with fascicle length change during knee flexion. *Physiol Rep, 2*(6). doi:10.14814/phy2.12044

Leitner, C., Hager, P. A., Penasso, H., Tilp, M., Benini, L., Peham, C., & Baumgartner, C. (2019). Ultrasound as a Tool to Study Muscle-Tendon Functions during Locomotion: A Systematic Review of Applications. *Sensors (Basel), 19*(19). doi:10.3390/s19194316

Lenhart, R. L., Francis, C. A., Lenz, A. L., & Thelen, D. G. (2014). Empirical evaluation of gastrocnemius and soleus function during walking. *J Biomech, 47*(12), 2969-2974. doi:10.1016/j.jbiomech.2014.07.007

Lichtwark, G. A., & Wilson, A. M. (2006). Interactions between the human gastrocnemius muscle and the Achilles tendon during incline, level and decline locomotion. *J Exp Biol, 209*(Pt 21), 4379-4388. doi:10.1242/jeb.02434

Liu, C. L., Zhou, J. P., Sun, P. T., Chen, B. Z., Zhang, J., Tang, C. Z., & Zhang, Z. J. (2020). Influence of different knee and ankle ranges of motion on the elasticity of triceps surae muscles, Achilles tendon, and plantar fascia. *Sci Rep, 10*(1), 6643. doi:10.1038/s41598-020-63730-0

Liu, M. Q., Anderson, F. C., Pandy, M. G., & Delp, S. L. (2006). Muscles that support the body also modulate forward progression during walking. *J Biomech, 39*(14), 2623-2630. doi:10.1016/j.jbiomech.2005.08.017

Liu, M. Q., Anderson, F. C., Schwartz, M. H., & Delp, S. L. (2008). Muscle contributions to support and progression over a range of walking speeds. *J Biomech, 41*(15), 3243-3252. doi:10.1016/j.jbiomech.2008.07.031

Maas, H., Noort, W., Baan, G. C., & Finni, T. (2020). Non-uniformity of displacement and strain within the Achilles tendon is affected by joint angle configuration and differential muscle loading. *J Biomech, 101*, 109634. doi:10.1016/j.jbiomech.2020.109634

Macaluso, A., Nimmo, M. A., Foster, J. E., Cockburn, M., McMillan, N. C., & De Vito, G. (2002). Contractile muscle volume and agonist-antagonist coactivation account for differences in

torque between young and older women. *Muscle Nerve, 25*(6), 858-863. doi:10.1002/mus.10113

Maganaris, C. N. (2003). Force-length characteristics of the in vivo human gastrocnemius muscle. *Clin Anat, 16*(3), 215-223. doi:10.1002/ca.10064

Maganaris, C. N., Baltzopoulos, V., & Sargeant, A. J. (1998). In vivo measurements of the triceps surae complex architecture in man: implications for muscle function. *J Physiol, 512 (Pt 2)*, 603-614. doi:10.1111/j.1469-7793.1998.603be.x

Malatesta, D., Canepa, M., & Menendez Fernandez, A. (2017). The effect of treadmill and overground walking on preferred walking speed and gait kinematics in healthy, physically active older adults. *Eur J Appl Physiol, 117*(9), 1833-1843. doi:10.1007/s00421-017-3672-3

Malcolm, P., Galle, S., Derave, W., & De Clercq, D. (2018). Bi-articular Knee-Ankle-Foot Exoskeleton Produces Higher Metabolic Cost Reduction than Weight-Matched Mono-articular Exoskeleton. *Front Neurosci, 12*, 69. doi:10.3389/fnins.2018.00069

Matijevich, E. S., Branscombe, L. M., & Zelik, K. E. (2018). Ultrasound estimates of Achilles tendon exhibit unexpected shortening during ankle plantarflexion. *J Biomech, 72*, 200-206. doi:10.1016/j.jbiomech.2018.03.013

Matson, A., Konow, N., Miller, S., Konow, P. P., & Roberts, T. J. (2012). Tendon material properties vary and are interdependent among turkey hindlimb muscles. *J Exp Biol, 215*(Pt 20), 3552-3558. doi:10.1242/jeb.072728

McGowan, C. P., Neptune, R. R., & Kram, R. (2008). Independent effects of weight and mass on plantar flexor activity during walking: implications for their contributions to body support and forward propulsion. *J Appl Physiol (1985), 105*(2), 486-494. doi:10.1152/japplphysiol.90448.2008

Merletti, R., Knaflitz, M., & DeLuca, C. J. (1992). Electrically evoked myoelectric signals. *Crit Rev Biomed Eng, 19*(4), 293-340.

Mian, O. S., Thom, J. M., Ardigo, L. P., Minetti, A. E., & Narici, M. V. (2007). Gastrocnemius muscle-tendon behaviour during walking in young and older adults. *Acta Physiol (Oxf), 189*(1), 57-65. doi:10.1111/j.1748-1716.2006.01634.x

Miller, M. S., Callahan, D. M., & Toth, M. J. (2014). Skeletal muscle myofilament adaptations to aging, disease, and disuse and their effects on whole muscle performance in older adult humans. *Front Physiol, 5*, 369. doi:10.3389/fphys.2014.00369

Miyoshi, T., Nakazawa, K., Tanizaki, M., Sato, T., & Akai, M. (2006). Altered activation pattern in synergistic ankle plantarflexor muscles in a reduced-gravity environment. *Gait Posture, 24*(1), 94-99. doi:10.1016/j.gaitpost.2005.07.010

Monaco, V., Coscia, M., & Micera, S. (2011). Cost function tuning improves muscle force estimation computed by static optimization during walking. *Conf Proc IEEE Eng Med Biol Soc, 2011*, 8263-8266. doi:10.1109/IEMBS.2011.6092037

Morse, C. I., Thom, J. M., Birch, K. M., & Narici, M. V. (2005). Changes in triceps surae muscle architecture with sarcopenia. *Acta Physiol Scand, 183*(3), 291-298. doi:10.1111/j.1365-201X.2004.01404.x

Narici, M. V., Maffulli, N., & Maganaris, C. N. (2008). Ageing of human muscles and tendons. *Disabil Rehabil, 30*(20-22), 1548-1554. doi:10.1080/09638280701831058

Narici, M. V., Maganaris, C. N., Reeves, N. D., & Capodaglio, P. (2003). Effect of aging on human muscle architecture. *J Appl Physiol (1985), 95*(6), 2229-2234. doi:10.1152/japplphysiol.00433.2003

Neptune, R. R., Kautz, S. A., & Zajac, F. E. (2001). Contributions of the individual ankle plantar flexors to support, forward progression and swing initiation during walking. *J Biomech, 34*(11), 1387-1398. doi:10.1016/s0021-9290(01)00105-1

Neptune, R. R., & Sasaki, K. (2005). Ankle plantar flexor force production is an important determinant of the preferred walk-to-run transition speed. *J Exp Biol, 208*(Pt 5), 799-808. doi:10.1242/jeb.01435

Neptune, R. R., Sasaki, K., & Kautz, S. A. (2008). The effect of walking speed on muscle function and mechanical energetics. *Gait Posture, 28*(1), 135-143. doi:10.1016/j.gaitpost.2007.11.004

Neptune, R. R., Zajac, F. E., & Kautz, S. A. (2009). Author's Response to Comment on "Contributions of the individual ankle plantar flexors to support, forward progression and swing initiation during walking" (Neptune et al., 2001) and "Muscle mechanical work requirements during normal walking: The energetic cost of raising the body's center-of-mass is significant" (). *J Biomech, 42*(11), 1786-1789. doi:10.1016/j.jbiomech.2009.04.029

Nilsson, J., & Thorstensson, A. (1989). Ground reaction forces at different speeds of human walking and running. *Acta Physiol Scand, 136*(2), 217-227. doi:10.1111/j.1748-1716.1989.tb08655.x

Nuckols, R. W., Dick, T. J. M., Beck, O. N., & Sawicki, G. S. (2020). Ultrasound imaging links soleus muscle neuromechanics and energetics during human walking with elastic ankle exoskeletons. *Sci Rep, 10*(1), 3604. doi:10.1038/s41598-020-60360-4

Oda, T., Kanehisa, H., Chino, K., Kurihara, T., Nagayoshi, T., Fukunaga, T., & Kawakami, Y. (2007). In vivo behavior of muscle fascicles and tendinous tissues of human gastrocnemius and soleus muscles during twitch contraction. *J Electromyogr Kinesiol, 17*(5), 587-595. doi:10.1016/j.jelekin.2006.04.013

Ogihara, N., Oishi, M., Kanai, R., Shimada, H., Kondo, T., Yoshino-Saito, K., . . . Okano, H. (2017). Muscle architectural properties in the common marmoset (Callithrix jacchus). *Primates, 58*(3), 461-472. doi:10.1007/s10329-017-0608-9

Onambele, G. L., Narici, M. V., & Maganaris, C. N. (2006). Calf muscle-tendon properties and postural balance in old age. *J Appl Physiol (1985), 100*(6), 2048-2056. doi:10.1152/japplphysiol.01442.2005

Orendurff, M. S., Segal, A. D., Klute, G. K., Berge, J. S., Rohr, E. S., & Kadel, N. J. (2004). The effect of walking speed on center of mass displacement. *J Rehabil Res Dev, 41*(6A), 829-834. doi:10.1682/jrrd.2003.10.0150

Orselli, M. I. V., Franz, J. R., & Thelen, D. G. (2017). The effects of Achilles tendon compliance on triceps surae mechanics and energetics in walking. *J Biomech, 60*, 227-231. doi:10.1016/j.jbiomech.2017.06.022

Panizzolo, F. A., Green, D. J., Lloyd, D. G., Maiorana, A. J., & Rubenson, J. (2013). Soleus fascicle length changes are conserved between young and old adults at their preferred walking speed. *Gait Posture, 38*(4), 764-769. doi:10.1016/j.gaitpost.2013.03.021

Pedowitz, D., & Kirwan, G. (2013). Achilles tendon ruptures. *Curr Rev Musculoskelet Med, 6*(4), 285-293. doi:10.1007/s12178-013-9185-8

Pekala, P. A., Henry, B. M., Ochala, A., Kopacz, P., Taton, G., Mlyniec, A., . . . Tomaszewski, K. A. (2017). The twisted structure of the Achilles tendon unraveled: A detailed quantitative and qualitative anatomical investigation. *Scand J Med Sci Sports, 27*(12), 1705-1715. doi:10.1111/sms.12835

Piazza, S. J., Okita, N., & Cavanagh, P. R. (2001). Accuracy of the functional method of hip joint center location: effects of limited motion and varied implementation. *J Biomech, 34*(7), 967-973. doi:10.1016/s0021-9290(01)00052-5

Purser, J. L., Weinberger, M., Cohen, H. J., Pieper, C. F., Morey, M. C., Li, T., . . . Lapuerta, P. (2005). Walking speed predicts health status and hospital costs for frail elderly male veterans. *J Rehabil Res Dev, 42*(4), 535-546.

Rajagopal, A., Dembia, C. L., DeMers, M. S., Delp, D. D., Hicks, J. L., & Delp, S. L. (2016). Full-Body Musculoskeletal Model for Muscle-Driven Simulation of Human Gait. *IEEE Trans Biomed Eng, 63*(10), 2068-2079. doi:10.1109/TBME.2016.2586891

Riley, P. O., Della Croce, U., & Kerrigan, D. C. (2001). Propulsive adaptation to changing gait speed. *J Biomech, 34*(2), 197-202. doi:10.1016/s0021-9290(00)00174-3

Roberts, T. J., & Gabaldon, A. M. (2008). Interpreting muscle function from EMG: lessons learned from direct measurements of muscle force. *Integr Comp Biol, 48*(2), 312-320. doi:10.1093/icb/icn056

Rubenson, J., Pires, N. J., Loi, H. O., Pinniger, G. J., & Shannon, D. G. (2012). On the ascent: the soleus operating length is conserved to the ascending limb of the force-length curve across gait mechanics in humans. *J Exp Biol, 215*(Pt 20), 3539-3551. doi:10.1242/jeb.070466

Sarrafian, S. K. (1993). Biomechanics of the subtalar joint complex. *Clin Orthop Relat Res*(290), 17-26.

Sawicki, G. S., Lewis, C. L., & Ferris, D. P. (2009). It pays to have a spring in your step. *Exerc Sport Sci Rev, 37*(3), 130-138. doi:10.1097/JES.0b013e31819c2df6

Scovil, C. Y., & Ronsky, J. L. (2006). Sensitivity of a Hill-based muscle model to perturbations in model parameters. *J Biomech, 39*(11), 2055-2063. doi:10.1016/j.jbiomech.2005.06.005

Sikdar, S., Wei, Q., & Cortes, N. (2014). Dynamic ultrasound imaging applications to quantify musculoskeletal function. *Exerc Sport Sci Rev, 42*(3), 126-135. doi:10.1249/JES.0000000000000015

Silder, A., Heiderscheit, B., & Thelen, D. G. (2008). Active and passive contributions to joint kinetics during walking in older adults. *J Biomech, 41*(7), 1520-1527. doi:10.1016/j.jbiomech.2008.02.016

Slane, L. C., & Thelen, D. G. (2014). Non-uniform displacements within the Achilles tendon observed during passive and eccentric loading. *J Biomech, 47*(12), 2831-2835. doi:10.1016/j.jbiomech.2014.07.032

Slane, L. C., & Thelen, D. G. (2015). Achilles tendon displacement patterns during passive stretch and eccentric loading are altered in middle-aged adults. *Med Eng Phys, 37*(7), 712-716. doi:10.1016/j.medengphy.2015.04.004

Studenski, S., Perera, S., Patel, K., Rosano, C., Faulkner, K., Inzitari, M., . . . Guralnik, J. (2011). Gait speed and survival in older adults. *JAMA, 305*(1), 50-58. doi:10.1001/jama.2010.1923

Sutherland, D. H., Cooper, L., & Daniel, D. (1980). The role of the ankle plantar flexors in normal walking. *J Bone Joint Surg Am, 62*(3), 354-363.

Szaro, P., Witkowski, G., Smigielski, R., Krajewski, P., & Ciszek, B. (2009). Fascicles of the adult human Achilles tendon - an anatomical study. *Ann Anat, 191*(6), 586-593. doi:10.1016/j.aanat.2009.07.006

Thorpe, C. T., Godinho, M. S. C., Riley, G. P., Birch, H. L., Clegg, P. D., & Screen, H. R. C. (2015). The interfascicular matrix enables fascicle sliding and recovery in tendon, and behaves more elastically in energy storing tendons. *J Mech Behav Biomed Mater, 52*, 85-94. doi:10.1016/j.jmbbm.2015.04.009

Thorpe, C. T., Riley, G. P., Birch, H. L., Clegg, P. D., & Screen, H. R. C. (2016). Fascicles and the interfascicular matrix show adaptation for fatigue resistance in energy storing tendons. *Acta Biomater, 42*, 308-315. doi:10.1016/j.actbio.2016.06.012

Thorpe, C. T., Riley, G. P., Birch, H. L., Clegg, P. D., & Screen, H. R. C. (2017). Fascicles and the interfascicular matrix show decreased fatigue life with ageing in energy storing tendons. *Acta Biomater, 56*, 58-64. doi:10.1016/j.actbio.2017.03.024

Thorpe, C. T., Udeze, C. P., Birch, H. L., Clegg, P. D., & Screen, H. R. (2012). Specialization of tendon mechanical properties results from interfascicular differences. *J R Soc Interface, 9*(76), 3108-3117. doi:10.1098/rsif.2012.0362

Thorpe, C. T., Udeze, C. P., Birch, H. L., Clegg, P. D., & Screen, H. R. (2013). Capacity for sliding between tendon fascicles decreases with ageing in injury prone equine tendons: a possible mechanism for age-related tendinopathy? *Eur Cell Mater, 25*, 48-60.

Tian, M., Herbert, R. D., Hoang, P., Gandevia, S. C., & Bilston, L. E. (2012). Myofascial force transmission between the human soleus and gastrocnemius muscles during passive knee motion. *J Appl Physiol (1985), 113*(4), 517-523. doi:10.1152/japplphysiol.00111.2012

Tijs, C., van Dieen, J. H., Baan, G. C., & Maas, H. (2016). Synergistic Co-activation Increases the Extent of Mechanical Interaction between Rat Ankle Plantar-Flexors. *Front Physiol, 7*, 414. doi:10.3389/fphys.2016.00414

Tilp, M., Steib, S., Schappacher-Tilp, G., & Herzog, W. (2011). Changes in fascicle lengths and pennation angles do not contribute to residual force enhancement/depression in voluntary contractions. *J Appl Biomech, 27*(1), 64-73.

van Gils, C. C., Steed, R. H., & Page, J. C. (1996). Torsion of the human Achilles tendon. *J Foot Ankle Surg, 35*(1), 41-48. doi:10.1016/s1067-2516(96)80011-1

Whittington, B., Silder, A., Heiderscheit, B., & Thelen, D. G. (2008). The contribution of passive-elastic mechanisms to lower extremity joint kinetics during human walking. *Gait Posture, 27*(4), 628-634. doi:10.1016/j.gaitpost.2007.08.005

Winter, D. A. (1983). Energy generation and absorption at the ankle and knee during fast, natural, and slow cadences. *Clin Orthop Relat Res*(175), 147-154.

Winter, D. A. (1990). *Biomechanics and Motor Control of Human Movement* (6th ed.): New York: Wiley.

Wolfram, S., Hodson-Tole, E. F., Morse, C. I., Winwood, K. L., & McEwan, I. M. (2020). Elongation differences between the sub-tendons of gastrocnemius medialis and lateralis during plantarflexion in different frontal plane position of the foot. *Gait Posture, 75*, 149-154. doi:10.1016/j.gaitpost.2019.10.020

Zajac, F. E. (1989). Muscle and tendon: properties, models, scaling, and application to biomechanics and motor control. *Crit Rev Biomed Eng, 17*(4), 359-411.

Zargham, A., Afschrift, M., De Schutter, J., Jonkers, I., & De Groote, F. (2019). Inverse dynamic estimates of muscle recruitment and joint contact forces are more realistic when

minimizing muscle activity rather than metabolic energy or contact forces. *Gait Posture, 74*, 223-230. doi:10.1016/j.gaitpost.2019.08.019

Zelik, K. E., & Franz, J. R. (2017). It's positive to be negative: Achilles tendon work loops during human locomotion. *PLoS One, 12*(7), e0179976. doi:10.1371/journal.pone.0179976

Zelik, K. E., Huang, T. W., Adamczyk, P. G., & Kuo, A. D. (2014). The role of series ankle elasticity in bipedal walking. *J Theor Biol, 346*, 75-85. doi:10.1016/j.jtbi.2013.12.014

Zhang, J., Fiers, P., Witte, K. A., Jackson, R. W., Poggensee, K. L., Atkeson, C. G., & Collins, S. H. (2017). Human-in-the-loop optimization of exoskeleton assistance during walking. *Science, 356*(6344), 1280-1284. doi:10.1126/science.aal5054